Enhanced Static Voltage Stability and Short Circuit Monitoring Performance and Optimization of Future Onshore AC Power Systems

Muhanad Ahmed

A thesis submitted for the degree of Doctor of Philosophy to the Department of Electronic and Electrical Engineering University of Strathclyde Glasgow, United Kingdom

August 2022

This thesis is the result of the author's original research. It has been composed by the author and has not been previously submitted for examination which has led to the award of a degree.

Signed:

Date:

Abstract

This thesis presents several techniques focussed on improving characterisation, estimation and optimization of various factors associated with future power system strength and stability, that are markedly changing as the transition to renewable energy-dominated power systems continues. Changing systems strength in transmission and distribution networks are presenting unique regional challenges limiting the integration of low carbon technologies due to various constraints imposed on the network. These include fault level headroom constraints in MV distribution networks and steady state stability limits in transmission networks during periods of high power transfer.

Specifically, a perturbation-coefficient based recursive least square (RLS) passive fault current estimation method, impedance matching bus-based and line-based static stability indices and voltage stability-constrained optimal power flow (VSCOPF) models are presented to facilitate enhanced system performance in future low-inertia/strength power systems. Alternative to model-based strategies for conducting short circuit studies, measurement based short circuit monitoring has presented effective means to facilitate active fault level management functions and support flexible distributed generation connections in MV distribution networks. The application of passive and active fault level estimation is presenting alternative means to support embedded generation connections in fault level constrained regions. This research therefore proposes a perturbation coefficient-based technique for passive short circuit estimation utilising RLS based methodologies. This improves existing OLS processes in fault current estimation as parameter estimates are continuously updated via gain vectors with the sum of square of errors recursively minimised with additional load perturbation events identified. Enhancements in the accuracy of the proposed estimation method are demonstrated utilizing extensive simulation-based studies relative to conventional estimation methods.

Declining system strength presents several challenges in monitoring and managing future networks with increased risks of classical voltage instability in weak networks

identified as an emerging challenge. Novel static line-based and bus-based voltage stability indices are developed based on the ratio of load current flowing in a line to the expected fault current flowing in the line and are based on impedance matching concepts during maximum power transfer. The proposed approach models shunt branch parameters, which have been historically neglected in two-bus equivalents and hence illustrate enhanced performance during stressed system conditions. Simulation-based studies on multiple test networks have demonstrated improved detection capability of the developed stability indicator against several bespoke static line stability assessment methods. Index characterization considering solid state transformer (SST), constant voltage and constant power factor DG models are also presented to illustrate stability performance in future system conditions.

The developed line index is incorporated into existing optimisation procedures for optimal generation dispatch with the inclusion of voltage stability criteria via voltage stability-constrained optimal power flow (VSCOPF). The proposed VSCOPF models incorporate the novel line stability indicator as part of an objective function in a multi-objective OPF formulation and as an inequality constraint. The proposed VSCOPF solution procedures demonstrate enhanced capability in increasing critical loadability, improved voltage performance, enhanced active/reactive generation dispatch and reduction in system losses relative to existing methods via simplified and robust calculation of proximity to collapse using static analysis techniques.

Acknowledgements

I would like to express my sincere gratitude and appreciation for the unwavering, unparalleled patience, support and mentorship from my supervisor Campbell Booth whose guidance and relentless motivation has been invaluable throughout this study.

Many thanks to Ibrahim Abdulhadi who always managed to provide an interesting and entertaining technical conversation and for his guidance during the early stages of my PhD. Thanks also to Federico Coffele for his support of my research work and input.

Thanks also to EEE colleagues Dimitrios Tzelepis, Waqquas Bukhsh , Qiteng Hong and Agusti Alvarez for their valuable input and engagement with my work.

Finally and most importantly, sincere thanks go to my caring and loving parents Mousa Ali Ahmed and Zeinab Abdulgadir for all their support, patience and prayers. Their continuous encouragement has been invaluable during my PhD journey. Thanks also to my siblings for always keeping an open mind and supporting me unconditionally.

Contents

List of figures

List of tables

1. Introduction

1.1 Research context and motivation

With the increasing uptake of renewable-based generation, integrated via power electronics converters, to meet global climate change targets and support the net zero transition as part of the growing global green economy, several decarbonization pathways, policies and proposals for reduction of emissions within each sector have been developed in GB [1]. Several challenges have been identified by system operators, regulators, equipment manufacturers and research institutions. These challenges include maximising renewable integration, and being able to plan, model, operate, control and protect future systems, which behave very differently from conventional, synchronous generation-dominated systems. Growing penetrations of low carbon technologies (LCT) – specifically the electrification of transport and heat, and possible integration of large-scale and smaller distributed storage (and technologies such as vehicle-to-grid), and proliferation of large-scale renewables (e.g. large wind farms) and smaller-scale distributed energy resources (DER), have and will continue to significantly change system behaviour, and these changes are expected to increase in the future. There is also the expectation that future energy systems, while being underpinned by electricity, may contain multiple energy vectors (e.g. green hydrogen) and interfaces between vectors, and this will also act to change electrical system performance and dynamics.

Reducing system strength and short circuit levels [2-4], for example, have presented unique challenges in planning and operating a power network at both transmission and distribution level. System strength can be defined as an inherent power system characteristic relating the availability of fault current at a given location which relates the magnitude of change in voltage following a fault [2]. Increased DER penetration in distribution networks have reduced available fault level headroom in fault level constrained regions, risking switchgear make and break design limits being exceeded [5, 6]. This in turn restricts the uptake of DER without delayed and costly network reinforcement and the provision of flexible DER connections and active management of distribution fault levels may provide alternative means for accelerated DER

deployment. Conventional strategies in fault level management have relied on offline, model-based short circuit studies [7] which have a number of limitations [8] due to simplifying assumptions inherent in existing IEC [9] and ANSI standards, leading to, in some cases, over-investment in network infrastructure [5]. This has recently led to the development and deployment of measurement-based active and passive fault level monitoring technologies utilised to facilitate active fault level management functions to support increasing DER penetration in distribution networks [5,6]. Conversely, transmission systems have seen an overall decline in regional short circuit levels (see figures 1.1 and 1.2) [10] increasing risks of system instability, protection maloperation and subsynchronous oscillations due to the weak nature of the interconnected network [3]. Several stability challenges in relation to weak, low system strength systems have been observed and reported in the literature by network operators [3, 11]. Classical steady-state voltage instability during small load disturbances occurs when an increase in system loading causes a net reduction at the active power gained at a bus and a critical stability condition is reached. This has become of increasing concern with higher renewable integration due to the higher voltage sensitivity to active and reactive power changes seen across weak networks during periods of high-power transfer [3]. Methods to monitor and manage short circuit level issues in transmission and distribution systems can therefore support the increased uptake and management of DER resources and is hence the focus of this thesis.

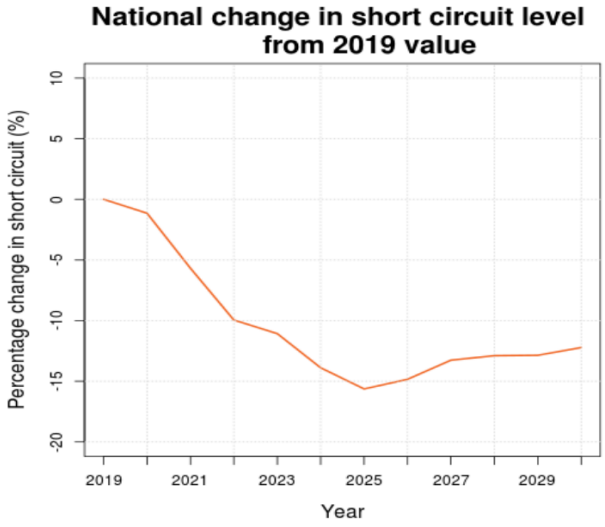

Figure 1.1 Forecasted decline in national short circuit levels between 2019-2030 [10]

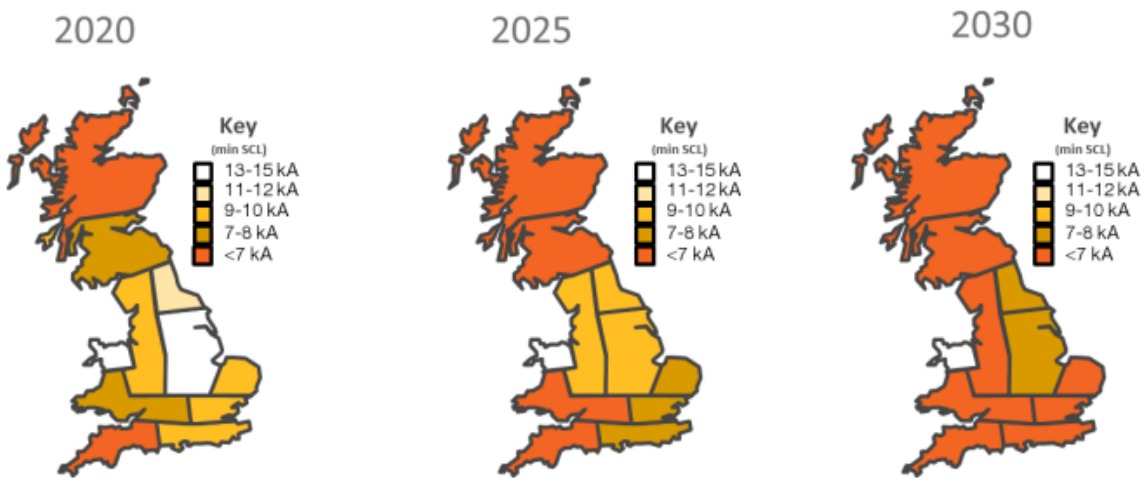

Figure 1.2 Regional changes in short circuit levels between 2020-2030 [10]

Bonneville Power Administration in the USA has encountered steady-state instability conditions [3] due to high penetration of wind power parks connecting long transmission lines where high sensitivities ($\frac{dV}{dP}$ and $\frac{dV}{dQ}$) have been observed leading to voltage collapse following wind ramp ups due to high equivalent system impedances seen at the collapse point (weak radial network condition). National grid ESO has identified voltage instability issues in the south east of England [11] under certain contingencies (double circuit faults) which result in high power transfers, and exports in long transmission corridors needing to be capped, to avoid system voltage collapse and has identified 59 sites which may encounter weak network conditions due to low availability of reactive power demand [11]. Figure 1.3 illustrates for a double circuit fault between Kemsley, Canterbury and Cleve Hill the System Security and Quality of Supply Standard (SQSS) limit may be reached during high power export periods [11] in the 400 kV system (e.g. winter peak demand periods), which requires additional voltage support via reactive power service provision to maintain dynamic voltage stability.

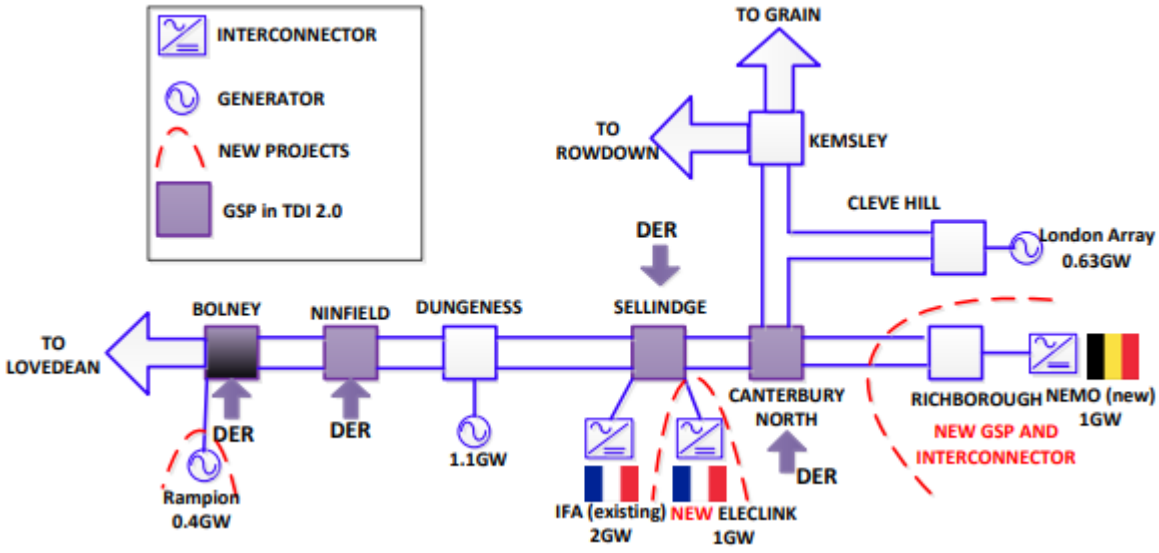

Figure 1.3 Voltage stability risks in South East England transmission network for a double circuit fault during high power export periods

This research focuses on the development of methods and tools to monitor system short circuit levels and steady-state voltage instability to facilitate online management of system strength in transmission and distribution systems via preventive control action. The inherent natural variation and perturbation of system load creates unique voltage and current signatures that can be utilised to passively monitor system fault levels during unfaulted, steady-state conditions. The application of static voltage stability indices[12] can also be utilised to identify critical lines and weak buses in a network in addition to available stability margins using steady-state RMS based methodologies [12]. Relative to time consuming dynamic time domain simulations, stability indices provide efficient means to perform static voltage stability assessment using algebraic methods. This research also investigates the application of line-based stability indices for the provision of optimisation solutions to maximize distance to collapse and critical loadability during maximum power transfer conditions via voltage stability-constrained optimal power flow (VSCOPF). Based on the aforementioned issues the main challenges addressed in this thesis include:

- Shortcomings and inefficiencies inherent in existing passive fault current estimation methods, which limit application in online fault level management functions can be enhanced through effective parameter estimation

methodologies. Improved modelling of downstream load perturbation events can further improve estimation performance relative to existing techniques.

- Limited concepts adopted for deriving line-based stability indices, which have predominantly relied on modelling two-bus network equivalents [13] may be expanded through alternative concepts for index development. Impedance matching theory can further provide alternative and improved means of deriving line-based stability indices as they have been predominantly utilised in bus-based index methods.
- Two-bus equivalent models utilised for development of stability indices have historically neglected shunt branch admittances [13-15], which may compromise accuracy of calculated indices. Development of indices accounting for shunt susceptance parameters (π models) may further improve performance and accuracy of existing index-based methods.
- Provision of flexibility in expressing stability indices as both line and bus-based indices can enhance monitoring capability as the voltage stability condition of both lines and buses can be evaluated utilising an improved index formulation.
- Improved performance of index-based VSCOPF solution procedures and dispatch can be achieved through improved modelling of stability indices through incorporation of full π transmission line models during index evaluation (accounting for shunt susceptance parameters).

1.2 Research contributions

A brief summary of the novel contributions made in this thesis is outlined below:

- A resistance and reactance based recursive least square fault level estimator based on a perturbation-coefficient technique is presented for passive upstream short circuit current measurement based on measurements of voltage phasors and active power before and after a downstream load perturbation
- Static line and bus based voltage stability indices utilizing impedance matching two bus equivalent including both series branch and shunt susceptance

parameters. The developed line current index (LCI) based on the ratio of the load current flowing in a line to the expected prevailing fault current flowing in the same line (for a fault at the receiving end bus) is reformulated to an equivalent bus current index (BCI) method and can therefore identify both critical lines and weak buses.

- Voltage stability constrained optimal power flow solution procedures incorporating the improved static line index as a constrained-based and multiobjective formulation for redispatch of system generation (synchronous) and the provision of control setpoints for enhanced stability margin capability and critical loadability during stressed system conditions.

1.3 Published Conference Papers

- Ahmed, M., Booth, C. and Coffele, F. (2018), Performance of fault-level estimation functions in future distribution networks. The Journal of Engineering, 2018: 978-981.

1.4 Thesis overview

Chapter 2 Provides an overview of existing methods, standards and limitations to fault level management via model-based methodologies adopted by DNOs and the emergence of measurement-based fault level monitoring technology as an alternative for enhanced management. A critical review of existing short circuit impedance methods and identified short comings will also be summarised. Steady state voltage stability assessment methods and techniques will be covered with an emphasis on limitations of index-based concepts and techniques outlined. Review of existing VSCOPF methodologies and identified gaps in the literature will be summarised with a focus on index based VSCOPF methods.

Chapter 3 Based on the identified short comings and objectives outlined in the previous chapter, the development of a perturbation coefficient recursive least square short circuit estimation method is presented utilising resistance and reactance based

RLS estimators. The developed short circuit impedance method assumes a downstream perturbation is modelled as an active power increment at a bus which neglects active power loss due to system voltage drops. The developed approach is evaluated using several test scenarios and test networks with summary and discussion of the main findings addressed.

Chapter 4 A line-based and bus-based voltage stability index method based on impedance matching concepts and a two-bus π transmission line model equivalent is presented with the technique validated against several test networks and performance compared against multiple existing line stability indices. The developed technique is based on the ratio of the load current flowing in a line to the expected prevailing fault current flowing in the same line considering shunt susceptance parameters. Simplified, steady-state constant power factor, constant voltage DG models and SST power flow models are incorporated to evaluate the impact on index performance.

Chapter 5 Multi-objective and constrained-based voltage stability-constrained OPF models are presented based on the previously developed line current index with performance evaluated against existing line index-based VSCOPF methods using several test network scenarios during stressed network conditions. Recommendations for extending and enhancing the performance of the developed VSCOPF are summarised including the incorporation of emerging reactive power injection models in the OPF for coordinated and economic system redispatch.

Chapter 6 Concludes by summarising the main research contributions and potential areas that require future work. Expanding the developed short circuit impedance methods for dynamic voltage stability monitoring, the application of active fault current level estimation and the incorporation of emerging reactive power injection models in VSCOPF will also be outlined for additional development and advancement of technology readiness levels of the developed techniques.

2. Literature review

This chapter reviews fundamental concepts and emerging practice of fault level management and monitoring and shows how the contributions made in this research and reported in this thesis address some of the future work requirements and identified shortcomings or areas for improvement in the reviewed concepts and literature. Limitations of existing offline short circuit study methodologies and standards will be discussed. Emerging fault management techniques and technologies will also be examined. Focus is attributed to topics associated with enhancing fault level management practice via fault level measurement and estimation.

This chapter also examines fundamentals of voltage stability analysis in the context of low system strength systems and identifies indexed-based methods as effective tools for static voltage stability monitoring. Focus on limitations of offline based tools in mitigating low system strength issues will be highlighted with index-based stability monitoring, one of the main contributions of this work, identified as a viable solution for online applications. This will be used as a springboard for the development of a static line-based index for steady-state stability monitoring in the context of weak networks where a line-based and bus-based stability index considering shunt susceptance parameters is later presented in this work.

Emerging activities in mitigating voltage stability in low system strength systems will be addressed with optimisation methods identified as a potential measure for system stability enhancement. Based on the developed static line stability index, voltage stability-constrained optimal power flow models are also presented in this research in latter chapters of this thesis. Section 2.1 reviews fundamentals of short circuit calculation methods and its short comings in model-based fault level management. Distribution network fault level monitoring methodologies and applications are introduced in sections 2.2 and 2.3 with a critical assessment of existing methods addressed. A review of fundamental concepts associated with steady-state voltage stability assessment and mitigation of low system strength systems are addressed in sections 2.4 and 2.5 respectively with short comings and limitations of existing index-

based methods discussed. A review of index-based and Jacobian-based VSCOPF methods will also be addressed.

A summary of the main research gaps identified in this chapter include limitations in existing parameter estimation methods for passive short circuit current estimation which have predominantly relied on ordinary least square methodologies. Short comings in modelling two bus equivalent static line indices which have historically neglected shunt susceptance parameters may further limit the accuracy of static stability monitoring capability. Limited concepts in deriving static line indices can be expanded through adoption of impedance matching theory for line index development. Improving the efficiency and performance of VSCOPF methods through adoption of simplified static based algebraic models of stability indices accounting for both series and shunt branch parameters for index evaluation.

2.1 Review of short circuit calculation methods

2.1.1 Voltage source method

The IEC60609 standard [9] outlines the procedures for calculating short circuit currents in three phase 50 Hz and 60 Hz systems through the voltage source method [8, 16]. In this approach an equivalent voltage source is introduced at the fault point. This voltage source is regarded as an ideal source applied at the fault location in the positive sequence domain and is the only active source in the system (all other sources short circuited). To account for network operating conditions[5, 8] including load flows, pre-fault voltages, transformer tap changers, etc., a c-factor multiplier is introduced to account for system voltage variations. Impedance correction terms are also introduced for transformers and synchronous generators based on statistical data and operating practice. The fault current is comprised of a symmetrical (periodic) and decaying (DC) component. With multiple sources of fault current injection, the total fault current is regarded as the vector sum of all sources in the network[8].

2.1.2 Superposition (complete) method

Relative to the voltage source method, the complete method [17] based on the ANSI standard accounts for system operating conditions through the application of a load flow to determine pre fault voltages. In weak network conditions it is assumed system load current is in close proximity to the fault current magnitude and is therefore also added to the fault current contribution (by superposition). This methodology reflects the true or operational fault currents without the simplified assumptions for short circuit calculation.

2.1.3 Limitations of offline model-based techniques

Sources of error in the IEC60609 standard [9] for example include the voltage c factor multiplier [7] to account for variations in system voltage and factor the influence of consumer load data, variation of inverter-based DG fault contribution with actual output levels, etc. There are factors not available to modellers which impact fault level studies [3] including the accuracy of models (EMT and RMS) which are dependent on both network measurements, impedance parameters, manufacturer data, etc. Distribution fault level infeed are also influenced by load fault level infeed, operational running arrangements, generation mix and technologies[7, 18] where not all information is readily available in real-time. Network models therefore do not readily provide a real-time representation of network fault levels which makes it more difficult to provide additional fault level headroom to facilitate increased low carbon DG penetration without costly reinforcement measures in constrained regions. Increased DG capacity connections therefore risk switchgear make and break limits and short circuit withstand capability being exceeded. Offline model-based methodologies for short circuit studies often result in conservative design limits being set, resulting in higher capital costs for plant installations [5]. There is therefore an increasing need for the development of measurement-based approaches [18, 19] to better reflect actual fault current levels and support active fault level management decisions and facilitate flexible DG connections through fault level monitoring. This can be achieved through active and passive methods where system perturbations are monitored and evaluated to obtain fault level measurements. This is further discussed in section 2.3.

Limitations in RMS and EMT based short circuit studies have been identified in mitigating low system strength issues including system stability, control interactions and converter instability. The application of RMS based fault studies are effectively positive sequence based which neglect DC, negative and zero sequence components [3]. Simulation programs also have large simulation time steps and may neglect responses from fast control loops and PLL controllers that are key drivers of instability modes in weak systems. The use of EMT programs utilise simplified generator models (neglecting dynamics of stator flux) which may lead to failure in detecting oscillations beyond 5 Hz [3] and other phenomena during weak system conditions. Close coordination between manufacturers and system operators may therefore be required to supply appropriate EMT models for stability and short circuit studies in converter dominated networks and improve network and IBG performance during low system strength conditions. Alternative to model-based strategies and associated shortcomings, online measurement-based enabled applications provide alternative means to address and circumvent high and low system strength challenges[18]. Short circuit current monitoring via estimation can therefore provide an effective tool in improving system operational challenges including fault level headroom bottlenecks and converter stability assessment in weak systems utilising measurement-based equivalent impedance methods. In this work, recursive least square methodologies are adopted to enhance existing ordinary least square passive fault current estimation approaches as parameter estimates are recursively updated with new perturbation events identified and will be discussed in latter sections of this thesis.

2.2 Review of fundamentals of measurement-based fault level estimation

2.2.1 Passive methods

Fault level measurement involves short circuit impedance estimation following small downstream load changes that initiate changes in voltage and current, from which an estimate of the source impedance (coupled with other known system impedances) can be derived to estimate fault levels – weaker systems will generally be more perturbed (in terms of relative changes in system voltage) in response to a change in load. At a

given monitoring location, reducing the system to a Thevenin equivalent allows direct estimation of system Thevenin or short circuit impedance and prospective fault current levels [20, 21]. With measurements of voltage and current obtained before and after a load change with subscripts taken as 1 (before load change) and 2 (after load change) respectively, the following equation applies:

$$Z_{sc} = \frac{\overline{U_2} - \overline{U_1}}{\overline{I_2} - \overline{I_1}} \tag{2.1}$$

Where $\bar{U} = U_{Re} + jU_{Im}$ and $\bar{I} = I_{Re} + jI_{Im}$ are the measured complex voltage and current phasors respectively. Sources of measurement errors include measurement drift as a result of fundamental frequency variation, where time synchronisation is frequently utilised to compensate for phase angle shift.

Several disturbances occurring over a period of time are typically detected (<0.5% voltage change [18, 22]) and stored for accurate fault level estimation through statistical processing of measurements. This includes the use of frequency distributions [20] and ordinary least squares [19]. Passive approaches require continuous monitoring and collection of multiple load events prior to estimation and may be limited to offline applications. Without the need to introduce external equipment for active disturbance provision, passive methods provide cost effective solutions for several applications including network model validation, remote monitoring in poorly instrumented regions, grid code (G59) compliance [7], etc.

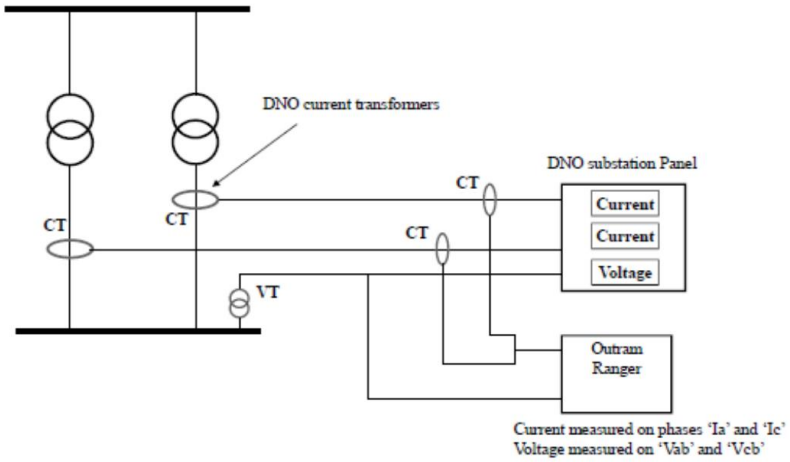

Figure 2.1 Fault level monitor connection schematic in a distribution substation [23]

An illustration of a fault level monitoring device connection is shown in figure 2.1. In this arrangement, the FLM directly interfaces with secondary substation monitoring systems with access to the primary instrumentation measurements (CTs and VTs). The Outram ranger component provides fault level estimation results for three phase systems in radial and interconnected sections of the network [23]..The FLM is connected to the secondary distribution transformer in a radial section of the network. A downstream change in load would initiate changes in current and subsequently voltage, providing upstream fault level information [23] through source impedance estimation (from equation 2.1). The FLM is required to distinguish between upstream and downstream disturbance sources in order to obtain the correct voltage and current signatures to perform estimation.

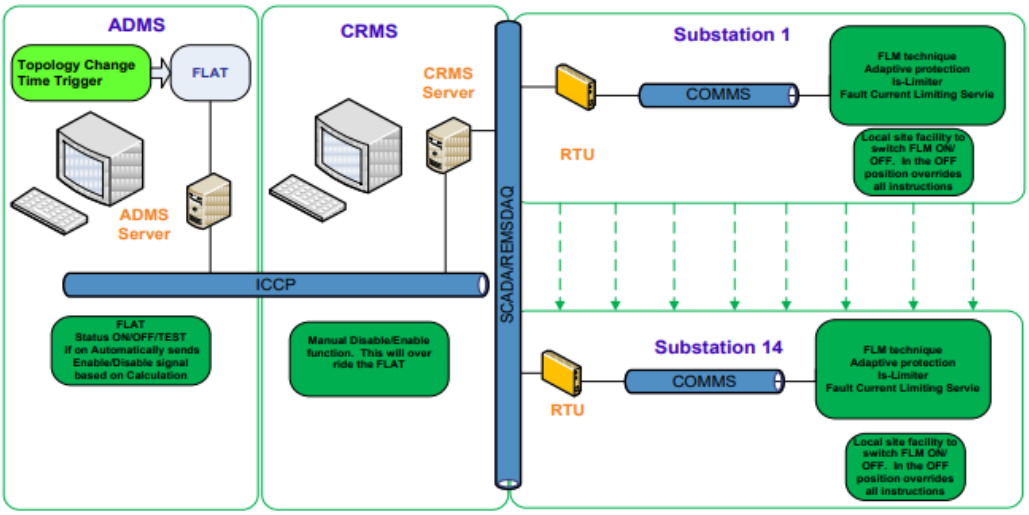

Figure 2.2 Active fault level management scheme via real-time FLM [24]

An application of FLM used to initiate fault level mitigation techniques is shown in figure 2.2 [24] with interface achieved through the automatic distribution management system (ADMS). This tool [24], integrated at the network management system (NMS) level, monitors network fault levels to check circuit breaker capacity (headroom) against actual network conditions in order to enable/disable mitigation functions (I_s-limiters, adaptive protection, fault current limiting). If monitored fault level is identified as exceeding circuit breaker switchgear fault level rating, the NMS sends a signal to the control room management system (CRMS) to enable a fault level mitigation measure via an Inter-control Centre Communication Protocol (ICCP) link.

Substation RTUs process control and status signals between on-site mitigation equipment and the ADMS in addition to CB switch status of monitored sites in the network model. This arrangement may be limited to active management applications to enable mitigation functions which may be costly for passive monitoring as no real-time mitigation strategies (fault current limiting, adaptive protection) can adopted. This may be suitable for MV applications as the introduction of active disturbances at HV may require additional power quality mitigation actions and resources to reduce impact on power quality. Discussion of the various fault level mitigation techniques will also be covered in the next section to summarise applications of short circuit monitoring in the context of fault level management of distribution networks under high DER penetration.

2.2.2 Active methods

In order to provide real-time fault level measurements [5], as opposed to aforementioned methods that rely on building up an estimate over time through analyses of several load changes and the subsequent system response in terms of voltage levels, the introduction of controlled external disturbances can achieve the desired functionality. Recent efforts utilise pulse closing technology [25] (see figure 2.3) and inductive load banks [26] for active disturbance provision. In the arrangement shown [5], a transient line to line fault is switched on to the network to generate the desired active disturbance via the pulse closer. Point on wave switching is utilised to minimise the impact of fault current magnitude on power quality by controlling the instant in which the fault is switched on to the network. Active FLM therefore facilitate real-time monitoring and visibility of network fault levels and support active fault level headroom management enabling flexible DG connections. Active methods therefore provide means to cost effectively increase renewable penetration without delayed network reinforcement and installation of fault current limiting devices as available headroom is monitored in real-time. A shortcoming of this approach however is the additional cost of equipment installation which may increase at higher voltage levels in addition to the introduction of power quality issues. Wide area monitoring of fault levels [26] using active methods also increase cost of infrastructure deployment and integration with existing systems.

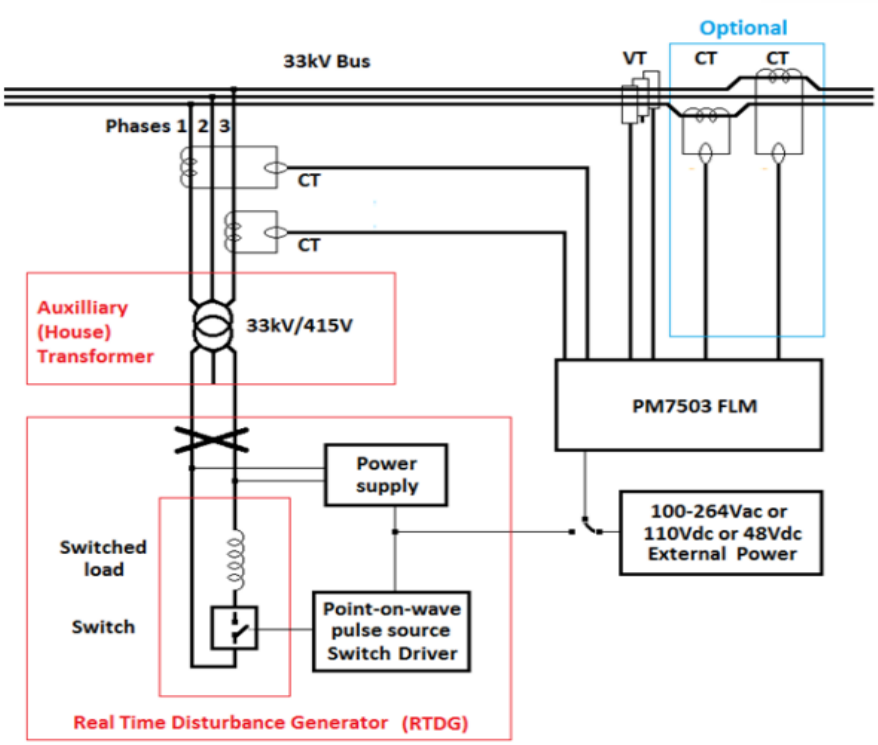

Figure 2.3 Active disturbance provision utilising pulse closing and point on wave switching [5]

2.2.3 Review of existing passive and active short circuit current measurement methods

An approach in [20] developed in 2003 proposes a portable PC-based instrument to derive phasor information from samples of voltage and current and extracts the complex fundamental components to estimate the equivalent short circuit impedance. Measurements are acquired at each cycle at a sampling rate of 1.6 kHz (32 measurements per cycle) and the equivalent Thevenin source impedance is obtained from the ratio of the difference in voltage and current (see figure 2.4). The approach makes use of a 12-bit, 8 channel ADC board where first harmonic components are calculated and sent to disk for post processing (in MATLAB) using DOS programming. Multiple case studies are investigated at various voltage levels including a 132 kV transformer feeding a rolling mill, a 400 kV AC/DC converter station where a 113 MVAr filter is switched to initiate a downstream perturbation and a 230V socket connecting a laser printer. A 5-minute measurement period is utilised

for the 132 kV and 230 V switching events with histograms used to extrapolate impedances whilst manual analysis of one-off events is employed for the 400kV perturbations. The approach makes use of a time synchronisation algorithm to deal with time varying frequency and associated phase errors introduced. The accuracy of the method strongly relies on accurate estimation of the changes in voltage phasors which are a function of both amplitude and phase angle. To overcome potential errors, time synchronisation is utilised for improved precision in obtaining phase angle differences between disturbances assuming slowly-varying system frequencies. With increased penetration of inverter interfaced generation, overall system inertia is seen to decline. The intermittency of renewable sources further exacerbates the assumption of slow varying grid frequencies following disturbances and high inaccuracies may be introduced during steady-state perturbation measurements. The performance of the time synchronisation mechanism may therefore be compromised in low inertia systems due to increased system frequency variability and higher ROCOFs which may impact estimation performance. The method also relies on statistical analysis of frequency distributions using histograms to reliably obtain numeric estimates of the short circuit impedance. This approach requires a large number of events to reliably determine an impedance value and relies on one-off estimates for each disturbance to quantify system fault levels. With disturbances occurring of various magnitudes, the approach is prone to measurement errors and may not reliably identify short circuit impedance for a finite number of events. For the 132 kV outlet between 1000-1500 events are collected, implying the approach relies on the statistics of multiple events due to small changes in system voltage during events [20]. Improvements in the statistical estimation processes may therefore be desirable to improve the efficiency and performance of the estimation.

Obtaining Thevenin impedances and equivalent source voltages through estimation of covariances of voltage and current following load perturbations was addressed in[21]. The approach makes use of power quality monitors to identify the level of voltage deterioration for voltage performance enhancement near industrial customer sites (e.g. saw mills). The method derives quantities from the Thevenin equivalent model through statistical analysis of voltage and current variations over a given time period. This includes monitoring the number of occurrences of measured impedances to construct

frequency distribution and histograms to reliably determine impedance estimates. This may require the collection of a large number of events (e.g 100 events) which may not be feasible for all monitoring locations and voltage levels and may only be suitable for power quality applications where monitoring interval periods are non-critical. The method also requires the occurrence of multiple load events (typically <0.5% voltage step) to accurately determine covariances in addition to short circuit impedance estimation which may not be reliable for online applications as a relatively large number of events are required to be obtained for both estimates. Low inertia networks may also introduce high frequency variations during disturbances which may cause large phase angle errors which compromise the accuracy of measured voltage changes as no time synchronisation is utilised.

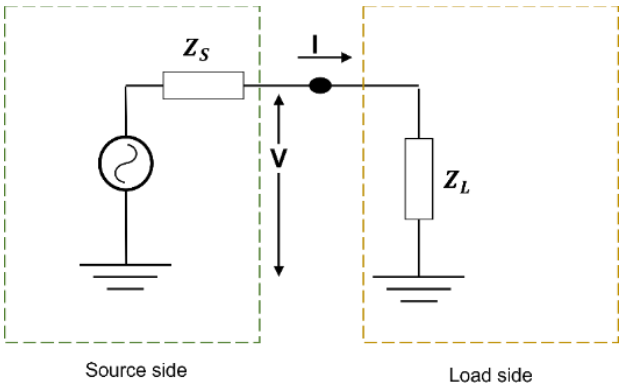

Figure 2.4 Simplified power system Thevenin equivalent model

Recent efforts have aimed to account for downstream distribution connected generation fault levels in addition to upstream grid fault contribution. A method in [19] proposes an online least squares model to simultaneously quantify both upstream Thevenin equivalent and downstream parameters from the equivalent circuit. This method assumes downstream generation fault contribution as a function of DG current rating and utilises an overcurrent multiplier to account for inverter-based fault current infeed. The method also aims to extract useful disturbances through the application of fuzzy logic identifiers to determine the confidence level of weighted measured disturbances.

The approach proposes the use of installed PMUs for high precision measurements or protection relays to implement the algorithm and therefore no additional monitoring infrastructure is required for estimation. A major short coming of this method is that it

is passive in nature and therefore cannot be utilised for real-time applications and may require additional hardware installed for active disturbance provision. The method assumes downstream DG fault contribution is wholly supplied from inverter connected DG as the employed overcurrent multiplier assumption as a function of rated current does not hold for induction generator and synchronous based sources.

The method also assumes a constant current representation of the DG source and does not consider phase angle of the current required for vector summation of upstream and downstream fault level contributors (algebraic summation only). With downstream DG fault contribution sourced from multiple generation technologies, fault current as a function of DG rating i.e. multiplier concept may not accurately represent downstream fault contribution. Load fault infeed is also not accounted for in the approach.

In an effort to address some of the previous short comings, an active, real-time short circuit measurement approach is discussed in [26]. This method proposes use of a linear regression model to correlate active (inductive load bank switching) and passive (natural load perturbations) measurements to predict missing data between naturally occurring events. Equivalent Thevenin impedance is quantified using the conventional approach and the introduction of an inductive load bank is utilised for controlled active disturbance generation for real-time estimation.

A shortcoming of this approach is that it assumes the availability of passive measurements at the 132 kV, 33 kV and 11 kV busbars which requires the fault level monitoring be centralised in order to retrieve monitored parameters at various measurement locations for estimation. With fault level constrained locations occurring at limited areas in the network e.g. high DG capacity installation regions, adoption of a centralised methodology may impose high cost of integration with existing infrastructure (e.g. substation and NMS communication infrastructure).

Active disturbance provision costs are a function of the voltage levels which require higher equipment ratings for resistive/inductive load bank installation which may not be economically feasible. The minute-by-minute switching of banks for active disturbance injection may cause power quality problems and introduce voltage performance issues particularly in long radial feeders which may impose additional

costs for voltage management. The method similar to the previous approaches employs statistical analysis methodologies for short circuit estimation but rely on collecting several one-off events to construct least square models.

From the above review [27], it can be deduced that improvements in the efficiency and performance of the statistical estimation methods and models may accelerate the provision of impedance estimates. Reliance on frequency distributions and ordinary least square regression models may be infeasible for passive monitoring in various network locations and voltage levels as a large number of events and measurement intervals are required for accurate estimates at acceptable confidence levels. Utilisation of recursive methodologies may further accelerate and improve upon existing estimation processes and is addressed in latter sections of the Thesis. Recursive least square modelling may enhance estimation performance as estimates are continuously updated via gain vectors and sum of square of errors continuously minimised following identified perturbations and measurements. In this regard, a passive recursive least square (RLS) estimation approach is proposed in this work for enhanced short circuit current measurement utilising a novel perturbation coefficient technique.

2.3 Review of fault level monitoring enabled mitigation and management techniques

As previously described, fault level monitoring facilitates the application of active fault level management functions in real or near real time conditions. This further supports flexible DER connections without the immediate need for additional infrastructure deployment and reinforcement. This includes network model validation in poorly instrumented region [7], network splitting and reconfiguration and adaptive protection. A brief outline of fault level monitoring enable management techniques is described in the next section

2.4.1 Network splitting and reconfiguration

A common approach to reduce the upstream fault level impact to support flexible DG connections is through network reconfiguration [27, 28]. Two network splitting arrangements are shown in figures 2.5 and 2.6 [27]. Assuming a fault occurring at the transformer incomer, the normally closed bus section circuit breaker can be opened thus increasing the upstream impedance path between the upstream grid and fault point hence reducing the fault current infeed.

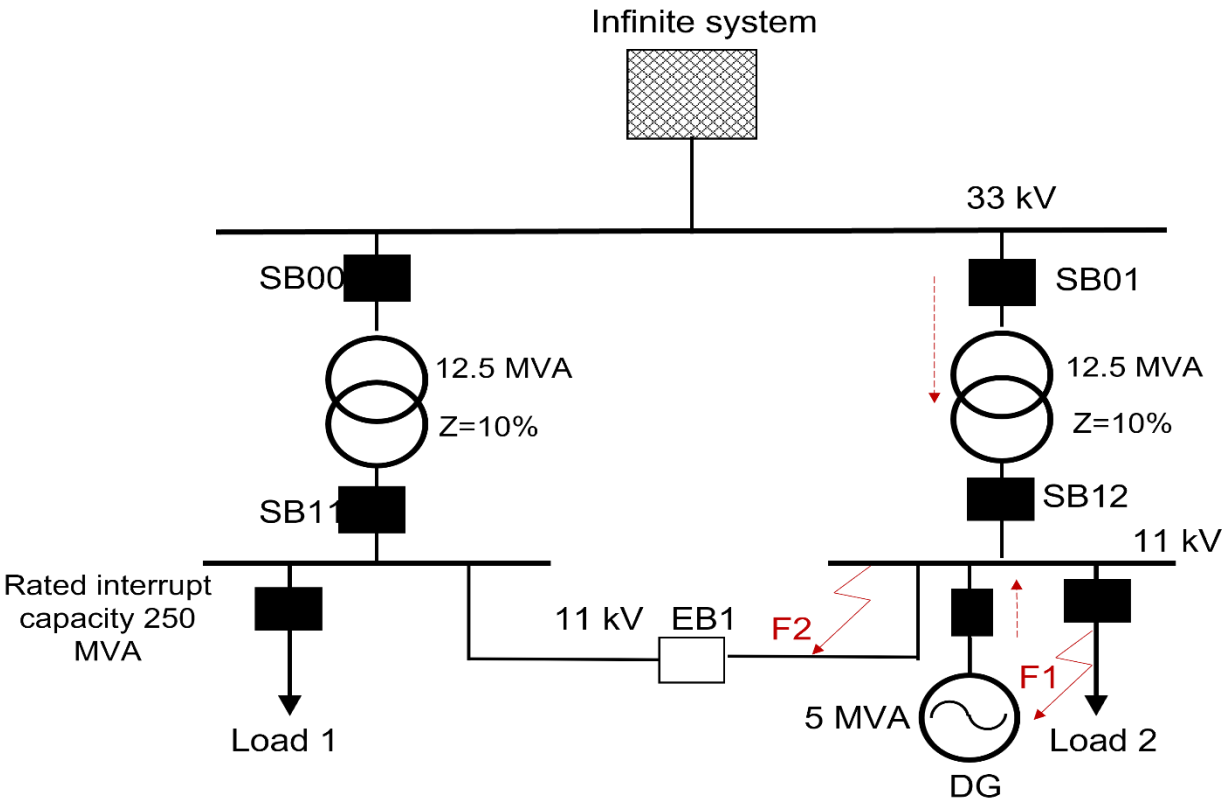

Figure 2.5 Network splitting arrangement for upstream fault level reduction

By splitting the network through opening of EB1, the impedance increases from 5% to 10%, reducing the magnitude of the fault current from the 33 kV network. An alternative (figure 2.6) arrangement may require the installation of an additional breaker (EB2) to transfer the DG and load connection from one bus to another after fault clearance (at F3) improving network flexibility and safety. During normal operation, breaker EB1 is normally open separating the 11 kV buses and is closed following a fault at the transformer incomer.

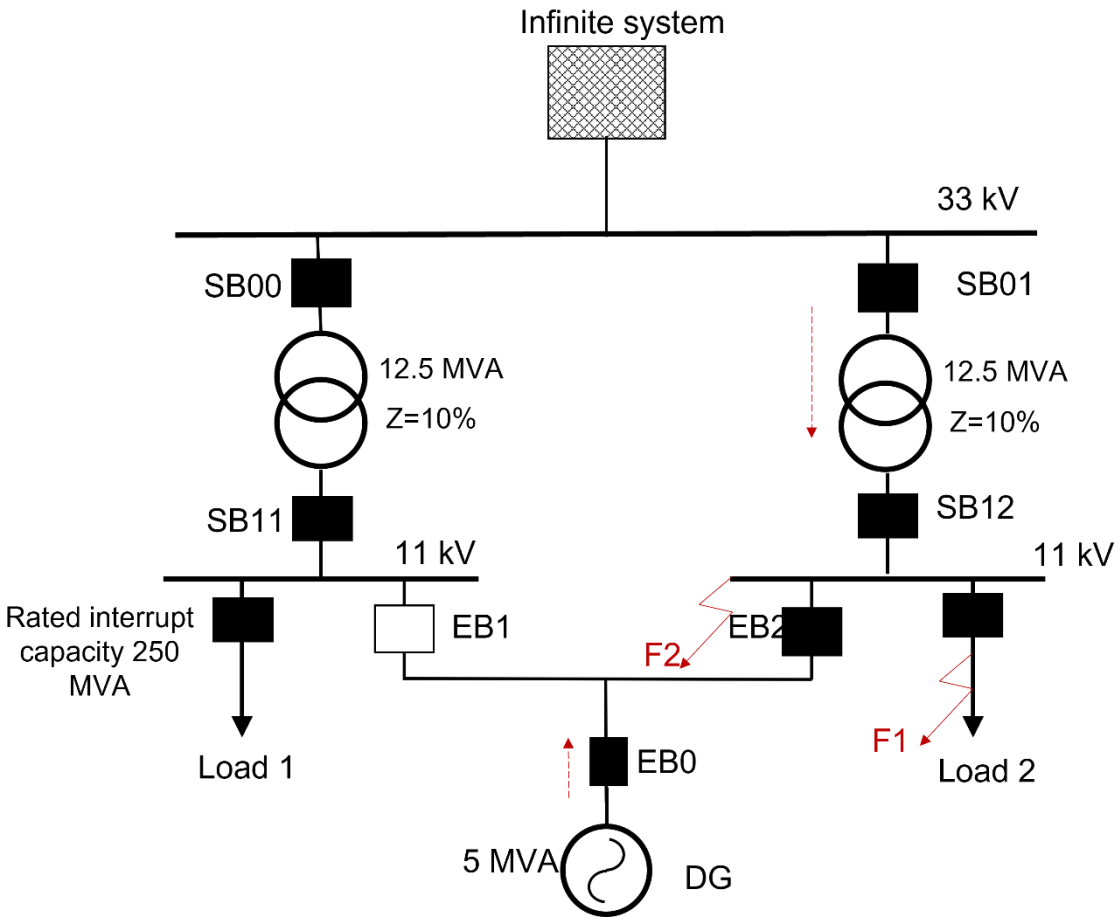

Figure 2.6 Alternative network splitting arrangement through bus sectionalsing

2.4.2 Adaptive protection

Recently-adopted techniques for fault level management make use of fault level monitoring and adaptive protection [29, 30] (AP) methodologies. In this approach, the network is split through resequencing of circuit breaker switching thus actively managing system short circuit capacity in constrained regions. This approach has been trialled for both radial and closed ring

network topologies [30]. For a radial network (figure 2.7) the AP operates using a two-stage arrangement with stage 1 tripping the bus coupler allowing each bus section to be supplied by a single transformer reducing upstream fault current. In the event of protection failure, a second stage is adopted to trip out the transformer LV breaker after

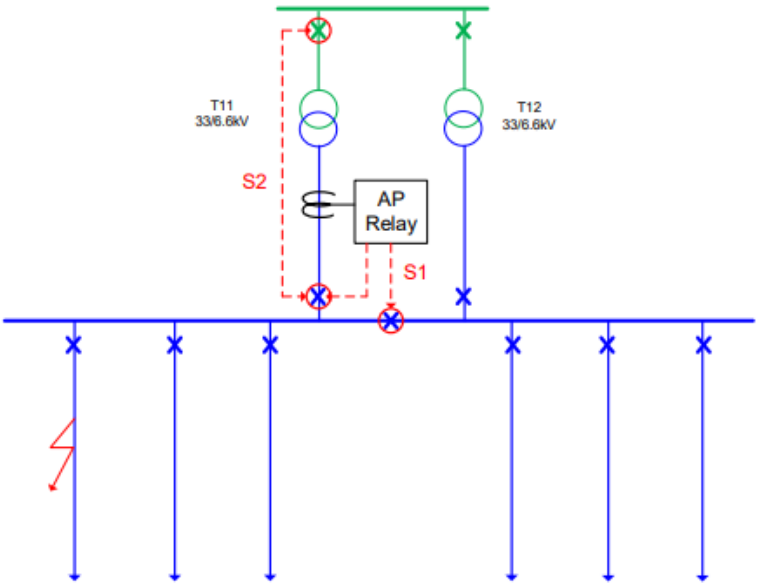

Figure 2.7 Two stage adaptive protection scheme for fault level management in a radial network

200ms, thus splitting the transformer parallel connection. In the closed ring arrangement (figure 2.8), both the ring feeder and bus coupler breakers are tripped splitting the parallel path between the bus sections. Upstream fault infeed is thus reduced as each section is supplied by a single transformer. Similar to the radial configuration a second stage is adopted in the event of a stage 1 failure to open the transformer breakers. Alternative to a real-time fault level input to the AP relay, a CT is installed to measure upstream conditions and trips instantaneously if a fault is detected based on a pre-set threshold. The AP relay operates in advance of the other protection relays with existing relay settings not altered to achieve measurement based active fault level management functionality.

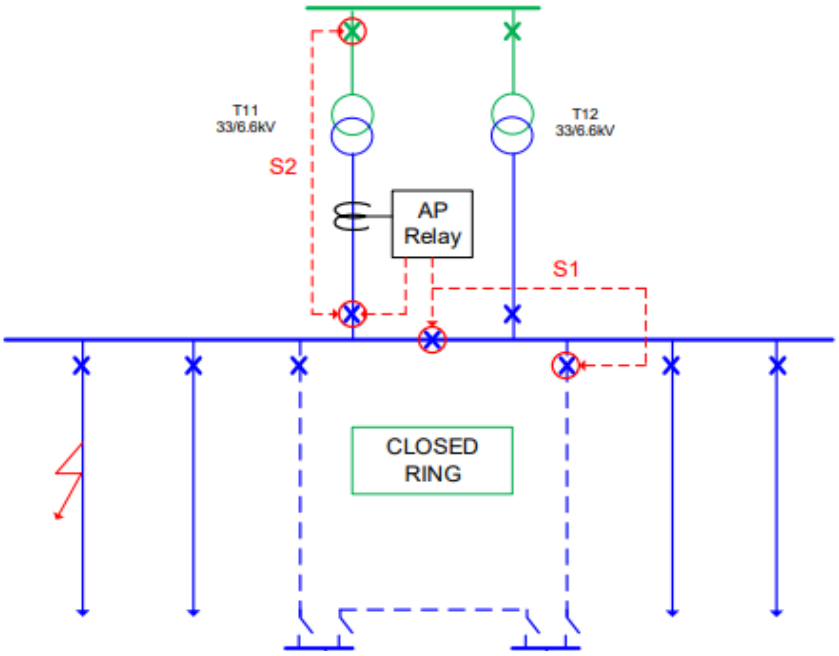

Figure 8

Figure 2.8 Closed ring adaptive protection scheme for fault level reduction

2.4.4 Active and passive flux discharging

A newly developed fault level mitigation technique that aims to reduce downstream fault infeed magnitudes and maintain short circuit headroom capacity make use of advanced voltage regulation and machine excitation control. This has been considered effective in reducing short circuit infeed magnitude of synchronous based DG. The approach involves temporary disconnection of a machines excitation system in order to reduce the flux linkages (maintained by the excitation voltage) involved in supplying fault current thereby reducing the fault contribution of a machine for a sustained period. Different methodologies have been trailed in regulating generator excitation during a fault for effective fault level management. This involves sudden disconnection of the field circuit to reduce the fault current magnitude supplied to the system.

Passive flux discharging (shown in figure 2.9) involves disconnecting the excitation system that maintain the flux linkages causing an overall fault current reduction of 9%. This involves disconnection of the field winding of the generator following fault detection reduce the magnitude of the break current supplied by the unit. The general

effect of passively disconnecting the generator's excitation system is to accelerate the rate of discharge in the field windings (and hence flux linkage) thereby reducing the overall fault contribution. This approach does not reduce the initial peak fault current and mainly impact breaking fault current infeed.

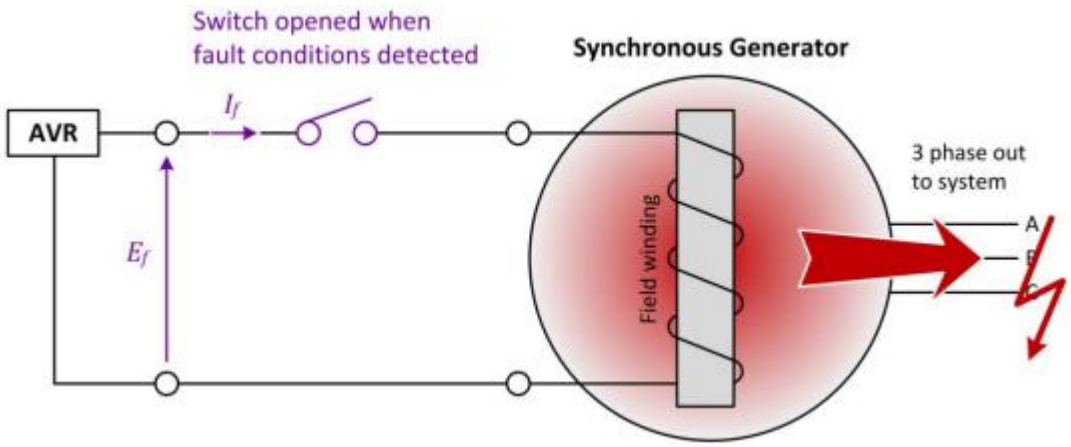

Figure 2.9 Passive flux discharging of a synchronous distributed generator

Similar to the passive flux discharge arrangement, active flux discharging adds an additional parallel switch and resistor to accelerate and increase the discharge process as illustrated in figure 2.10. The additional branch is switched on fault inception to connect a resistance in series with the field winding. This effectively causes a faster rate of decay of fault current in the machine. A 25% reduction in breaking fault current is achieved however implementation of this scheme is costly and complex as the technique cannot be retrofitted and requires alteration of the excitation system design.

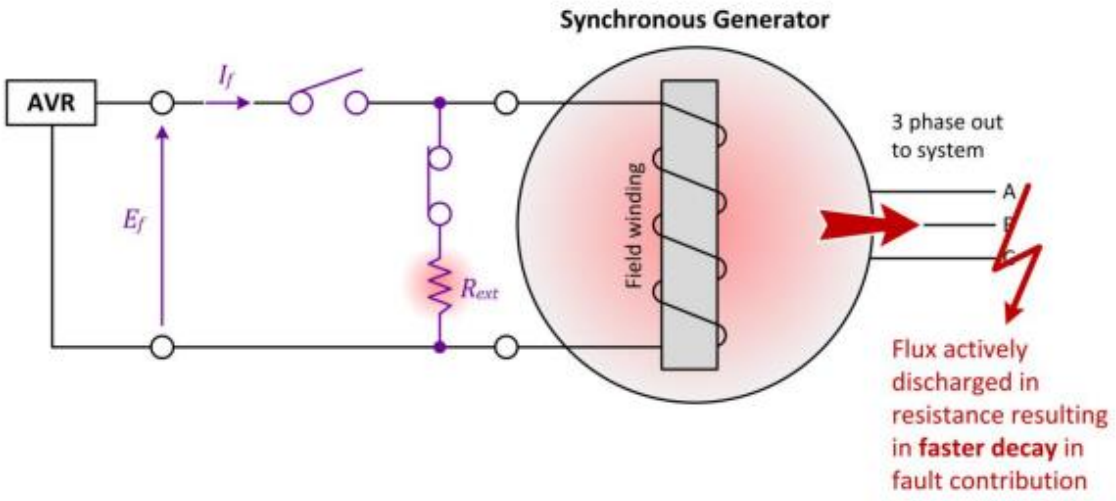

Figure 2.10 Active flux discharging of a synchronous generator using resistive parallel switching

Active flux discharging generally aim to further reduce the magnitude of the fault contribution by introducing a parallel switch and external resistance parallel with the field winding in order to further impact the flux decay occurring in the generator during the flux discharging process. This involves dissipating the field voltage across the resistance which greatly reduces the fault contribution by the generator as the flux linkage developed at the windings decay at a much faster rate as a result of the dissipation or the drop in the excitation voltage across the generators excitation circuit. Tests involved have so far shown an approximate reduction of 25% in the overall break current contribution of a synchronous generator which has shown the effectiveness of this method in reducing or managing the fault contribution of generators. The main disadvantage of this approach is the general need for advanced machine excitation which can be regarded as costly and complex and cannot be retrofitted into existing systems without altering the excitation system design. Fault level measurement enabled mitigation functions (adaptive protection, fault current limiting) may therefore be more effective in active management of available headroom relative to flux discharging methodologies.

2.4 Review of fundamentals of voltage stability assessment

2.4.1 Introduction

Voltage stability phenomena can occur as either dynamic or steady-state instability. Dynamic voltage stability occurs following system events and disturbances and is related to the inability of the system to control and maintain bus voltages within permissible limits across the network [31]. Steady state instability arises when gradual small disturbances in the network moves the system to a critical operating point where the network is unable to sustain a steady-state condition following additional load increase[32, 33]. Different analysis methods and tools have been developed to analyse static [12, 13, 34-37] and dynamic instability [38-41]. The focus in this thesis is the identification and monitoring of steady-state voltage instability using static, index-based methodologies.

With increasing complexity in planning and operating weak power networks under high penetration of power electronic interfaced generation [3, 4], voltage instability conditions are of increasing concern [11] . Low system strength systems and weak grids increase the risk of voltage instability due to insufficient available resource to maintain the system within a stable steady-state operating envelope. Weak networks result in high sensitivity of active and reactive power to changes in voltage magnitude which increases the risk of voltage collapse. During periods of high power transfer and fewer online synchronous generation, large voltage drops are seen across the network as the reactive loss is proportional to the square of the current, lowering system voltage and reducing available margins and loadability [3].

A number of voltage stability issues have been identified in networks during weak grid and high penetration of renewable conditions. The Bonneville power administration (BPA) area in the US for example have experienced steady-state instability under high wind power park (WPP) penetration. With a WPP (operating in power factor control mode) connected to the midpoint of a long 230 kV transmission line, in a relatively weak part of the network, high active and reactive power sensitivities were observed [3]. During a wind ramp up, the network had experienced voltage collapse with the event analysed using classical PV analysis [38].

The southeast of England has seen a significant increase in the penetration of wind and solar generation and costs of maintaining transmission voltages in the southeast region has been exponentially rising with bulk power transferred to major demand centres. The electricity system operator National Grid ESO (Electricity System Operator) has identified voltage instability conditions in the event of a double circuit fault in the route between Canterbury and Kemsley leaving one radial route to deliver bulk power to London and other demand centres [11, 42]. This resulted in the need to limit prefault power flows to avoid system voltage collapse, resulting in increased financial implications to cap power exports from renewable sources and requiring additional reactive resource to remain online (to manage system voltages). The ESO proposes utilisation of distribution connected DER capability through a DER reactive power service to support emerging weak network constraints. By implementing the proposed control solution in 19 voltage zones in the GB transmission system, an overall saving of £96m could be achieved by 2050 [11].

The development of voltage stability monitoring and mitigation solutions may therefore address emerging weak network issues (e.g. steady-state voltage instability) and is the motivation in this work. The next section summarises common voltage stability assessment methods and emerging mitigation measures currently being adopted by network operators.

2.4.2 PV and QV curves

A common approach for static voltage stability assessment [43] is through power-voltage (PV) analysis. System loading is increased in steps with bus voltages monitored at each step until voltage collapse is reached. During low loading conditions, the active power gained at the bus (receiving end) dominates over the voltage drop to satisfy the active power demand increase. A slow decline in system voltage is experienced in this region (see figure 2.11). As system loading is further increased, a proportional increase in the magnitude of the voltage drop across the system is observed and a faster decline in system voltage occurs [43, 44]. At the critical condition, this drop becomes equal in magnitude to the receiving end bus voltage (critical voltage) and voltage collapse occurs (knee point of the curve). This satisfies

the maximum power or impedance matching condition where system impedance equates the load impedance at the studied bus[44, 45]. Various types of reactive compensation devices (shunt capacitors, STATCOM, SVCs) can further enhance voltage stability performance. This can be illustrated in the PV curve by achieving higher knee point values and critical voltages i.e the nose curve is shifted to a higher critical loadability position in proportion to the MVAR injection via compensation.

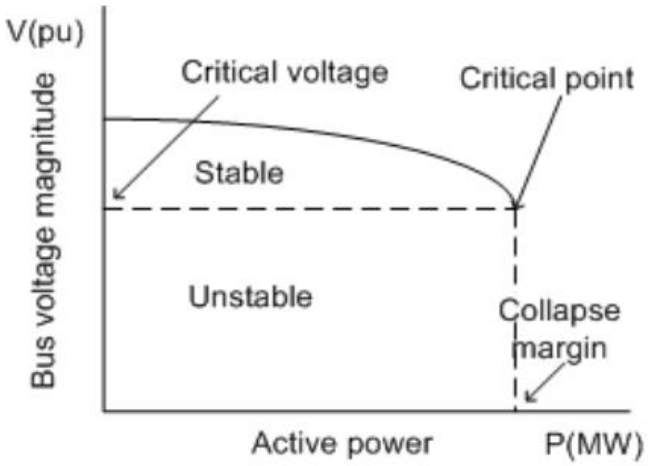

Figure 2.11 Power-voltage (PV) curve

QV curves study the relation between the reactive power injection and bus voltage and is used to determine the maximum reactive load a bus can sustain before system voltage collapses. The curve traces what a given bus's voltage would be as MVAR load increases at a given loading margin as shown in figure 2.12 and is useful in identifying reactive sensitivities[31, 43]. This tool is also useful in identifying reactive injection requirements to avoid voltage instability.

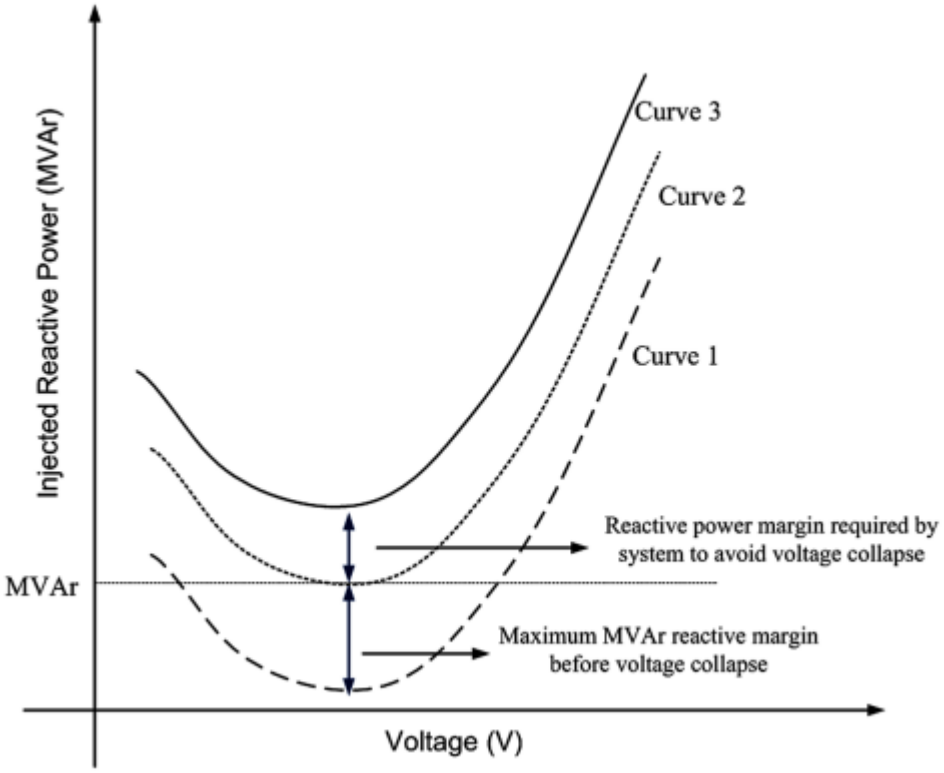

Figure 2.12 Determination of reactive power margin requirements using QV curves

2.4.3 Continuation power flow

A well-established Jacobian-based voltage stability assessment method is the continuous power flow[46, 47,48] approach based on branch tracing methodologies. In this approach, the power flow nonlinear equations make use of local parameterisation techniques to reformulate the load flow equations. A load factor λ is added to implement a load change step in the load flow simulation and is described using

$$P_{L\,i}=P_{Li\,0}+\lambda(K_{Li}S_{base}\cos\theta_i) \tag{2.2}$$

$$Q_{L\,i}=Q_{Li\,0}+\lambda(K_{Li}S_{base}\sin\theta_i) \tag{2.3}$$

$P_{L\,i}Q_{L\,i}$Where $P_{Li\,0}$and $Q_{Li\,0}$ represent the active and reactive loading at the initial or base loading condition, K_{Li} is a multiplying factor representing the rate change of increase in load , θ_i is the power factor angle and S_{base} is the chosen MVA power used to scale λ with respect to the base case condition.

The continuation power flow (CPF) approach make use of a predictor-corrector step (figure 2.13) to identify a prediction of the next solution and locating the next curve point by correcting the prediction. The technique therefore identifies the location of the solution with respect to the preceding solution. The predictor step estimates the next solution with the step size tangent to the solution path (tangent vector). The correction step corrects the approximation of the predictor estimate of the modified power flow equations. Throughout this thesis the CPF method is utilised to perform static voltage stability assessment and derive developed stability indices at a given operating point and at critical loadability (knee point). Under stable normal conditions, the system operating point varies with system loading (λ) and can be tracked using linear analysis techniques. At the knee point, the system becomes non-singular and is said to reach a bifurcation condition where linear analysis methodologies no longer hold and predictor-corrector CPF analysis is required to trace the PV curve beyond the knee point.

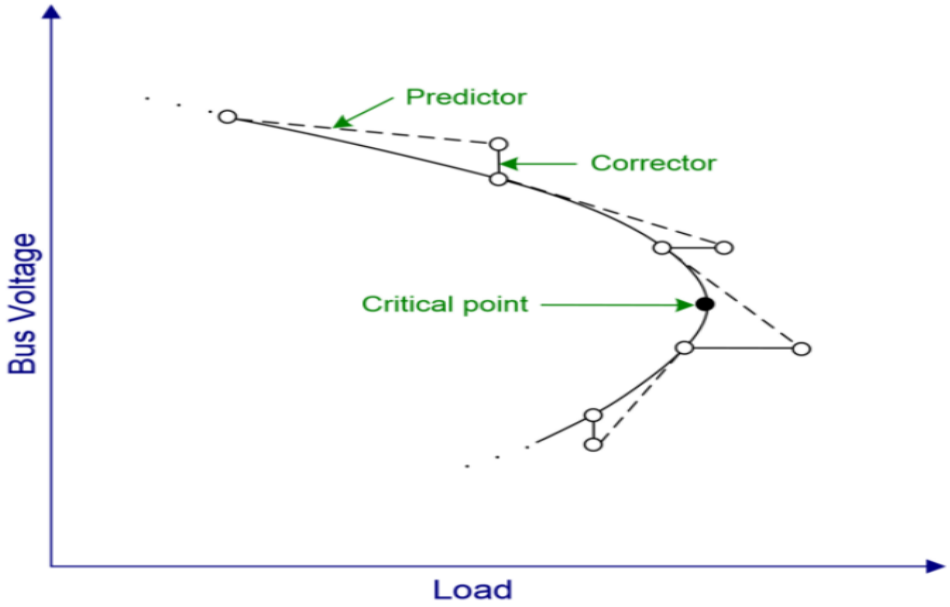

Figure 2.13 Continuation power flow predictor-corrector solution approach

2.4.4 Index based methods

In an effort to improve the computational efficiency of voltage stability (VS) analysis methods, the use of static techniques utilise stability indices for VS assessment [12, 49]. This is employed predominantly in steady-state analysis procedures. As steady-state network models are employed, index-based approaches are useful in identifying

critical lines and weak buses in the system but may be less accurate in calculating stability margins and dynamic/time domain approaches may be required for improved accuracy [59]. As steady-state network models are employed, VSIs can broadly be categorised into Jacobian and system variable based approaches using bus and line-based indices [31] . Jacobian based methods [50, 51] for example have relatively high computational times and utilise dynamic models whilst variable based methods model voltage stability as algebraic equations improving computational efficiency enabling its application in online/real-time environments. Stability indices have been utilised in applications including DG sizing and placement[52], allocation of reactive compensation (capacitors, FACTs) [53], system planning and applications involving countermeasures against instability [54, 55] (Stability-constrained OPF).

A simple two-bus representation of a power system can be used to study the voltage collapse point characteristics of VSIs [36, 56]. A power-voltage quadratic equation is derived from the real and reactive power flows in the model and at the collapse point, the Jacobian matrix becomes singular and the voltage equation have two pairs of real roots [13, 36]. Any further increase in load creates real and imaginary parts and the roots become complex. Alternatively, when the discriminant of the voltage equation is positive, then the system is regarded as stable. At maximum loadability, this discriminant is equal to zero and the system is said to have reached a critical state. Several static VSIs have been developed from this two-bus representation. This maximum or critical loading condition is explained by equation (2.4) below [36]:

$$V_R^4 + 2P_R + (2Q_R X - V_S^2)V_R^2 + (P_R^2 + Q_R^2)Z = 0 \qquad (2.4)$$

2.4.5 Modal analysis

This method, based on a reduced Jacobian matrix, assumes the system is voltage stable if there is an increase in bus voltage magnitude with a reactive power injection at each bus. The system is therefore regarded stable with a positive Q-V sensitivity and unstable if there is a negative Q-V sensitivity for at least one bus [57]. An underlying assumption in this approach considers the incremental relationship between Q and V at different operating conditions, keeping P constant. The Jacobian matrix is reduced to:

$$\Delta Q = (J_{QV} - J_{Q\theta} J_{P\theta}^{-1} J_{PV}) \Delta V = J_R \Delta V \quad (2.5)$$

This is then decomposed (orthogonal decomposition) to the following expression:

$$\Delta V = \zeta \cdot \Lambda^{-1} \cdot \eta \cdot \Delta Q \quad (2.6)$$

Where ζ, η are the right and left eigenvectors for matrix J_R and Λ is the diagonal eigenvalue matrix. The system is regarded voltage stable if all the eigenvectors values remain positive[57].

2.5 Review of existing static stability indices for voltage collapse prediction

As previously described, the application of voltage stability indices has been utilised for static, steady-state voltage stability monitoring and has gained increasing attention in several power system applications. This includes DG and FACTs placement and sizing problems [58], security-constrained OPF preventive action initiation [59] and for identification of weak lines and buses during critical loading and system contingencies [60]. Several classifications have been identified for static indices including bus-based and line-based indices, system variable and Jacobian-based indices in addition to classifications regarding the concepts to which the indices are derived including impedance matching theory, solution of the power and voltage quadratic equations, Jacobian matrix non-singularity and maximum power transfer. The authors in [12] provide a substantive overview of developed static stability indices available in the literature.

Evaluation and comparison of the performance of multiple line-based indices using real-time digital simulation (RTDS studies) have been discussed in [34, 56]. The authors identify several quantitative measures for comparison to assess index performance including last value prior to voltage collapse, first value following instability, index linearity at the stable region (using R^2) and rate of increase. The purpose is to develop a statistical model for future prediction based on the linearity of the index. As the power-voltage characteristic of a bus with increased loading is nonlinear with the rate of voltage magnitude decline high at low loading and exhibits a slow rate of decline during high loading (large system voltage drops), the behaviour of the indices may consequently exhibit nonlinearity. The index characteristic of the

bus is also dependent on the equivalent system impedance seen by the bus [39], the load impedance magnitude and load type, which may be unique for each bus in the network, may result in varied levels of linearity for multiple buses. This may therefore compromise a predictive model based on assumed index linearity of a bus or line. Other dynamic characteristics of the system my influence index characteristics including generator automatic voltage regulation (AVR) action, reactive capability (curves) of online generation and location of reactive injection sources (STATCOMs, static var compensators (SVC), etc.).

Recent efforts make use of PMU monitoring to predict voltage collapse in real-time through measurement-based stability indices. The authors in [35] identify several bus-based stability index methods suitable for real-time applications including impedance stability index (ISI), transmission path stability index (TPSI) based on a voltage phasor concept and a voltage index predictor (VIP). The majority of the studied indices are based on the same theoretical formulations and concepts (PV curve knee point [43]) which yielded similar performance attributes in terms of voltage collapse prediction. It should also be noted there has been limited development of line-based indices based on impedance matching concepts as they have been predominantly utilised in bus-based stability indices. Therefore, there has been limited performance evaluation of line stability indices based on varied theoretical concepts, with impedance matching based line indices having limited development in the literature. A static line index based on impedance matching theory is presented in this work and is addressed in later chapters of this thesis.

Several line-based indices have been developed in the literature for instability identification based on quantifying the determinant and solving the power and voltage quadratic equation derived from load bus active and reactive injections [56, 59, 60]. Developed indices include fast voltage stability index (FVSI) [36], line stability indices, L_{mn}, LQP [59, 60] and the voltage collapse proximity indicator (VCPI)[59] which have been extensively studied and utilised in various power system applications [56]. These indices have been derived from a simplified two-bus equivalent model which neglect shunt branch admittance parameters in the assumed equivalent model. Transmission line charging and susceptance effects may impact voltage stability

performance due to the local reactive injection inherently provided. This may impact index values for different types of indices due to the localized reactive support provided. For example, the LQP index developed in [59] is dependent on the reactive power flow of a line which may vary based on shunt parameter magnitudes at a given operating condition and may therefore exhibit compromised accuracy. Considering shunt branch admittances may therefore improve accuracy of developed line stability indices as they have predominantly been neglected in two bus models. The use of a π transmission line-based two-bus equivalent model may be utilised to develop an improved line-based index and will be addressed in latter chapters of the thesis.

Recent approaches aim to address some of the shortcomings of variable based indices by considering effects of transmission line charging and shunt branch parameters to improve line modelling in the stability problem [15]. A method developed in [15] proposes use of ABCD parameter-based transmission line models to solve voltage quadratic equations previously investigated in [36] to obtain the stable conditions of a line accounting for shunt parameters. The method is able to perform online stability assessment and determine available stability margins during critical and contingency based conditions. Conventionally, ABCD parameters are calculated using model-based approaches which rely on several assumptions and approximations. For example, conductor sag effects change over time in addition to temperature variation dependence of impedance parameters. Online methods using synchro phasors have recently been utilised for ABCD parameter estimation [61, 62] and can further improve parameter-based methods. Developed line indices based on ABCD parameters calculated offline may therefore not accurately reflect the stability proximity and measurement-based approaches may be more desirable. Estimated margins may provide overoptimistic estimates resulting in insufficient preventive action being implemented.

Other methods [62] make use of artificial neural networks based on feedforward ANN models with error back propagation. This approach relies on a finite number of existing line indices as inputs into the model. The performance of the ANN may be constrained for larger networks as the solution is computationally intensive, time consuming and may not be robust for online applications where line indices have been predominantly

utilised. ANN approaches may not be generically applicable and require re-training for different systems and configurations. Flexibility in index formulations may be desirable as indices have predominantly been developed and classified as line-based and bus-based indices and approaches to reformulate indices to identify both critical lines and buses may enhance stability evaluation and offer flexibility for various monitoring applications (index-based DG placement and sizing, VSCOPF, etc.). Line and bus-based stability indices are proposed in latter chapters of this thesis which may offer flexibility in the stability evaluation and its adoption for various system applications.

From the above review it has been determined that there have been limited developments in two-bus equivalent index methods considering shunt branch parameters which have conventionally been neglected and may compromise accuracy of calculated indices. The development of static line indices based on impedance matching concepts, which have been predominantly attributed to bus-based indices may expand existing methodologies and concepts on line index development utilising two-bus equivalents. Introducing flexibility in defining and expressing stability indices to evaluate the voltage stability condition of both lines and buses may also enhance stability evaluation capability. The motivation in this work is therefore to develop a static line and bus-based stability index based on impedance matching theory and concepts, considering shunt susceptance parameters using an equivalent two-bus π transmission line model and will be covered in latter chapters of this thesis.

2.6 Methods for mitigation against voltage instability and low strength power systems

2.6.1 Synchronous condensers

With the increased decommissioning of synchronous generation, synchronous condensers have become an attractive solution in improving system strength [1, 2, 63]. As renewable resources are typically electromagnetically decoupled from the main grid connection and often interfaced via power electronics converters, there is a lack (or absence) of system inertia and short circuit provision capability from inverter interfaced generation and is required to be compensated to cover the shortfall of reduced synchronous generation. Synchronous condensers have provided a viable

solution for the provision of several services normally obtained from synchronous generation units. The ability to provide dynamic reactive support and high short circuit current enhances network performance and provide network operators flexibility in managing weak regions in the network thus improving system stability and supporting increased nonsynchronous penetration.

2.6.2 Shunt compensation and hybrid technologies

The use of reactive compensation such as shunt capacitors and FACTs support dynamic reactive provision and reactive resource availability thus supporting bus stiffness and system short circuit levels at steady-state and contingency conditions [2]. These devices provide localised support functions and further support nonsynchronous generation integration as system short circuit ratios are improved thus avoiding dynamic voltage instability and inverter connection issues (e.g. control interaction and oscillations).

Recent developments [64] propose the use of hybrid technologies to mitigate low system strength constraints including dynamic instability through timely reactive power service delivery. A hybrid STATCOM and synchronous condenser functionality is proposed in the Phoenix project [64] in GB to provide enhanced reactive power services. Through the combination of STATCOM and condenser functionality, the solution approach provides a complimentary solution in which the shortfalls of each technology is compensated by the alternative system hence achieving hybrid functionality. In the Phoenix solution a 4 pole, 50Hz, 1500 RPM synchronous condenser together with a 70 MVA MMC-based VSC STATCOM provides a combined condenser solution. The hybrid synchronous compensator-STATCOM arrangement is illustrated in figure 2.14. The condenser branch contributes to system recovery during frequency excursions and improve system inertia levels. The STATCOM branch is able to inject and absorb reactive power during dynamic events hence restoring the system during voltage dips and faulted conditions thus avoiding voltage instability. Major components of the STATCOM unit include a modular multi-level inverter VSC configuration (delta connected) and an air-cooled phase reactor. A controlled three phase sinusoidal voltage is produced by the VSC which injects/absorbs reactive power in relation to the system voltage connected to its

terminals. When the system voltage is higher than the VSC voltage the STATCOM operates as an inductive component and when system voltage is lower than VSC setpoint voltage, a capacitive functionality is achieved injecting reactive power to the system. The master control system is a microprocessor-based system able to perform monitoring and control requirements of the hybrid synchronous condenser in addition to achieving remote operation.

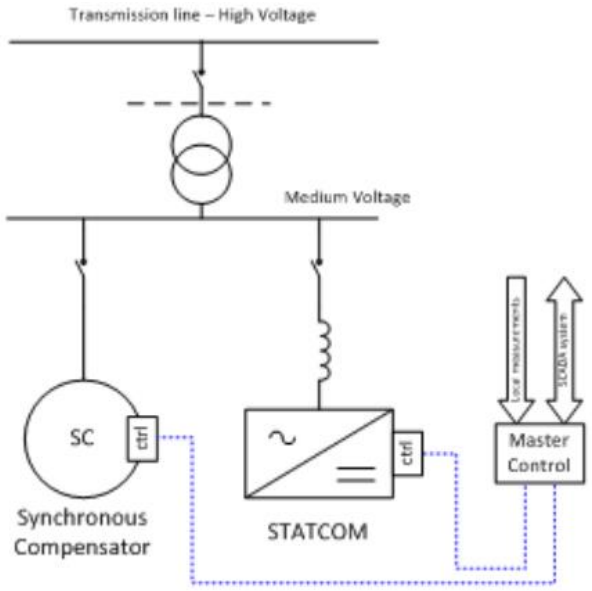

Figure 2.14 Hybrid synchronous condenser-STATCOM connection arrangement [64]

2.6.3 Network optimisation and preventive redispatch

As an alternative to the installation of reactive compensation for increasing system short circuit levels, the use of optimisation tools may provide an alternative instability mitigation measure to support weak networks in operational and planning environments [65, 66]. The availability of centralised unit commitment [4], economic dispatch and OPF engines [67] in the control room allow redispatching preventive and corrective actions to be implemented online to address network bottlenecks and constraints. The application of transient[68, 69], rotor angle [69] and voltage stability-constrained OPF [70] have predominantly allowed initiation of control measures on available network devices to address network constraints. The provision of redispatching control setpoints for synchronous generation, shunt capacitors, FACTs, etc., can be utilised to provide mitigation of impending network constraints thus facilitating operational flexibility. With weak networks increasing risks of voltage

instability, security constrained optimisation can initiate online preventive control and improve stability margins using online system resources. In modern deregulated power networks, the operation of the system is broadly implemented through day ahead operation and redispatch and 5-minute real-time dispatch mechanisms[1, 4]. The National electricity market of Australia (NEM) for example performs security constrained DC optimal power flow in 5-minute dispatch intervals to operate the system within security limits (transient stability-constrained OPF).

Recent efforts in GB aiming to mitigate weak network constraints harness reactive resource availability from distribution-connected generation utilising OPF-based methodologies [11] for the calculation of setpoints of DER controllers. The developed control system (termed DERMS) determines a voltage setpoint (via an OPF component) for the DER to facilitate reactive support via voltage droop control (see figure 2.15). Any difference between setpoint and measured voltages would result in a reactive power injection at its output terminals (similar to STATCOM operation) thus delivering the required service. This also illustrates the potential for unlocking new markets and services for system stability support during steady-state and contingency conditions. Network optimisation and preventive action may therefore be a viable approach to address operational constraints in low system strength systems with increased penetration of nonsynchronous generation.

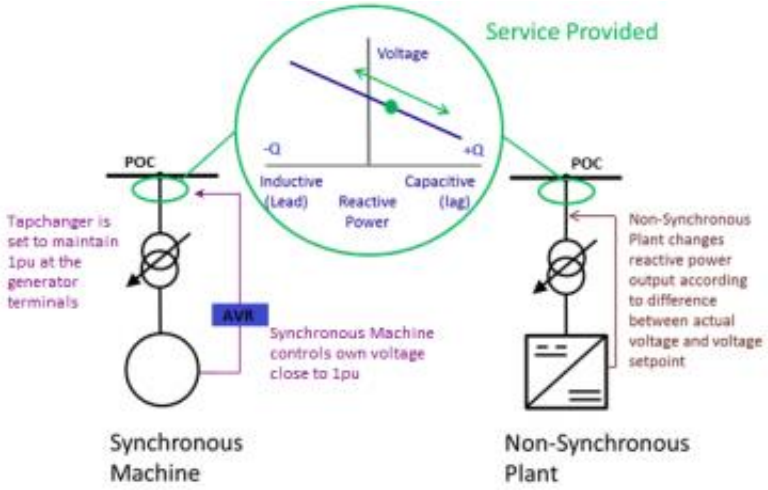

Figure 2.15 DER reactive power service provision for system stability enhancement via voltage droop control [11]

2.7 Review of existing VSCOPF methodologies and techniques

2.7.1 Background

With power systems today being operated in more stressed conditions with limited upgrades in generation and transmission systems, increased uncertainty in operating conditions with increasing renewable penetration, the integration of complex control devices (FACTs, HVDC links), system security and strength are becoming increasingly weakened [4, 71]. The application of security-constrained optimal power flow (SCOPF) has therefore become an important tool in day ahead operational planning and real-time operation of deregulated power networks [67]. The modelling of transient stability, voltage stability and rotor angle stability has been one of the challenges in implementing SCOPF for preventive and corrective control under stressed and contingency conditions.

Problems associated with the implementation of VSCOPF can broadly be categorised into two main challenges: issues associated with developing an efficient non-linear optimisation solution to solve the OPF, and the application of analytical methods to represent voltage stability criteria in the OPF model (which aim to satisfy a specific system objective).

In contrast, analytical methods aim to implement voltage stability conditions in an OPF in the form of algebraic equations in order to solve a VSCOPF problem. The main motivations behind this include simplicity, computational efficiency and robustness in implementing an optimisation solution. Conventional OPF constraints including voltage and thermal limits are incorporated in OPF formulations in the form of algebraic models and hence introducing voltage stability conditions using similar methods and models is more desirable from a computational perspective. As voltage stability is regarded as a dynamic system condition, represented through the use of differential equations[75] in time domain simulations, recent efforts have also aimed to reformulate these conditions in the form of algebraic models to simply the solution procedure. Alternative to this approach, the application of voltage stability indices [12, 76] provides an alternative methodology to represent voltage stability in an OPF using algebraic modelling and can therefore achieve the desired simplicity and

computational efficiency for online implementation and is hence the main motivations in this work. The enhanced line-based stability index proposed in this thesis is incorporated into a VSCOPF solution procedure for enhanced voltage stability performance at critical loadability utilising two-bus equivalent π models considering shunt branch parameters. The developed index can be directly incorporated as an inequality constraint or in a multiobjective formulation for system stability enhancement and is addressed in sections 5.3.1 and 5.3.2.

The application of voltage stability indices (VSI) has been a well-established technique in power system optimisation problems to enhance system security, operation and reliability. The inclusion of indices have been utilised in several applications including allocation and sizing of FACTs devices [77], optimising reactive power dispatch [78, 79], reducing system losses and operational costs[66]. in addition to optimising generation dispatch through VSCOPF solution procedures. A number of methods have been developed to incorporate voltage stability criteria in the conventional OPF model for VSCOPF implementation using VSIs. These approaches can broadly be classified into index based (system variable) or Jacobian based methods [80].

2.7.2 Static index-based stability-constrained optimal power flow

An established technique to incorporate voltage stability in an OPF is through the utilisation of bus and line-based stability indices. The well-established L-index detection method is utilised to improve voltage stability performance through an OPF procedure in [81] . The VCPI index based VSCOPF is solved both as constraints and part of the cost function in [76] to apply preventive control action during contingencies and critical loadability. A number of limitations to line based indexed VSCOPF are addressed in [75, 82] where the performance, accuracy and robustness properties of indices are compared for the selection of a suitable index for effective VSCOPF implementation. An index was selected for VSCOPF implementation based on its higher reduction in real power loss, reactive power generation and voltage stability enhancement. The selected index (VCPI [83]), based on the two-bus equivalent model, neglect shunt branch admittance parameters for index calculation and may compromise accuracy and VSCOPF performance for effective preventive control. As the approach is based on the ratio of active power flow to the maximum

power at the stability limit, accounting for reactive injection from shunt branches further reduces active power loss in the line which may impact the assumed maximum power transfer (knee point) and hence compromise accuracy of the calculated index. This may also lead to less effective VSCOPF dispatch and may increase operating costs and reduce effectiveness of stability margin improvement due to the simplifying assumptions. Accounting for line shunt susceptance parameters in the line model may further reduce reactive generation dispatch levels reducing system losses (via localised reactive support) and improving available reactive reserves. There is therefore limited application of line-based VSCOPF procedures that account for shunt admittance parameters in the incorporated stability indices.

Other classifications to VSI-based approaches include system admittance-based and system-variable based indices in which major differences in performance and trade-offs reside in computational performance and accuracy of stability prediction. It can be regarded that admittance-based methods are more accurate in estimating proximity to collapse and stability margin estimation, however assessment of such indices is computationally intensive requiring dynamic network models and time domain simulations for accurate margin assessment which may be less suitable for applications requiring online VSCOPF implementation. Variable based indices are effective in identifying critical lines and buses and are efficient in providing an OPF solution as static network models are employed for stability prediction. Conventionally, index based VSCOPF methods have utilised simplified transmission line model assumptions in stability prediction which have neglected line shunt branches. Recent approaches consider ABCD [15] transmission line models to address some of the inaccuracies inherent in existing VSI methods. However, these improved line model-based VSIs have not been evaluated in VSCOPF problems. The developed line-based stability index taking into account shunt branch parameters presented in chapter 4 will be incorporated in a VSCOPF formulation to maximize distance to collapse and is presented in Chapter 5.

2.7.3 Jacobian based VSCOPF methods

Other techniques that incorporate voltage stability criteria into the OPF procedure can be classified as Jacobian based methods. This includes the application of bifurcation

analysis to identify saddle node/collapse points to be incorporated it the OPF model[66, 75]. Other methods consider base and critical loading formulations, thus modelling stability margins (difference between current and critical operating point) in the OPF problem to maximise distance to collapse (knee point of the PV curve). In this approach a global minimum stability margin is defined for the network to account for all system buses taken as the difference between the current and critical operating/loading point. A number of critical buses may exist in the system (multiple $Z_{th} = Z_L$ locations) with varying loading margins and therefore the inclusion of a single system minimum may not effectively ensure adequate margins across the network under all operating conditions. The approach also proposes a linear combination formulation where distance to collapse is incorporated in the objective function. This methodology relies on weighting factors to vary the "weight" of the cost function as a trade-off between generation and voltage security costs. Determination of the weighting factors rely on offline OPF and distance to collapse studies which depend on the characteristics of a specific network. This may impose inaccuracies in weighting value selection in different networks which may impact system operating costs and VSCOPF performance [75, 84] . Jacobian based methods may therefore present additional complexities in solving the OPF further reducing computational efficiency.

Other techniques incorporate single (N-1) and multiple contingencies (N-2) in the OPF formulation [84] which make use of singular value decomposition to identify the minimum singular value of the power flow Jacobian (modelled as inequality constraints in the OPF). This approach relies on iterative processes to satisfy the VSCOPF and therefore adds an additional computational burden which can be time consuming for larger systems (scaling constraints). Recent VSCOPF developments [55] reformulate the VSCOPF problem due to recent advances in optimisation algorithms where stability detection is identified through non singularity in the power flow Jacobian. The proposed approach models the stability problem as second order conic where the non-singularity quantifies available margins and is solved via a convex relaxation OPF reformulation.

With power systems being operated closer to their limits already and more so in the future [67], in addition to increasing penetration of nonsynchronous generation, the application of online VSCOPF can be regarded as an effective tool for initiating preventive control action and redispatch of system components to address stability bottlenecks in weak networks as offline methods (dynamic/EMT modelling and time domain analysis) are inadequate in operational timescales. From the previous review, the application of index-based VSCOPF can provide effective and efficient means of implementing preventive redispatching as index-based tools directly incorporate voltage stability criteria as algebraic models in the OPF. Enhancements in the accuracy of index-based methods by considering shunt susceptance parameters may further improve accuracy of modelled index constraints and formulations in the OPF model and hence improve VSCOPF performance. Bus-based stability indices derived from impedance matching theory have been extensively modelled in VSCOPF formulations however impedance matching line stability indices considering shunt branch parameters have had limited application in the VSCOPF solution procedure. The development of improved line based static indices considering shunt admittances based on impedance matching concepts may further enhance VSCOPF performance capability and is the methodology adopted in this work.

2.8 Chapter summary and conclusions

This chapter has reviewed fundamentals of fault level monitoring, steady-state voltage stability analysis and voltage security constrained optimal power flow methods. Applications of both voltage stability and short circuit level management and mitigation are examined based on current research and industry pilot projects. A critical review of the relevant literature on short circuit measurement methods, static voltage stability indices and VSCOPF methods has been presented, with key limitations and shortcomings of existing techniques and concepts outlined for further research. Key findings of the review include shortcomings in the estimation processes and statistical models utilised in fault level estimation as both frequency distribution histograms and ordinary least square regression underperform for efficient passive short circuit impedance parameter estimation. Application of recursive least square methodologies provides additional enhancements in passive fault level measurement applications as parameter estimates are continuously updated (via gain vectors) with

the sum of square of measurement errors recursively minimised. A perturbation-coefficient RLS based passive short circuit estimation procedure is presented in Chapter 3 to address identified limitations. Shortcomings in the concepts adopted for line stability index development that neglect shunt branch effects have been highlighted with impedance matching having limited applications in line-based indices. The inclusion of shunt susceptance parameters using two-bus equivalent π transmission line models in line-based indices have not been previously addressed and have been conventionally neglected. A static line index based on the ratio of the load current flowing in a line to the expected prevailing fault current flow for a receiving end bus fault considering shunt parameter effects is therefore proposed in this research. Impedance matching VSCOPF methods have predominantly incorporated bus-based stability indices in the OPF model where line-based methods considering shunt branch effects having limited attention in the literature for VSCOPF implementation. From the improved line index developed in this work, constrained-based and multiobjective VSCOPF solution procedures are proposed and will be outlined in Chapter 5. Based on the reviewed literature a number of key areas of development have therefore been identified and will be addressed in latter chapters of this thesis.

3. Perturbation coefficient-based passive short circuit current measurement approach utilising recursive least square estimation

Distribution network operators are currently facing increasing pressure to offer low-cost distribution generation (DG) connections for low carbon generation plants to meet carbon emission targets and support the GB net-zero transition in 2050 [1,5, 25]. These are introducing several operational challenges to accommodate renewable-based DG due to the technical constraints imposed from newly connecting generation including voltage, thermal and short circuit capacity constraints. The management of fault levels and assuring that accurate knowledge of their levels in real or near-real-time is available is of increasing concern as the design limits of plant and the mechanical and thermal withstand capability are required to be ensured thus maintaining safety and network security risks whilst facilitating timely low-cost connections. Current strategies to facilitate fault level-constrained DG installations include network reinforcement and upgrades, which result in high cost and capital expenditure, and in some cases, result in newly connecting projects being economically and technically infeasible. Other approaches include network reconfiguration and installation of fault current limiting devices at substation or DG plant location. Emerging methodologies involve management of fault levels in real-time through the provision of network fault level measurements [6] in constrained locations to support active management [25] of short circuit headroom thus releasing additional non-firm capacity. A critical review of existing literature on short circuit measurement methods and limitations was addressed in chapter 2 where major shortcomings in estimation processes have been highlighted to illustrate how the proposed method addresses identified limitations and how it “fits” with the body of existing work in this space.

This chapter proposes a passive fault level measurement methodology through the application of a perturbation coefficient-based recursive least square estimation

algorithm. The chapter begins by introducing the current industry standards adopted for short circuit current calculations and its inherent limitations and challenges in the context of fault level management. The methodology of the proposed passive short circuit estimation approach is outlined in section 3.2. Testing and validation studies on a number of distribution network test models [138] are presented with results compared against simulated fault current values under varied upstream grid fault level conditions and is discussed in section 3.3.

The current industry standard for calculation of short circuit currents in three phase systems is the IEC 60909 [8, 9, 16, 85], where the equivalent voltage source method is adopted for manual calculation of fault currents in networks. Several simplifications and assumptions are incorporated to account for system operating conditions, including pre-fault voltages, transformer tap positions and loading levels. Recent efforts have aimed to evaluate the sensitivity of calculated make and break fault levels to network parameters [7] to identify which require high accuracy or measurement precision for fault level studies and improving the performance of "offline" based analysis through adjustment of model parameters. These include tap changer positions, load fault infeed, model impedance parameters and generator operating power factors which have a direct impact on calculated pre-fault voltages. Sources of error in the IEC60609 standard include the voltage c factor multiplier [8] which scales the source voltage to account for variations in system operating conditions and factor the influence of consumer load data, variation of inverter-based DG fault contribution with actual output levels,etc.

The current industry adopted approach for fault level management is based on short circuit studies utilising sophisticated tools and models accounting for system configuration, construction, fault contribution of industrial and commercial customers [5], etc. However, there are factors not available to modellers which impact fault level studies including the accuracy of models which are dependent on both network measurements and impedance parameters. Distribution fault levels are also influenced by several factors including upstream grid fault contribution, load fault level infeed, operational running arrangements [7], where not all information is readily available in real-time. Network models therefore do not readily provide real-time representation of network fault levels [5] which makes it more difficult to actively provide additional

fault level headroom to facilitate increasing penetration of low carbon DG. Model-based approaches for fault current calculation often result in conservative design limits being set, resulting in higher capital costs for plant installations. There is therefore an increasing need for the development of measurement-based approaches to accurately reflect actual network fault levels to support active fault level management decisions in addition to validating network models via fault level monitoring.

Methods to measure short circuit currents can broadly be categorised into passive [19, 86] and active [22] methods. Passive fault level estimation involves obtaining short circuit measurements based on natural variations [86] in network load in order to establish a Thevenin equivalent model of the system. Active methods introduce external disturbances in the network to obtain real-time measurements of short circuit currents. Both approaches present several advantages and disadvantages: active methods for example require installation of additional equipment including inductive load banks [22] and pulse closers[25], which may impose power quality issues and cost implications at higher voltage levels thus limiting wide area fault level monitoring. Passive methods may be less reliable for active fault level management as they are dependent on network load behaviour and naturally occurring variations to obtain estimates. Passive methods may therefore be useful in operational planning and model validation applications as they are cost effective and can be easily transformed into active schemes and therefore offer flexibility.

3.1 Development of a novel perturbation coefficient-based recursive least square short circuit current estimation approach

The authors in [41] propose formulae to model the net active power increment at a bus following a downstream load event during small load perturbations. In this approach, the net active power gained at a bus is composed of two terms; the active power increase due to connection of additional load $\Delta G_L$and the active power lost on original load due to the voltage drop ΔV across the system to supply the additional load demand. The assumed active power injection model is independent of load type as it is derived from load flow and Jacobian matrix concepts. This can be expressed as [41]

$$\Delta P_L = (V + \Delta V)^2 \Delta G_L + (2V + \Delta V) G_L \Delta V \quad (3.1)$$

Where V is the pre-event bus voltage, ΔV is the voltage drop following a load change, ΔG_L is the additional load admittance/conductance following a load perturbation, G_L is the pre-disturbance load admittance/conductance ($G_L = \frac{P_L}{V^2}$). During normal loading conditions, we can assume that the term $(V + \Delta V)\Delta G_L \gg (2V + \Delta V) G_L \Delta V$ as the *increase* in system loading dominates over the *decrease* in receiving end bus voltage V_R. In other words, the power loss across the lines as a result of the increased voltage drop is relatively small in comparison to the active power gained from the connection of the additional load. There is therefore a net active power increase supplied to the bus, neglecting the active power loss term from equation 3.1

$$\Delta P_L = (V + \Delta V)^2 \Delta G_L \quad (3.2)$$

This can be expressed as a current injection ΔI_L gained at the bus obtained from

$$\Delta I_L = \frac{\Delta P_L}{V} \quad (3.3)$$

Expanding equation (3.2) and from (3.3) we have

$$\Delta I_L = \frac{V^2 \Delta G_L + 2V \Delta V \Delta G_L + \Delta V^2 \Delta G_L}{V} \quad (3.4)$$

A generalised form to estimate the equivalent Thevenin impedance at a bus is taken as the ratio of the variation of the bus voltage to the variation in bus current following a downstream load perturbation. Taking $Z_{th} = \frac{\overline{V_2} - \overline{V_1}}{\overline{I_2} - \overline{I_1}}$ and $\Delta G_L = \frac{\Delta P_L}{V^2}$ where $\overline{V_1}, \overline{V_2}, \overline{I_1}, \overline{I_2}$ are the pre and post disturbance voltage and current phasors expressed in rectangular form, the equivalent Thevenin impedance can now be expressed as

$$Z_{th} = \frac{V \Delta V}{\Delta P_L + \frac{2 \Delta P_L \Delta V}{V} + \frac{\Delta V^2 \Delta P}{V^2}} \quad (3.5)$$

Rearranging the above equation with respect to the voltage measured at the bus following a load perturbation event we have

$$V = \left(\frac{\Delta P_L}{\Delta V} + \frac{2 \Delta P_L}{V} + \frac{\Delta V \Delta P}{V^2}\right) Z_{th} \quad (3.6)$$

Taking the term $\frac{\Delta P_L}{\Delta V} + \frac{2\Delta P_L}{V} + \frac{\Delta V \Delta P}{V^2} = A$ regarded as a perturbation coefficient in this problem, results in the following

$$V = A\, Z_{th} \tag{3.7}$$

Taking the real and imaginary components of the measured voltage and perturbation coefficient respectively as $V_i = V_{re} + jV_{im}$and $A_i = A_{re} + jA_{im}$

$$Z_{th} = \frac{V_{re} + jV_{im}}{A_{re} + jA_{im}} \tag{3.8}$$

This can be simplified to the following expression

$$Z_{th} = \frac{V_{re}A_{re} + V_{im}A_{im}}{A_{re}^2 + A_{im}^2} + \mathrm{j}\frac{V_{im}A_{re} - V_{re}A_{im}}{A_{re}^2 + A_{im}^2} \tag{3.9}$$

It is known that $Z_{th} = R_{th} + jX_{th}$ therefore

$$R_{th} = \frac{V_{re}A_{re} + V_{im}A_{im}}{A_{re}^2 + A_{im}^2} \tag{3.10}$$

And

$$X_{th} = \frac{V_{im}A_{re} - V_{re}A_{im}}{A_{re}^2 + A_{im}^2} \tag{3.11}$$

Alternatively, the above expressions can be written in the following form

$$V_{re}A_{re} + V_{im}A_{im} = (A_{re}^2 + A_{im}^2)\, R_{th} \tag{3.12}$$

$$V_{im}A_{re} - V_{re}A_{im} = (A_{re}^2 + A_{im}^2)\, X_{th} \tag{3.13}$$

Equations 3.12 and 3.13 can be expressed in terms of a generalised linear regression model and can be described using

$$y = H\theta + w \tag{3.14}$$

Where y is the output vector and is a dependant variable in the linear system shown and is a function of measured voltage and perturbation coefficient previously

described. H is the regressor vector, obtained from the real and imaginary components of A. R_{th}, X_{th} are the Thevenin resistance and reactances and represent the parameter vector θ, of the system to be solved via least square estimation. w can be regarded as a measurement error and is the difference between the model output and estimated output. In this problem, a recursive least equation (RLS) estimation algorithm is adopted to solve the above system and obtain estimates of the equivalent system resistances and reactances (RLS parameters), hence obtaining estimates of the short circuit impedance (Z_{th}) and short circuit current following small load disturbances. As system loading is continuously varying, an approach to recursively estimate equivalent impedances through updated measurements (following load perturbations) can improve estimation accuracy as the sum of squares of measurement errors is continuously minimised. This allows the estimates to be quantified closer to the true value of the equivalent short circuit impedance and hence improve overall fault level estimation performance. Expressing the above equation in full matrix form and following n measurements from a series of consecutive load changes, the above expressions can be described using:

$$\begin{bmatrix} V_{re1}A_{re1} + V_{im1}A_{im1} \\ V_{re2}A_{re2} + V_{im2}A_{im2} \\ \vdots \\ V_{ren}A_{ren} + V_{imn}A_{imn} \end{bmatrix} = \begin{bmatrix} A_{re1}^2 + A_{im1}^2 \\ A_{re2}^2 + A_{im2}^2 \\ \vdots \\ A_{ren}^2 + A_{imn}^2 \end{bmatrix} [R_{th}] + \begin{bmatrix} u_1 \\ u_2 \\ \vdots \\ u_n \end{bmatrix} \tag{3.15}$$

$$\begin{bmatrix} V_{im1}A_{re1} - V_{re1}A_{im1} \\ V_{im2}A_{re2} - V_{re2}A_{im2} \\ \vdots \\ V_{imn}A_{ren} - V_{ren}A_{imn} \end{bmatrix} = \begin{bmatrix} A_{re1}^2 + A_{im1}^2 \\ A_{re2}^2 + A_{im2}^2 \\ \vdots \\ A_{ren}^2 + A_{imn}^2 \end{bmatrix} \cdot [X_{th}] + \begin{bmatrix} v_1 \\ v_2 \\ \vdots \\ v_n \end{bmatrix} \tag{3.16}$$

The closed form solution to obtain the parameter vector $\tilde{\theta}$ and hence the equivalent short circuit impedance parameters is given by:

$$\tilde{\theta} = (H^T H)^{-1} H^T y \tag{3.17}$$

and

$$\tilde{\theta}_n = \tilde{\theta}_{n-1} + K_n(y_n - H_n\tilde{\theta}_{n-1}) \quad (3.18)$$

Where K_n is an estimation gain vector. In this regard, the new estimate $\tilde{\theta}_n$ is modified from the previous estimate $\tilde{\theta}_{n-1}$ by a correction term $(y_n - H_n\tilde{\theta}_{n-1})$ through the gain vector thus providing an update to the estimate when a new measurement or perturbation is identified. In this problem, the output vector y_n for the R_{th} and X_{th} RLS models are taken as $V_{ren}A_{ren} + V_{imn}A_{imn}$ and $V_{imn}A_{ren} - V_{ren}A_{imn}$ respectively. The next section evaluates the performance of the proposed online parametric estimation approach for passive short circuit current estimation during downstream load disturbances utilising a number of test networks and case studies.

3.2 Testing and validation of the proposed RLS-based passive short circuit estimation approach

3.2.1 Simple distribution network model

To illustrate the performance of the proposed short circuit current estimation procedure, a simplified distribution network model is developed (figure 3.1). The network is a typical UK HV/MV distribution network configuration which connects the HV network (at 33 kV) to the MV/LV networks. The model is composed of three HV/MV sections with each section interfacing two 33/11 kV transformers running in parallel. The upstream network fault level is assumed to vary between 250 and 1000 MVA where measurements are obtained at the secondary terminal of the transformer connecting bus 1 at 11 kV (location M1). Three consecutive load step changes are applied at LV of 15 kW, 5 kW and 5 kW at 0.2, 0.4 and 0.6 seconds respectively to simulate passive load perturbation events (figure 3.2). Measurements of voltage, current and active power are obtained and input to the recursive least square algorithm which estimates the Thevenin impedance parameters and subsequently the prospective breaking short circuit current (symmetrical fault current) based on the methodology outlined in the previous section. In this work, only the upstream RMS component of the short circuit current is evaluated using the proposed estimation approach. Simulation based fault studies are then run with three phase faults applied at bus 1 to obtain the upstream RMS break current at the monitoring point under various upstream

grid fault conditions with results compared to the estimates obtained from the RLS estimator.

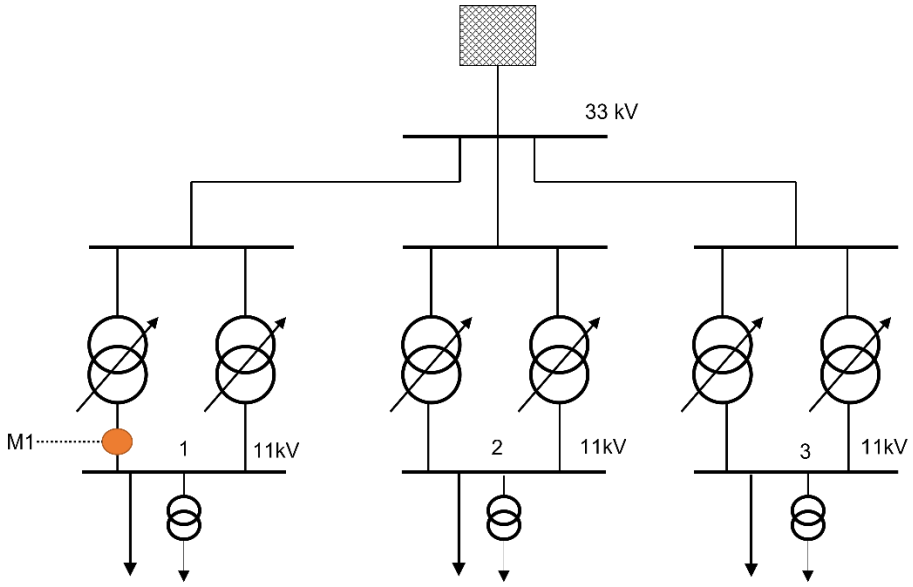

Figure 3.1 Simple distribution network model

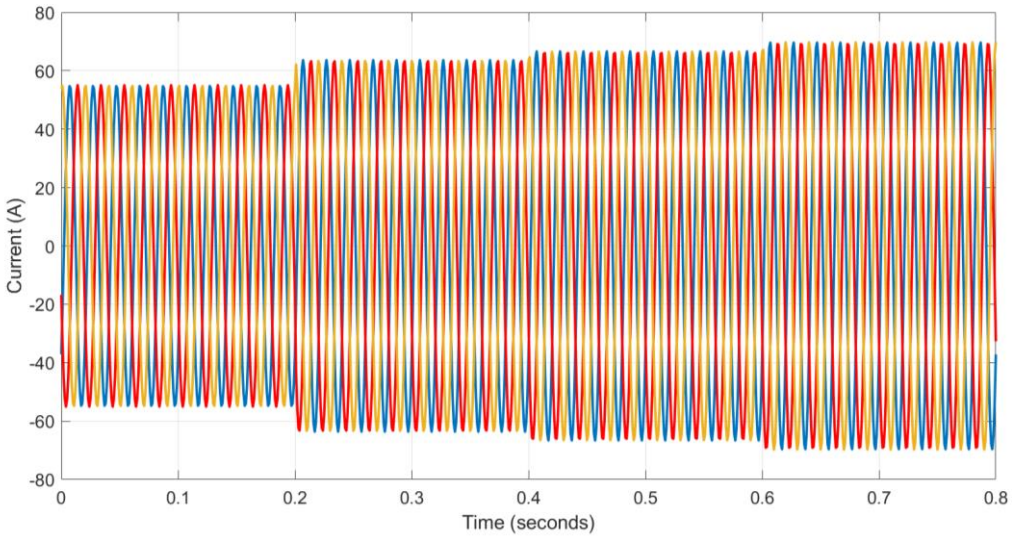

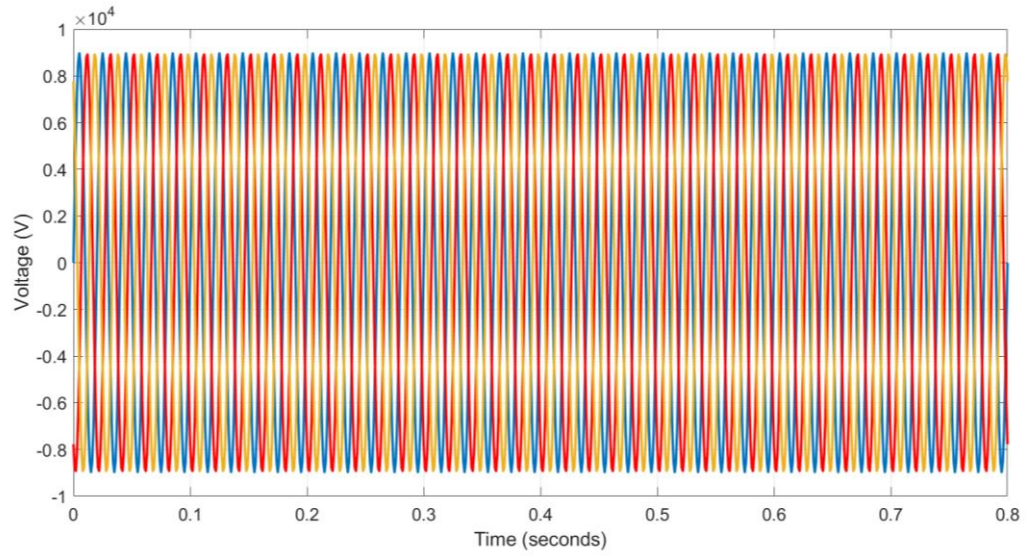

Figure 3.2 Current and voltage measurements at M1 following load variation at bus 1

Table 3.1 compares the estimated RLS Thevenin parameters with calculated Thevenin values using the conventional method ($Z_{th} = \frac{\Delta V}{\Delta I}$). Results generally indicate the proposed RLS model is accurately able to determine Thevenin equivalent values for a range of assumed upstream fault levels. It can be seen that R_{th} estimates are generally more accurate than X_{th} values with the majority of estimation errors <0.4% with X_{th} estimates at <1.3%. The largest estimation error for R_{th} is seen at 250 MVA with an error of 0.38% and a 1.295% error is apparent for the X_{th}estimate. The overall trend shows estimation errors increasing for lower or weakened upstream fault level conditions relative to a stronger network. This may be justified as higher equivalent source impedance for weak networks increases system voltage drops generally and this additional active power loss (due to voltage drops) for weaker networks is neglected in coefficient estimation as outlined in the previous section. The accuracy of the assumed net active power gain at the bus (from equation 3.2) is further compromised in weak network conditions due to higher voltage drops and system losses. However, results indicate high accuracy and effectiveness in determining the Thevenin parameters utilising the proposed approach and may therefore able to determine the equivalent short circuit currents from the derived short circuit impedance Z_{th}

Table 3.1 Comparison between estimated and calculated RLS Thevenin parameters

Fault MVA	$R_{th\ est}(\Omega)$	$R_{th}(\Omega)$	Error (%)	$X_{th\ est}(\Omega)$	$X_{th}(\Omega)$	Error (%)
250	0.075847	0.075561	0.378677	0.506137	0.512789	-1.29709
300	0.062617	0.062417	0.320905	0.429648	0.435118	-1.25714
350	0.053346	0.053198	0.27969	0.374655	0.379314	-1.22818
400	0.046492	0.046377	0.248983	0.333211	0.337281	-1.20683
450	0.041222	0.041129	0.22706	0.300813	0.304433	-1.18914
500	0.037049	0.036971	0.209006	0.274754	0.278026	-1.1767
550	0.033656	0.033589	0.198068	0.253745	0.256735	-1.16477
600	0.030847	0.030789	0.188351	0.235879	0.238639	-1.15623
700	0.026455	0.026408	0.175856	0.207647	0.210047	-1.14262
800	0.023199	0.023159	0.173764	0.186632	0.188766	-1.13049
900	0.020675	0.020639	0.176163	0.170551	0.172486	-1.12189
910	0.020453	0.020417	0.174792	0.168963	0.170881	-1.12248
920	0.020234	0.020198	0.175181	0.167503	0.169402	-1.12138
930	0.020023	0.019988	0.175907	0.166284	0.168168	-1.12051
940	0.019819	0.019785	0.176192	0.164859	0.166726	-1.11996
950	0.019614	0.01958	0.17573	0.163555	0.165407	-1.11964
960	0.019424	0.019389	0.176456	0.162087	0.163919	-1.11765
970	0.019218	0.019184	0.178095	0.160975	0.162794	-1.11782
980	0.019035	0.019001	0.179099	0.159816	0.161621	-1.11627
1000	0.018656	0.018622	0.179665	0.157363	0.159138	-1.11583

Table 3.2 compares the estimated ($I_{sc\ est}$) and simulated ($I_{sc\ act}$) fault currents under various upstream grid fault level magnitudes. $I_{sc\ est}$ is obtained from $\frac{V}{Z_{th}}$ where V is the pre-disturbance voltage phasor and Thevenin equivalent impedance is derived from RLS parameter estimates of R_{th} and X_{th}. $I_{sc\ act}$ is obtained through simulation-based fault studies where three phase faults are applied at bus 1 with the current measured at the transformer secondary (at 11 kV). The maximum estimation error obtained is -0.73% at 920 MVA. Estimation errors ranging from 2.58%-5% between simulated and estimated fault current values for various load types were reported in [19] however lower errors can be seen utilizing the proposed approach. There is also no apparent correlation between fault MVA and estimation error and therefore short circuit estimation performance is not impacted by strong and weak network conditions. It should also be noted that estimation errors are below $\pm 1\%$ which illustrate the

effectiveness and accuracy of the proposed approach for passive short circuit current estimation of the studied model. Comparison between simulated and estimated fault current levels is shown in figures 3.3 and 3.4 for a 1000 MVA upstream grid fault infeed.

Table 3.2 Comparison of estimated and modelled (actual) fault currents for the simplified distribution network model

Fault MVA	$I_{sc\,est}$ **(A)**	$I_{sc\,act}$ **(A)**	**Error (%)**
250	12252.62692	12309.00	-0.45798263
300	14447.79637	14500.00	-0.36002503
350	16580.7417	16602.00	-0.12804665
400	18654.04055	18641.00	0.06995629
450	20673.43104	20729.00	-0.26807351
500	22643.33286	22658.00	-0.06473271
550	24527.97666	24571.00	-0.17509805
600	26394.08024	26323.00	0.27003093
700	29999.17483	30096.00	-0.32172104
800	33393.61304	33190.00	0.61347708
900	36558.77008	36641.00	-0.22442051
910	36902.84053	36718.00	0.50340578
920	37226.09229	37500.00	-0.73042057
930	37500.94781	37322.00	0.47947003
940	37826.09841	37654.00	0.45705213
950	38129.04806	38291.00	-0.42295041
960	38475.56882	38661.00	-0.47963369
970	38743.40689	38647.00	0.24945503
980	39026.05742	38901.00	0.3214761
1000	39637.25336	39510.00	0.32207887

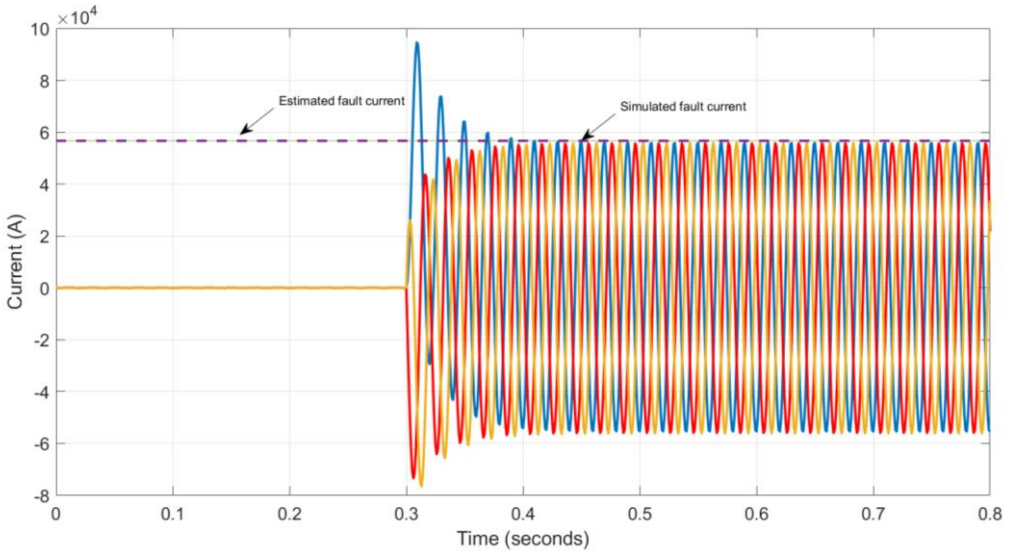

Figure 3.3 Estimated RLS fault level vs simulated fault at bus 1

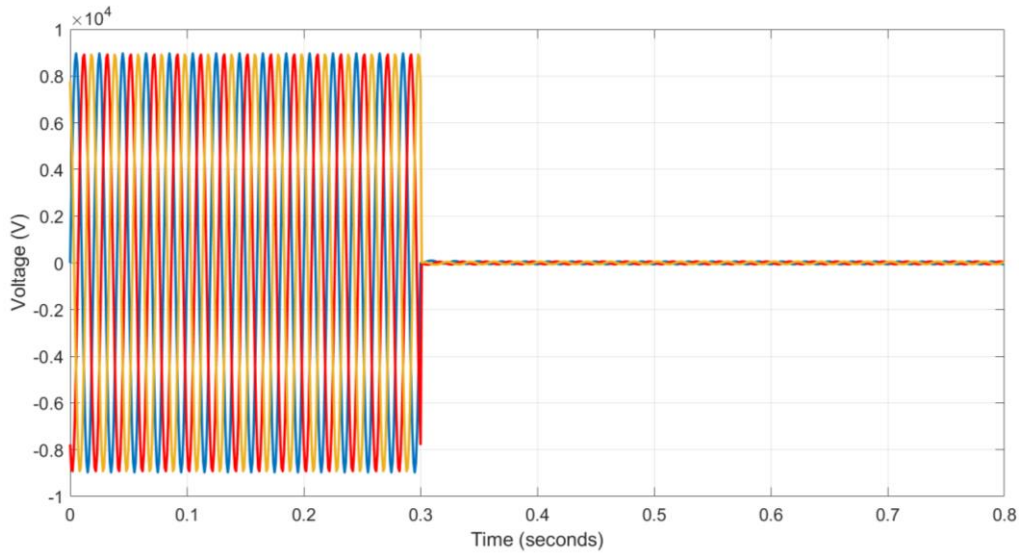

Figure 3.4 Voltage measurement following simulated fault at bus 1

Figure 3.5 illustrates the RLS error output of the model following the 3 perturbation events previously described which make use of a one-step-ahead predictor to estimate difference between model output and estimated output. The figure illustrates as more perturbations are identified the model error is continuously reduced as the recursive estimation minimises the sum of square of errors and updates the parameter estimate via the gain vector. This shows that as additional perturbations are captured, the estimation model updates the estimate and the error is reduced thus improving

performance. This therefore illustrates the effectiveness in adopting recursive least square regression to enhance estimation performance in passive short circuit current measurement applications as estimates are continuously updated and errors recursively reduced following identified perturbations relative to ordinary least square methodologies. The next section investigates the proposed approach on an IEEE distribution test feeder model to evaluate method performance on more realistic network conditions with results compared to simulated fault current values.

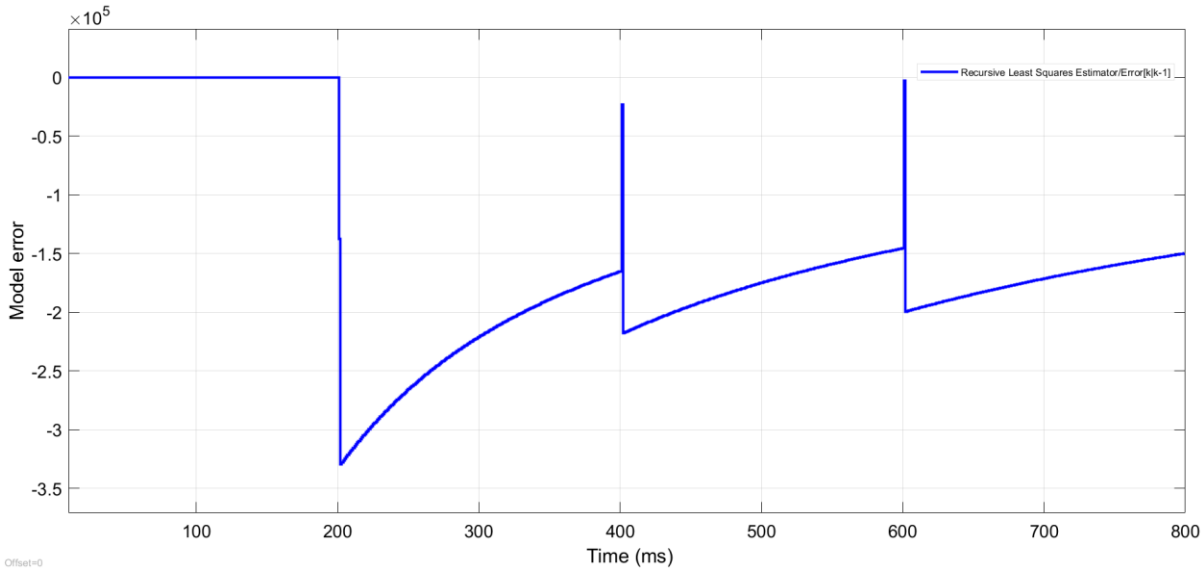

Figure 3.5 RLS model error reduction with multiple sequential load perturbation events are included in the calculation

3.2.2 Impact of perturbation location on estimation accuracy

To evaluate the performance of the proposed RLS based estimation method on disturbance location, a case study consisting of applying 500 kW perturbations in various locations along the LV line has been investigated. In this study, the location of the constant impedance load was varied between 0.1 m and 1000 m to illustrate the impact on estimation accuracy for LV perturbations. From table 3.3, results generally indicate that the closer the perturbation is from the measurement location the higher the accuracy. There is also a cut off distance where estimation accuracy greatly diminishes where a 400 m distance can be regarded as the maximum disturbance location to yield acceptable results within 10% accuracy at LV (400 V). This is because the developed Thevenin equivalent parameter method neglects line voltage drops and

only considers the drop across the load terminals. This impacts the assumed net active power gained at the bus as active power losses/voltage drops also impact this value and become proportionately larger for distances further away from the measurement location.

Table 3.3 Impact of perturbation location (electrical distance) on estimation performance and accuracy

Distance (m)	ΔV (%)	Z_{th}	$R_{th\,est}$	$X_{th\,est}$	$I_{sc\,actual}$	$I_{sc\,est}$	Error (%)
0.1	0.2076	0.0789 + 0.5138i	0.0875	0.4932	12309	12673.171	2.9585
10	0.2055	0.0707 + 0.5100i	0.1090	0.4812	12309	12866.515	4.5293
50	0.2061	0.0726 + 0.5124i	0.2168	0.4141	12309	13580.407	10.3290
100	0.2056	0.0776 + 0.5132i	0.1182	0.4836	12309	12750.084	3.5834
400	0.1928	0.0746 + 0.5143i	0.2167	0.4138	12309	13588.672	10.3962
800	0.1661	0.0781 + 0.5156i	0.2764	0.2930	12309	15760.125	28.0374
1000	0.1501	0.0713 + 0.5095i	0.2733	0.2405	12309	17439.059	41.6773

3.2.3 Impact of perturbation magnitude on estimation accuracy

To assess the performance of the RLS estimation performance to load perturbation magnitude, a case study was performed with load steps varied between 250 kW-2MW. In this study, the disturbance source was located at a 1m distance from the measurement location to minimise the impact of line length inaccuracy on estimation performance. From table 3.4, results generally indicate higher estimation errors for large load step changes relative to smaller perturbations (e.g. 250 kW). Increased loading results in higher drops across the system relative to the drop across the load which are not accounted for in the developed Thevenin equivalent method. In other words, as load perturbation magnitude increases, the active power lost on the load due to voltage drop (and higher loading) increases, which is assumed negligible in the developed approach. This indicates that for very large load perturbations greater than 1.5 MW, the estimation accuracy degrades to within 10% error as the power loss across the line infeed becomes significant. The method also illustrates good sensitivity to voltage disturbances as a perturbation magnitude of 0.1 % (ΔV) yielded an error of 1.866% whilst a 4.46% error for a 2% voltage disturbance was reported in [19] assuming a motor load perturbation. However, both perturbation magnitude and event location impact estimation performance and neglecting impact of system losses

becomes significant for distant load events and large load step changes as both incur a large active power loss comparable in magnitude to the load perturbation change which impact the assumed net active power increment at the measured bus.

ΔP(kW))	ΔV (%)	Z_{th}	$R_{th\ est}$	$X_{th\ est}$	$I_{sc\ actual}$	$I_{sc\ est}$	Error (%)
250	0.1048	0.0753 + 0.5112i	0.08196	0.4996	12309	12542.823	1.8659
500	0.2064	0.0753 + 0.5112	0.08677	0.4902	12309	12757.2	3.6069
600	0.2462	0.0753 + 0.5112i	0.0886	0.4864	12309	12843.511	4.3079
800	0.3243	0.0753 + 0.5112i	0.09209	0.4791	12309	13017.065	5.7174
1000	0.4005	0.0753 + 0.5112i	0.0953	0.4718	12309	13191.830	7.1367
1250	0.4933	0.0753 + 0.5112i	0.0991	0.4630	12309	13411.933	8.9243
1500	0.5835	0.0753 + 0.5112i	0.1027	0.4543	12309	13633.805	10.7262
2000	0.7561	0.0753 + 0.5112i	0.1089	0.4376	12309	14082.605	14.3711

Table 3.4 Impact of LV perturbation magnitude on estimation performance

3.2.4 IEEE 13 node test feeder

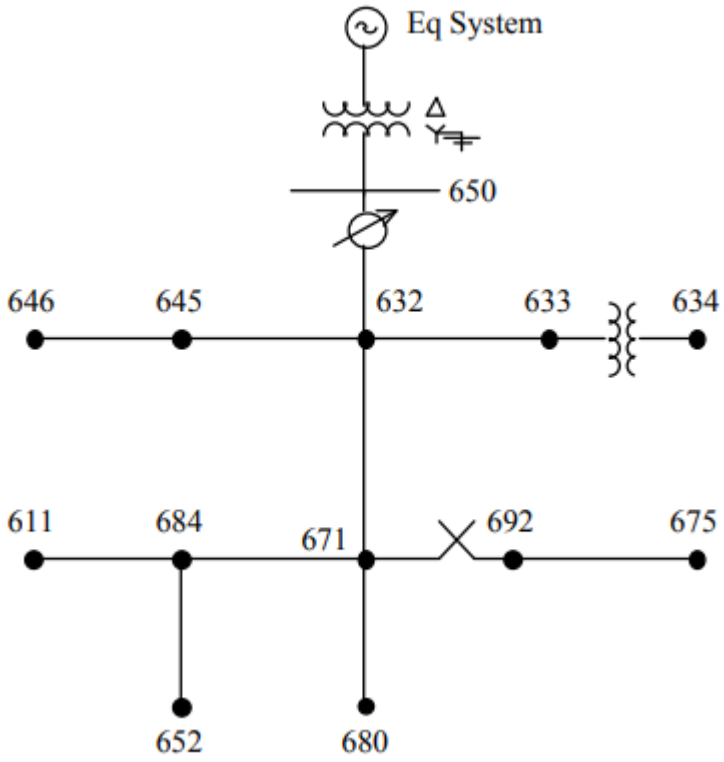

Figure 3.6 IEEE 13 node test feeder model [138]

To illustrate the performance of the proposed short circuit estimation method on a realistic test network, the IEEE 13 node test feeder (figure 3.6) was chosen to validate the approach through a number of case studies. The model is composed of balanced and unbalanced loads connected at MV and LV. The model is connected in a radial configuration at an MV voltage of 4.16 kV and is interfaced to the transmission grid through a 115/4.16 kV transformer. In this study the regulating transformer action is neglected in the model i.e. no tap changing action occurs during the perturbation period. As in the previous case study, a number of consecutive load perturbations are applied with measurements obtained from bus 632, taken as the transformer secondary from which the system is supplied. Three load changes of 15 kW, 5 kW and 5kW at 0,2, 0.4 and 0.6 seconds respectively are switched on downstream from the measurement location (at MV) and obtained measurements are utilised to construct the RLS models described (from (3.15) and (3.16)). Upstream grid fault levels are varied between 100-250 MVA in steps of 10 MVA, and the Thevenin parameters and short circuit level are estimated in each case and compared with the conventional Thevenin equivalent calculation method with fault current levels obtained from simulated faults. Performance of the RLS estimator and the estimation errors in each case are compared for evaluation of the proposed method.

Table 3.5 compares the estimated and calculated Thevenin parameters at various upstream fault levels for the IEEE 13 node feeder utilising the proposed RLS-based estimator. Results generally indicate the method obtains comparable estimates relative to the conventional approach, outlined previously, irrespective of the upstream fault level infeed with estimated values obtained recursively relative to conventional ordinary least square methodologies. Higher estimation errors are seen for resistance estimates as the system R_{th} is relatively small (0.058-0.023) at various grid fault levels relative to equivalent reactance values. This indicates a stronger dependence of the short circuit current estimate on estimated system reactance due to negligible upstream resistance values ($X_{th} \gg R_{th}$) with the $\frac{X}{R}$ taken as 3 in this study. This shows that the overall short circuit estimation performance is within reasonable accuracy, as upstream fault levels are a strong function of system reactance, where estimation errors are low utilising the proposed least square approach. In both cases, as upstream fault level is

increased, estimation performance and accuracy is improved indicated by the progressively lower error values as shown from the previous study.

Table 3.5 Comparison of estimated (RLS) and calculated Thevenin parameters for the IEEE 13 node test network

Fault level (MVA)	$R_{th\,est}(\Omega)$	$R_{th\,cal}$ **(Ω)**	**Error (%)**	$X_{th\,est}$ (Ω)	$X_{th\,ecal}$ (Ω)	**Error (%)**
100	0.082639	0.057685	43.25861	0.153452	0.173056	-11.328
110	0.074655	0.052441	42.36023	0.141175	0.157324	-10.2646
120	0.068059	0.048071	41.58024	0.130697	0.144213	-9.37211
130	0.062521	0.044373	40.89759	0.121655	0.13312	-8.61246
140	0.057807	0.041204	40.2957	0.113774	0.123611	-7.95808
150	0.053748	0.038457	39.76138	0.106846	0.115371	-7.38854
160	0.050217	0.036053	39.28409	0.10071	0.10816	-6.88836
170	0.047117	0.033933	38.85531	0.095236	0.101798	-6.44562
180	0.044375	0.032047	38.46812	0.090325	0.096142	-6.05096
190	0.041933	0.030361	38.11681	0.085893	0.091082	-5.69696
200	0.039744	0.028843	37.79668	0.081875	0.086528	-5.37765
210	0.037771	0.027469	37.50378	0.078215	0.082408	-5.08818
220	0.035984	0.026221	37.23482	0.074867	0.078662	-4.82455
230	0.034357	0.025081	36.987	0.071793	0.075242	-4.58345
240	0.032871	0.024036	36.75793	0.068961	0.072107	-4.36211
250	0.031507	0.023074	36.54558	0.066344	0.069222	-4.1582

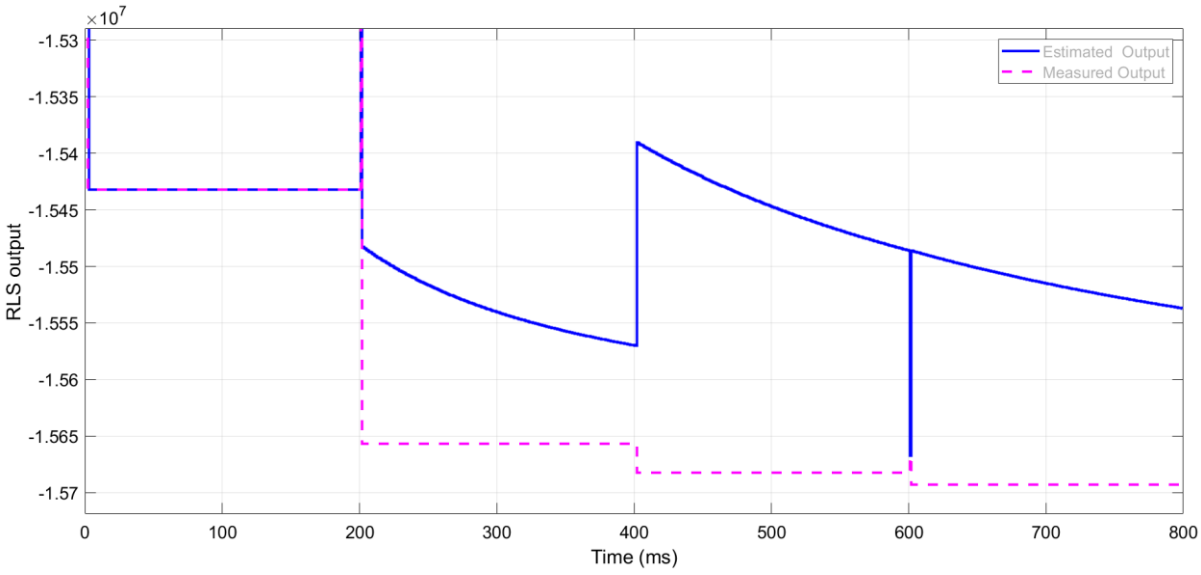

Figure 3.7 Simulated vs measured RLS output for Thevenin resistance estimator at 100 MVA fault level

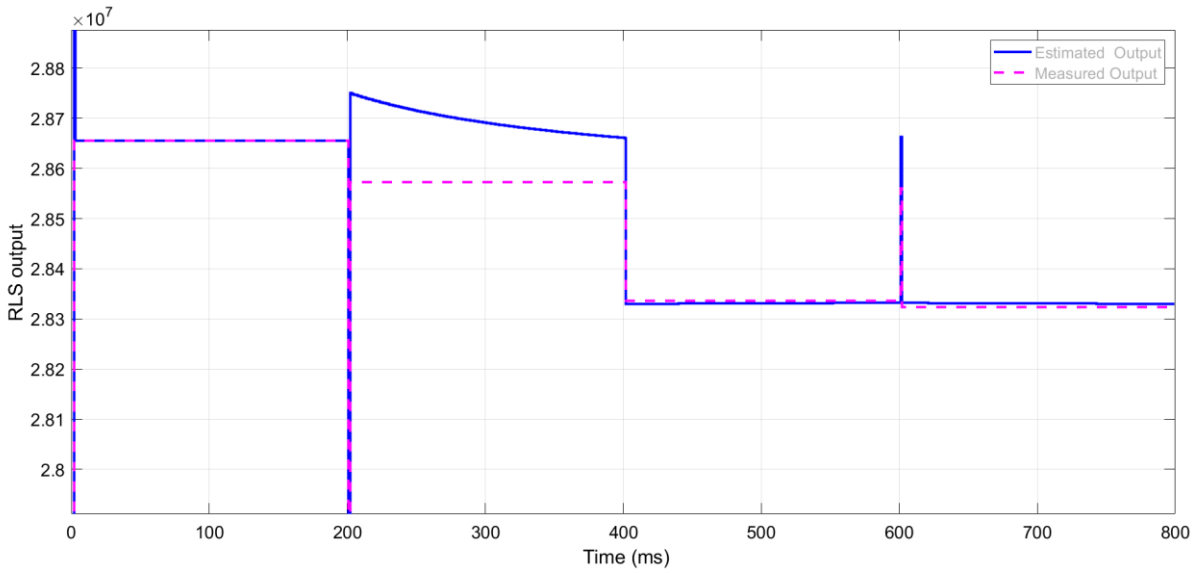

Figure 3.8 Simulated vs measured RLS output for Thevenin reactance estimator at 100 MVA fault level

Analysis of the performance of the RLS estimation procedure can be achieved through evaluation of measured and estimated/predicted RLS model outputs. Figures 3.7 and 3.8 illustrate RLS model output comparisons for the estimated parameters at 100 MVA whilst figures 3.9 and 3.10 illustrate outputs for 250 MVA. The overall trend indicates that as further perturbations are applied at 400 and 600ms differences between measured and estimated model outputs are reduced. This illustrates that as additional measurements are obtained following load events, the RLS model is updated and the accuracy in estimating equivalent parameters is improved as estimation errors are recursively minimised following additional perturbation measurements. It can also be seen that reactance parameter estimates indicate a smaller error between estimated and measured model outputs as shown in table 3 where errors are relatively lower for reactances relative to resistance estimates as the resistance estimator quantifies relatively low resistance values (0.082-0.031) which compromises RLS model accuracy. It can therefore be deduced that the reactance-based estimation model exhibits superior performance relative to the resistance estimator with the overall short circuit impedance value predominantly reactive (higher $\frac{X}{R}$ ratio of 3). However, differences between measured and predicted outputs for both estimators (R_{th} and X_{th}) are negligible with relatively small model errors which do not adversely impact model performance as parameter estimates are close to their true values. To further improve

estimation accuracy, additional perturbations may be required to further minimise discrepancies between predicted and measured RLS outputs. Other factors that may affect accuracy include disturbance magnitude and location (MV/LV, distance from measurement location, etc.) which have been outlined in the previous case study.

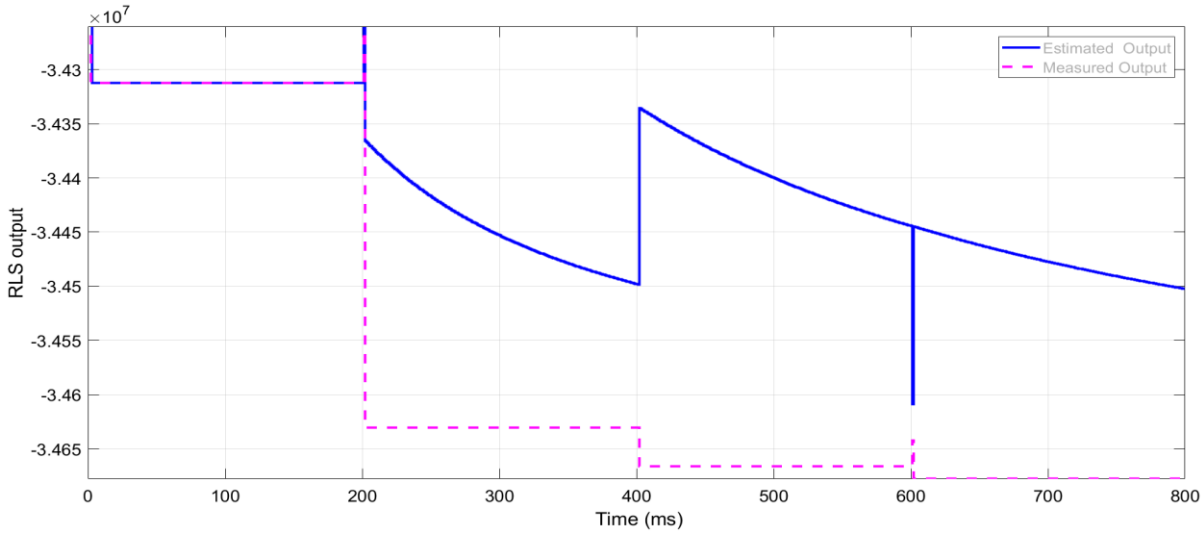

Figure 3.9 Estimated vs measured RLS output for Thevenin resistance estimator at 250 MVA fault level

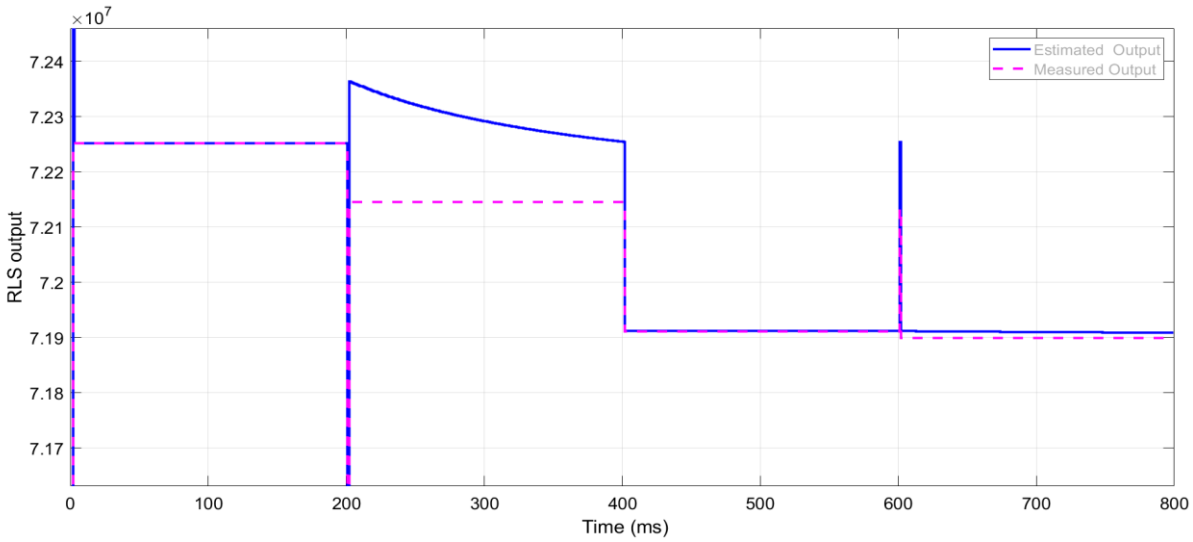

Figure 3.10 Estimated vs measured RLS output for Thevenin reactance estimator at 250 MVA fault level

Table 3.6 Comparison of estimated and simulated fault currents for the IEEE 13 node test network

Fault level (MVA)	$I_{sc\ est}$**(kA)**	$I_{sc\ act}$ **(kA)**	**Error (%)**
100	13.78039	13.43858	2.54349
110	15.03939	1.48E+01	1.617481

120	16.29911	1.61E+01	1.236708
130	17.55939	1.75E+01	0.339359
140	18.8201	1.88E+01	0.106915
150	20.08116	2.02E+01	-0.58832
160	21.3425	2.15E+01	-0.73256
170	22.60407	2.28E+01	-0.85934
180	23.86584	2.42E+01	-1.38085
190	25.12776	2.55E+01	-1.45976
200	26.38982	2.69E+01	-1.89657
210	27.652	2.82E+01	-1.94325
220	28.91429	2.95E+01	-1.98547
230	30.17666	3.09E+01	-2.34092
240	31.4391	3.22E+01	-2.36304
250	32.70162	3.36E+01	-2.67376

Similar to the previous study, Table 3.6 compares estimated and simulated fault current levels at various upstream fault level infeeds. Three phase faults are applied at the grid infeed (bus 632) and measured fault currents are compared to the estimated RLS parameter values. It should also be noted that voltage and current measurements obtained during steady-state perturbations are extracted from the same location where the fault is applied for accurate comparison of fault levels. Results generally indicate good estimation performance of fault currents as the estimation errors are relatively low at various upstream grid fault infeeds (<%3). A maximum error of -2.67% is obtained for a 250 MVA upstream grid fault infeed whilst an a maximum error of 5% was reported in [19] for an electric arc furnace load perturbation utilizing OLS regression estimation. This shows the RLS based approach is reliable for passive short circuit monitoring as estimates are within reasonable accuracy to the expected fault current levels that may flow in the network. It should also be noted that the detailed model utilised illustrates good performance for both simplified and realistic network models. The proposed online parametric estimation approach may therefore be suitable for online implementation where actual voltage and current measurements are passively monitored to quantify system short circuit current following a series of naturally occurring load disturbances. The proposed approach can also be easily incorporated into active fault level estimation applications through the provision of an active or artificial downstream disturbance source (e.g. inductive load bank at substation auxiliary transformer) for real-time fault level measurement [23]. Recent

state of the art technology for system strength measurement includes the patented Grid-Sonar™ developed by Reactive Technologies [26]

3.3 Chapter summary and conclusions

This chapter has presented a perturbation coefficient based passive short circuit current estimation method utilising recursive least square methodologies. The developed approach models a downstream load perturbation as a net active power gain at a bus neglecting active power loss due to system voltage drops. Measurements of complex voltages and active power are input into a recursive least square estimation algorithm in order to quantify equivalent resistance and reactance estimates. These are then utilised to obtain the short circuit impedance at a given monitored location and subsequently short circuit current. The developed method is tested and validated on a simplified 11 kV distribution network model and a 4.16 kV IEEE 13 node feeder model utilising a number of case studies with results compared to simulated fault current values. The model performance of the RLS estimator is evaluated through comparisons between model predicted and measured outputs with estimation errors seen to be continuously minimised as additional event measurements are input into the RLS model with the sum of square of errors recursively minimised. This illustrates enhanced estimation performance relative to ordinary least square methods with errors within $\pm 3\%$ for a range of assumed upstream grid fault levels relative to simulated fault values.

4. Development of enhanced impedance matching line and bus-based stability indices for classical voltage stability monitoring

From the previous review chapter, a number of limitations have previously been identified in the literature regarding the performance of existing line stability indices [87]. These include the impact of load power factors, transmission X/R ratios and effect of bidirectional power flows which compromise the accuracy of existing indices. Established methods have also conventionally relied on the two-bus equivalent system models [14, 36, 88, 89] to obtain the real roots of the power and voltage quadratic equations which have neglected the effect of shunt branch admittances. This may further exacerbate negative aspects associated with the accuracy and reliability of existing index methods as line shunt susceptance has a direct impact on the parameters utilised to quantify the indices due to inherent line reactive injection. These include sending end bus voltages, reactive power flows and network voltage drops and line losses which directly affect the stability limits and margins in the network. Obtaining the discriminant of the power and voltage equations using the two-bus model has also limited the concepts and methodologies adopted to obtain line indices with limited developments using alternative concepts. The use of concepts such as impedance matching during maximum power transfer which have predominantly been utilised in bus stability index methods [39] may also be desirable.

Therefore, this chapter builds on the previous concepts and methodologies in developing line voltage stability indicators considering shunt branch admittances using a two-bus equivalent π model of a transmission line. The proposed index is based on the ratio of the load current flowing in a line to the expected fault current [89,90] flowing in the same branch. The criterion for identifying the proximity to voltage collapse is based on impedance matching theory and does not require an equivalent

Thevenin model to detect instability. The proposed approach is mathematically simple and hence computationally efficient thereby improving the robustness and cost effectiveness of existing index-based approaches for online static stability assessment. The developed method can be utilised for online voltage stability monitoring using local measurements to determine the condition of voltage stability and available margins at a given operating condition. The proposed static line index can also be reformulated as a bus-based index and therefore provides flexibility in identifying critical lines and weak buses of a given network expanding evaluation capability. The next section summarises the methodology of the developed line index.

4.1 Development of static stability indices for voltage instability monitoring based on impedance matching two-bus equivalent models

4.1.1 Equivalent two-bus π model and impedance matching

As previously discussed, the proposed indices utilise a two-bus equivalent π model methodology where sending and receiving end voltages, system admittance and bus impedance (Z_{bus}) matrix parameters are evaluated to identify the voltage instability condition of the network. The developed index utilises a π transmission line model to account for both series and shunt branch parameters to further enhance the inaccuracies inherent in existing two bus methods [14,36,87] which have neglected shunt effects. In this approach the underlying theory for voltage instability identification is based on impedance matching concepts where the equivalent Thevenin impedance and load impedance at a bus are equated and regarded as the criterion of instability detection. The next section outlines the concepts and methodology adopted to develop proposed line stability indicator.

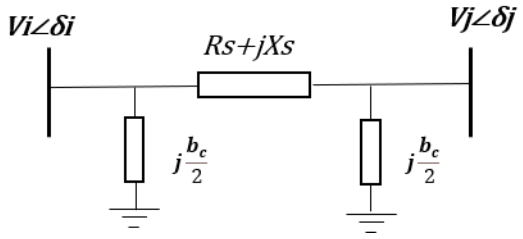

Figure 4.1 Simple two-bus equivalent π transmission line model

Assuming a simplified two-bus equivalent network shown in figure 4.1, the nodal current injections can be described from

$$I_{bus} = Y_{bus}V \tag{4.1}$$

Where Y_{bus} is the system admittance matrix and V is the complex bus voltages across a given network. Alternatively, system currents can be described in terms of the complex current injections [47] flowing in the branches where

$$I_{br} = Y_j V_j \tag{4.2}$$

Here, the parameter Y_j can be regarded as the system branch admittance matrix which relate the bus voltages to the branch currents across the network. The network admittance elements can be obtained from

$$Y_j = Y_{ij}C_i + Y_{jj}C_j \tag{4.3}$$

Where C_i, C_j are connection matrices used to define the system admittance matrix and the connectivity of the buses in the system. From the two-bus system shown, the bus admittance matrix is described using

$$Y_{br} = \begin{bmatrix} y_s + j\frac{b_c}{2} & -y_s \\ -y_s & y_s + j\frac{b_c}{2} \end{bmatrix} \tag{4.4}$$

Where

$$y_s = \frac{1}{r_s + jx_s} \tag{4.5}$$

Using equations (4.2), (4.3) and (4.4) ,the branch current injections seen at the receiving end bus is given as

$$I_{br} = Y_{ij}C_jV_j + Y_{jj}C_jV_j \tag{4.6}$$

$$I_{br} = (-y_sC_i + (y_s + j\frac{b_c}{2})C_j) * V_j \tag{4.7}$$

As previously mentioned, the motivation behind this work is to develop an approach to detect and identify the voltage stability state of the system in terms of the lines and buses in the network. When a system is gradually loaded and approaches its steady-state stability limit, it is assumed that the magnitudes of the load impedances of the network approach the equivalent source impedance quantities of the connecting buses. At the theoretical critical stability condition the voltage drops across the lines become equal in magnitude to the receiving end bus voltages [44] which result in a net active power decrease at the associated bus. This critical stability condition can be described by

$$\frac{Z_L}{Z_{th}} = 1 \tag{4.8}$$

Where Z_L and Z_{th} are the equivalent load and Thevenin impedances as seen from a load bus respectively.

This impedance matching condition refers to the maximum theoretical power transfer a line can sustain [44] prior to the network reaching a critical network state. Equation (4.8) shows that when the load impedance reaches the equivalent system Thevenin impedance, the network reaches its steady-state stability limit. In other words, when the load current flowing in the line or branch becomes equal in magnitude to the

expected fault current level flowing in the line, the network reaches an unstable state and system voltage collapse occurs. This can be described mathematically by

$$\frac{Current\ flowing\ in\ the\ branch}{Expected\ fault\ current\ flowing\ in\ the\ line} = \frac{|I_{br}|}{|I_{fl}|} \tag{4.9}$$

4.1.2 Line current index stability indicator

The proposed index simply states that when the ratio of the load current flowing in the line and the magnitude of the expected fault current level [90] (for a fault at the receiving end bus) flowing in the same line is unity, the critical stability condition is reached. In order to develop a suitable stability index for the given problem, the use of static techniques and methodologies is employed. The authors in [90, 91] propose formulae for the calculation of expected fault currents flowing in the system so as to incorporate fault level constraints in a standard OPF procedure for DG capacity allocation [91]. In order to quantify the network fault current levels, the authors propose an approach that relates OPF variables to the expected fault currents flowing in the lines for a fault at bus f. This is illustrated in figure 4.2 for a fault at the receiving end bus. The application of the expected fault current method is adopted in this work to quantify a line voltage stability index based on the ratio of branch currents to the expected fault current assuming a fault at the receiving end bus. The expected fault current of a line can be described using [90, 91]

$$I_{ij}{}^{f} = \frac{= (V_i - V_j - (FSF_{if} - FSF_{jf})V_f}{z_{ij}} \tag{4.10}$$

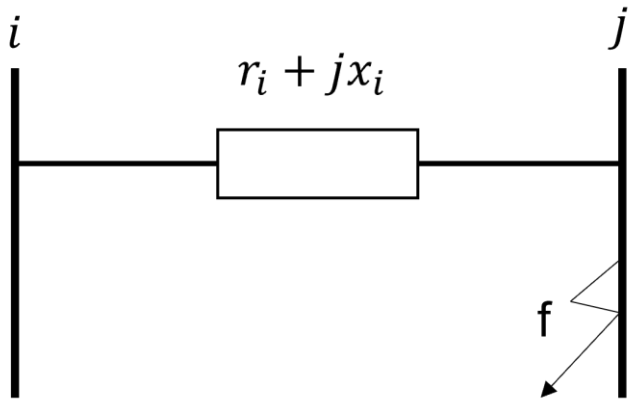

Figure 4.2 Illustration of expected fault current calculation

$$FSF_{if} = \frac{Z_{if}}{Z_{ff}} \tag{4.11}$$

Where $I_{ij}{}^{f}$ is the fault current flowing in line *i,j* for a fault at bus *f*. V_i is the prefault sending end voltage phasor for bus i, V_j Is the receiving end voltage phasor for bus j . FSF_{if}, FSF_{jf} are fault sensitivity factors [90,91] for lines *i,f, and j,f,*. V_f is the prefault voltage phasor at the faulted bus, z_{ij} is the line impedance for line *i,j*. Z_{if} *and* Z_{ff} are elements of the bus impedance matrix (where $Z_{bus} = Y_{bus}^{-1}$)

Assuming a fault occurs at the receiving end bus V_j, equation (4.10) can now be described as

$$I_{ij}{}^{j} = \frac{(V_i - V_j - (FSF_{if} - 1)V_j}{z_{ij}} \tag{4.11}$$

From equations 4.2, 4.9 and 4.11 the proposed LCI is defined as

$$LCI_k = \frac{|I_L z_{ij}|}{|(V_i - V_j - (FSF_{if} - 1)V_j|} \tag{4.12}$$

The line current index considering line shunt susceptance for the two-bus π model shown is given as

$$LCI_k = \frac{\left(-y_s C_i + (y_s + j\frac{b_c}{2}\right) * C_j V_j}{V_i - V_j - (FSF_{if} - 1)V_j} \tag{4.13}$$

The proposed index termed the Line Current Index (LCI) for an arbitrary line k can be employed to quantify the voltage stability state of a line at a given loading condition and identify the critical branches in the system. The index value varies between 0 and 1 and at the maximum loading condition reaches unity i.e. $Z_L = Z_{th}$. The index is able to assess the stability condition of a network using steady-state quantities (static analysis) with minimal computation efforts. This simple approach therefore allows voltage stability assessment in a fast and efficient manner and can be utilised as a screening tool for online voltage stability applications. The physical significance of equation 4.12 shows that when the voltage drop across a line (numerator) becomes equal in magnitude to the receiving end bus voltage (denominator) then then the stability limit [44] is reached. This further illustrates the improved approach in the developed index as the physical meaning behind the method is easily interpretable relative to previously developed line indices

From the proposed index the available loading margin (difference between current and critical loading of a load bus) can be quantified using

$$I_{L\,margin} = (1 - LCI) * I_{fl} \tag{4.14}$$

$$MW_{margin} = \frac{V_i V_j - V_j^2 - \left(FSF_{if} - 1\right)V_j^2 \cos\theta}{z_{ij}} \tag{4.15}$$

This can also be expressed in terms of available active and reactive power margins at a given loading condition and can be described by

$$MVAR_{margin} = \frac{V_i V_j - V_j^2 - \left(FSF_{if} - 1\right)V_j^2 \sin\theta}{z_{ij}} \tag{4.16}$$

The proposed line index can also be expressed in terms of a bus-based index and is termed the bus current index (BCI) in this work. This is defined as the ratio of the total branch current injections flowing into a bus to the total expected branch fault current flowing into the same bus which satisfies the impedance matching condition during

maximum power transfer. When this index becomes unity, the bus under study is said to have reached its critical state (line impedance equates load impedance). This is defined as

$$BCI = \frac{\sum_{i=1}^{N_{br\ bus}} I_{br\ j}}{\sum_{i=1}^{N_{br\ bus}} I_{fl}} \tag{4.17}$$

Where $N_{br\ bus}$ is the number of branch injections flowing into a bus j, I_{br} is the branch current flowing during normal loading and I_{fl} is the expected fault current flowing in a branch for a fault at the receiving end bus. This expression can also be descried as

$$BCI = \frac{\sum_{\boldsymbol{j=1}}^{\boldsymbol{N_{br\ bus}}} Y_{ij} C_j V_j^2 + Y_{jj} C_j V_j^2}{\sum_{\boldsymbol{j=1}}^{\boldsymbol{N_{br\ bus}}} (V_i - V_j - \left(FSF_{if} - 1\right) V_j} \tag{4.18}$$

4.1.3 Constant PQ and PV DG modelling

To evaluate the impact of distributed generation operating modes on steady-state voltage stability and index performance [3], simplified steady-state DG models are chosen to illustrate constant power factor and constant voltage control modes. As voltage instability occurs following a steady-state operating condition, simple load flow modelling methodologies are adopted to model DG as PV and PQ nodes [92]. Constant power factor DG models are therefore modelled as negative loads and constant voltage DG modelled as PV generator nodes[92]. In the event the reactive power limit of the PV generator is reached (governed by setting the power factor limits), the reactive injection is fixed at the limiting value and operates as a PQ generator (constant power factor mode).

4.1.4 SST model

Solid state transformers or smart transformers [93-96] are offering a promising solution relative to traditional low frequency transformers in terms of improving the efficiency and operation of power systems. Currently a number of trial projects have been implemented to facilitate the integration of LCTs in UK distribution networks. In addition to the voltage conversion inherent in transformer functionality, SSTs are able to offer both AC and DC supplies in their low voltage terminals and therefore reduce system losses occurring with the conversion to DC. The capability of load sharing with

other conventional transformers (and SSTs) can be regarded as an additional capability achieved by SSTs. At the HV terminals, SSTs are able to inject and absorb reactive power and therefore also offer voltage control functionality to the HV network (as a function of the SST rating). Depending on the prevailing network condition a reactive power setpoint is sent to the SST controller (analogous to STATCOM operation), however the amount of reactive power that can be controlled is dependent on the LV demand. The maximum availability of reactive power that can be injected or absorbed from the system is given by

$$Q_{ST,max} = \pm\sqrt{S_{ST}^2 - P_L^2} \tag{4.19}$$

The overall implementation of the SST is essentially comprised of three stages and are summarised as follows [96]. The first stage is a conventional AC/DC rectifier in which the incoming AC supply is transformed into its DC equivalent prior to a second DC conversion (stage 2) to a lower voltage level. This LVDC system is again converted to an AC equivalent in order to satisfy the LVAC supply and hence achieve the desired transformation functionality (stage 3).

The voltage control/reactive injection functionality of SSTs in the HV network may be regarded inherent to the operation of STATCOM units (see figure 4.3) where the injection and absorption of reactive power is dictated by a droop characteristic initiated by the exceedance of a deadband value and is essentially controlled via an external control system. The voltage measurements or setpoints determine the output reactive power required to maintain the network voltages within statuary values. In this regard, connection of SSTs to weak HV feeders may offer additional solutions to the voltage management issue during weak network conditions inherent in long radial lines and also support voltage stability performance.

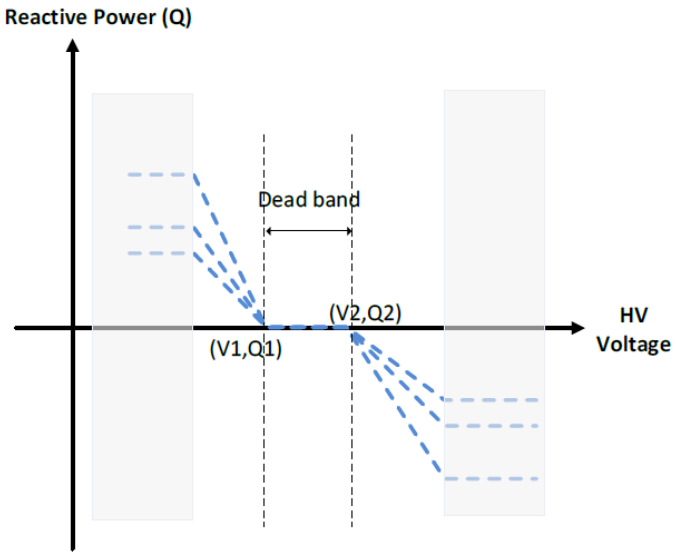

Figure 4.3 SST/STATCOM voltage control performance

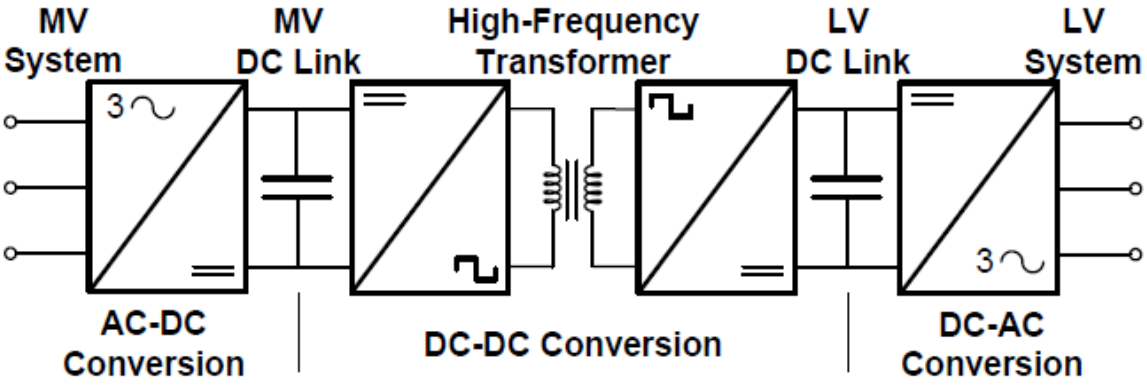

Figure 4.4 Three-stage solid state transformer model

The authors in [96] propose a two-terminal SST model suitable for power flow calculations and steady-state analysis. The approach models a three-stage smart transformer configuration (as shown in figure 4.4) consisting of an MV stage, an isolation stage and an LV stage that includes bidirectional functionality. The SST is modelled as a two terminal element where the MV and LV sides are decoupled and are therefore able to separately supply the MV and LV networks (figure 4.5). The MV stage is modelled as a load element consisting of the active power demanded by the LV side plus the losses across the transformer. The LV side is modelled as a constant voltage source serving the associated LV demand through active and reactive power

injection to the LV system. This two-terminal model is slightly modified for this study in order to include the reactive power capability of a smart transformer at the HV side and is achieved through the addition of a capacitive element across the HV terminal and is therefore able to inject reactive power to the HV network and hence simulate the HV AC reactive capability of the SST on its HV side. With SST being an emerging component in providing reactive power injection and voltage control functionality in HV networks, the evaluation on its impact on voltage stability is studied in this section. This model would later be utilized to assess its impact on the proposed static stability index. A number of studies are conducted to implement and evaluate the performance of the SST power flow model for load flow, voltage regulation, and voltage stability analysis and are summarised below

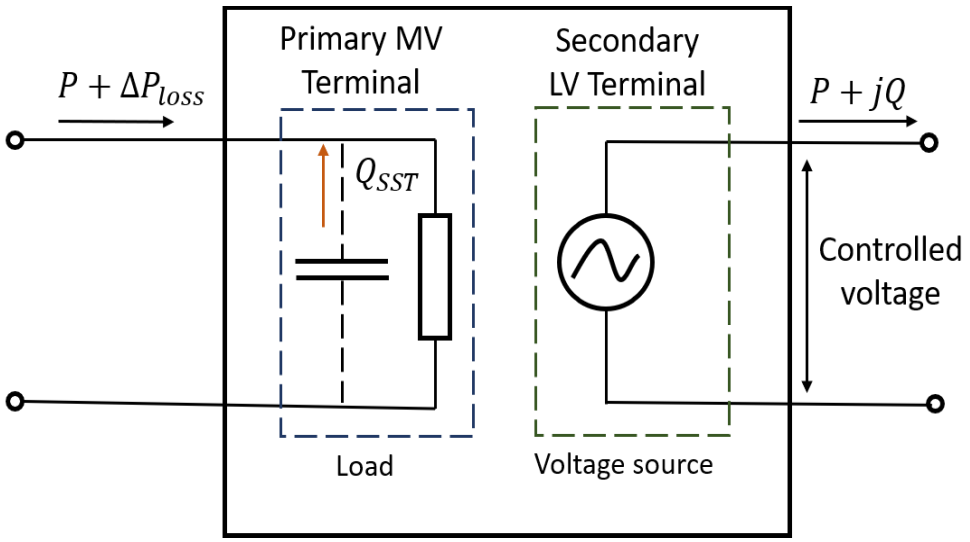

Figure 4.5 Simplified equivalent two terminal SST model (average model) [96]

The IEEE 14 bus network was selected to validate the performance of the SST model described. In this study, the transformer connecting buses 5 and 6 is removed and replaced with the SST model. The synchronous compensator connected at bus 6 is also disabled to evaluate reactive injection capability of the SST only. Reactive compensation is varied between 30-100 MVAR to study its impact on the system. Figure 4.6 illustrates the voltage profile of the network when different reactive injection values are supplied from the SST. The general trend shows that for increasing reactive power injections, the overall system voltage profile is seen to proportionately increase. The highest increases in bus voltages is shown to occur at buses 4 and 5 as

they are in close proximity to the injection source (SST HV terminal). Other adjacent buses (9,10,11) at the MV side are also seen to experience higher voltage magnitudes whilst generator buses are shown to be unaffected (buses 1,2 and 3). It can therefore be deduced that the SST reactive power injection magnitude provides an improvement in system voltage profiles for load buses.

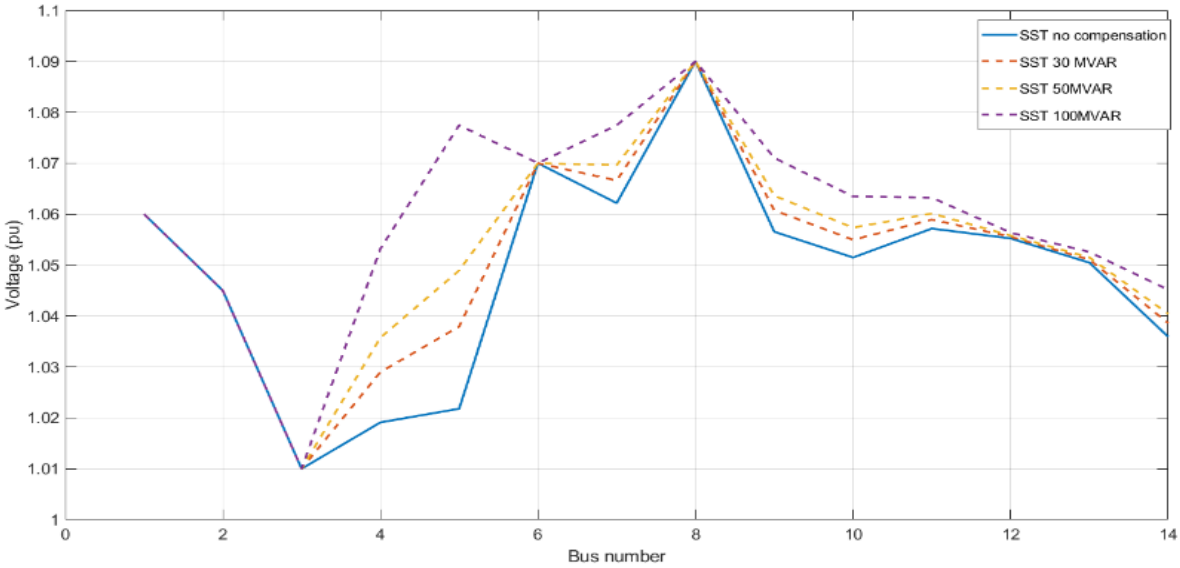

Figure 4.6 Impact of increasing SST reactive power capability on the system voltage profile

A PV study was also applied to the test network to illustrate the reactive power capability of the SST model at different MVAR injections and its overall impact on the knee point of the PV curve. Figure 4.7 shows the PV characteristic at bus 5 which illustrates that for increasing reactive injection from the SST terminal the overall knee point of the PV curve is seen to increase which improves the critical loadability for bus 5. This generally illustrates the ability for SST reactive injection functionality to

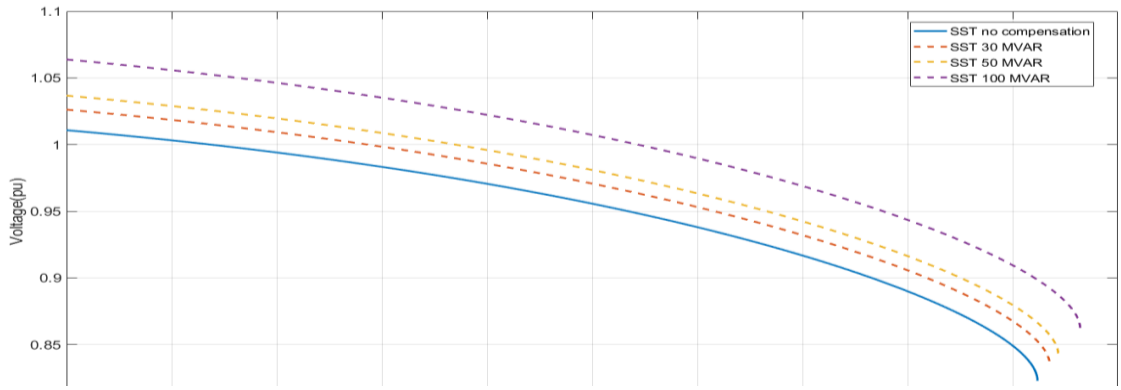

Figure 4.7 Bus 5 PV curve at different SST reactive power injection magnitudes

improve voltage stability performance across the network and enhance system strength. The overall improvement in the knee point of the PV curve is shown to be impacted at a proportional rate with increasing MVAR injection with the reactive injection varied between 30 and 100 MVARs. This shows that increased reactive power capability from an SST can improve the system performance as the maximum power that can be supplied to the buses is increased.

The next section evaluates the performance of the proposed method using a number of test networks and is compared against existing line index methods

4.2 Testing and validation studies of the proposed line stability index

4.2.1 Study description and test networks

In order to evaluate the performance of the proposed static line index, a continuation power flow study is applied to determine the knee point across system and identify the critical stability points of the load buses. Active and reactive loading at each bus is increased from base load by a factor 2.5 until maximum loadability is reached indicating system voltage collapse. The developed LCI index is calculated from equation (4.13) and performance evaluated using a number of case studies and compared against existing line indices previously described. Case studies investigate the effects of load power factors (modelled as constant power loads), transmission X/R ratios, DG control modes (constant voltage/constant power factor), penetration levels and SST power flow models on index performance. The developed LCI is evaluated using the IEEE 30 bus and IEEE 118 bus test systems.

4.2.2 Impact of active and reactive loading on the developed index for the IEEE 30 bus system

In this study, active and reactive loading is increased on all load buses until system voltage collapses via a continuation power flow with LCI calculated at each load increment. Figure 4.8 illustrates the LCI characteristic for bus 20. As system loading is increased, the branch currents flowing in the lines approach the expected fault current values and at maximum loadability, the currents become equal in magnitude

illustrating the stability limit is reached. A loading multiplier as a function of initial or base case loading is utilized to measure system loading at a given operating point. It can also be seen that at higher loading levels, the rate at which the index increases become higher as the system approaches the knee point of the PV curve or maximum loading condition. The figure also illustrates different trajectories for active and reactive loading. This shows that the nature of the load impacts the overall characteristic of the index at a given loading condition. Further studies will evaluate the impact of different load power factors on index performance. At a given loading point or operating condition, the index value generally shows the proximity to collapse or available loading margin. When the critical limit is reached, the line index approaches unity. This characteristic differs for each line as the respective fault current levels and corresponding branch currents are not equal in value. It can be seen that line 25 exhibits highest criticality and is therefore the weakest relative to lines 9 and 31 as the corresponding LCI value is maximum at the stability limit. Lines 25 and 31 are bothc onsidered critical for both active and reactive loading whilst line 9 remains stable (LCI< 1) for both loading conditions. It can also be observed that at a given loading point, the lines closer to instability can be identified (indicated by higher index magnitudes).

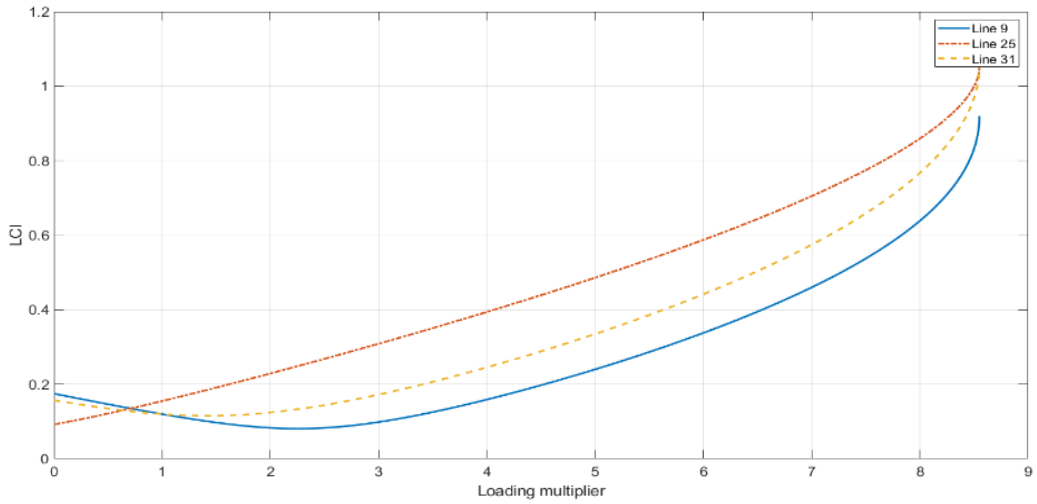

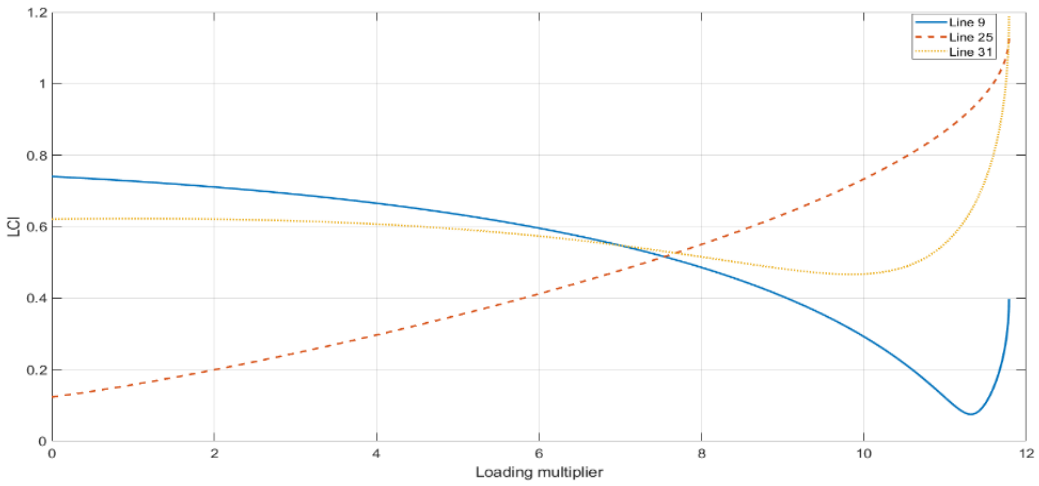

Figure 4.8 LCI index performance for (i) active and (ii) reactive loading at bus 20

Figure 4.9 and 4.10 show the impact of active and reactive loading on line indices across the branches for loading at buses 15, 20 and 30. For the active loading case, lines 10 and 26 have been identified as the critical lines in all bus loading scenarios. Active loading at bus 20 has additionally identified a critical line for line 31. Similarly, different critical lines are identified for reactive loading at the selected buses. This shows that loading at various buses impacts the stability performance differently for a given network. It can also be observed that the number of critical lines identified for the reactive loading case illustrates lower stability performance than in the case for active loading. This can be justified as the higher transmission of reactive power results in larger voltage drops across the system resulting in lower stability margins when compared to the active power loading case. In other words, increased reactive power demand would reduce the maximum active power transmission capability of the network as a result of larger drops across the system which moves the system closer to the knee point of the power-voltage curve.

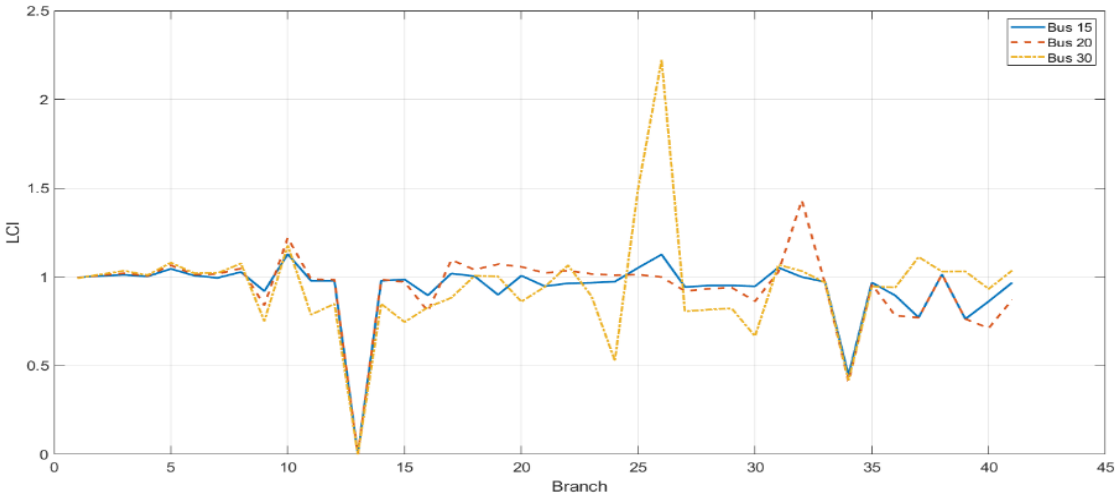

Figure 4.9 System line stability indices using developed method for active loading at buses 15, 20 and 30

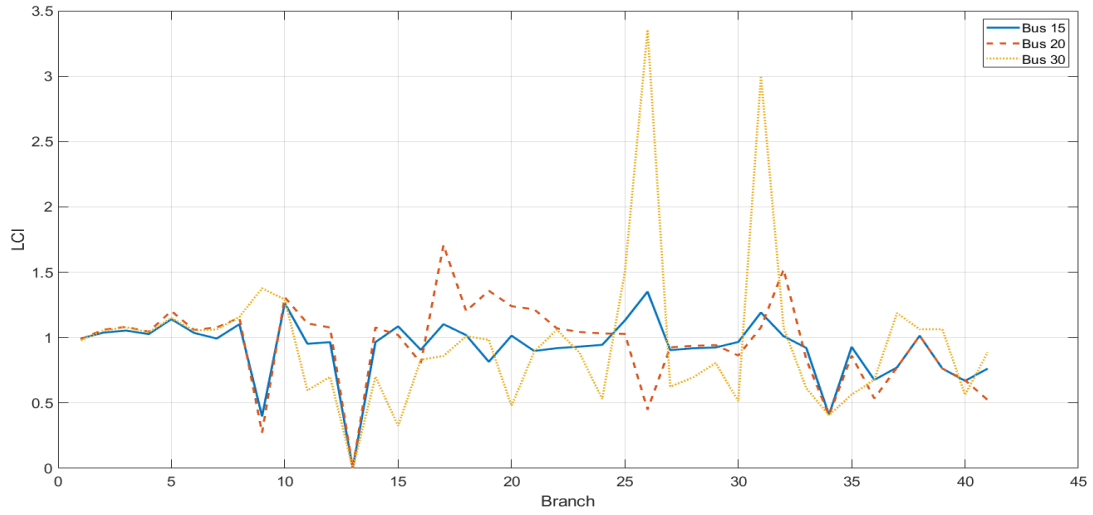

Figure 4.10 System line stability indices using developed method for reactive loading at bus 20

Results also illustrate the LCI index demonstrates improved accuracy and is comparable in performance relative to existing line index methods (Table 4.1). For the majority of the selected lines, at the critical stability condition the index values approach a value of 1 pu. Table 4.1 shows the LCI index exhibits similar performance characteristics to the L_{mn} indicator as the values of the lines are similar in magnitude. The LQP index estimates lower values at the stability limit (e.g. line 10) illustrating inferior performance in comparison the L_{mn} and LCI indices, as they approach the theoretical limit of 1 for a critical line. This generally indicates the effectiveness of LCI in determining the correct value of the index of a line at the stability limit.

Table 4.1 Comparison of line stability indices of selected lines for the IEEE 30 bus network

Line	**LCI**	**L_{mn}**	**LQP**
8	1.01294	0.80132	0.52015
10	1.01381	1.16427	0.64228
12	0.95030	1.44930	0.59946
15	0.86119	1.09019	0.81820
20	0.91549	1.00449	0.18541
26	1.14637	1.19054	0.14231
31	1.06876	0.85836	0.26430
34	1.58006	0.40093	0.22185
39	1.10584	0.58957	0.26968

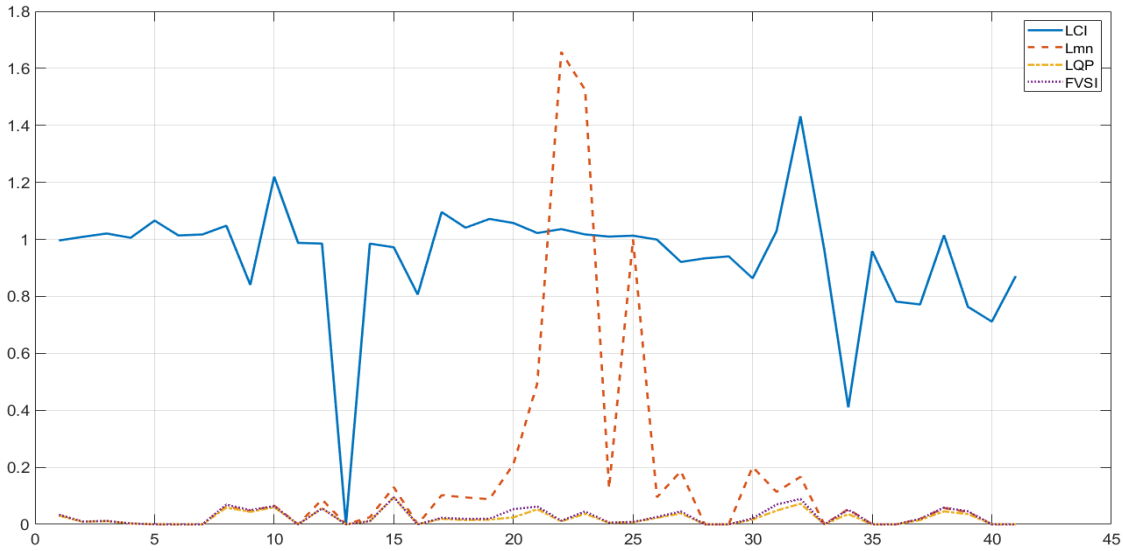

Figure 4.11 Comparison of system line indices against developed LCI index

From figure 4.12 as system load is gradually increased the indices follow a similar trajectory as the system approaches its stability limit, with both L_{mn} and LCI reaching an index value of 1.16427 and 1.01381 respectively. The index trajectory shows a linear characteristic up to a loading multiplier of 2 pu with the rate of increase becoming non-linear up to the collapse point. Both the LQP and FVSI settle at a value of 0.65 illustrating the critical condition does not reach the theoretical of 1. Similarly,

for line 26, both the L_{mn} and LCI indicators reach a value of 1.19054 and 1.14637 respectively at the stability limit and both methods correctly identify the critical line. The LQP index exhibits a lower value for line 26 illustrating a misclassification of a critical line. Figure 4.13 illustrates the LCI characteristic for lines 15,26 and 38 from base case to critical loading with lines 26 and 38 identified as critical lines. Relative to existing line index methods (FVSI, Lmn, LQP), the proposed LCI obtains comparable values at the stability limit and follows a similar trajectory from base case to critical loadability, and is able to reach/exceed the theoretical stability indicating a critical condition is reached. The approach incorporates shunt admittance and susceptance parameters in index calculation (equation 4.13) which have been neglected in existing methods illustrating improved performance.

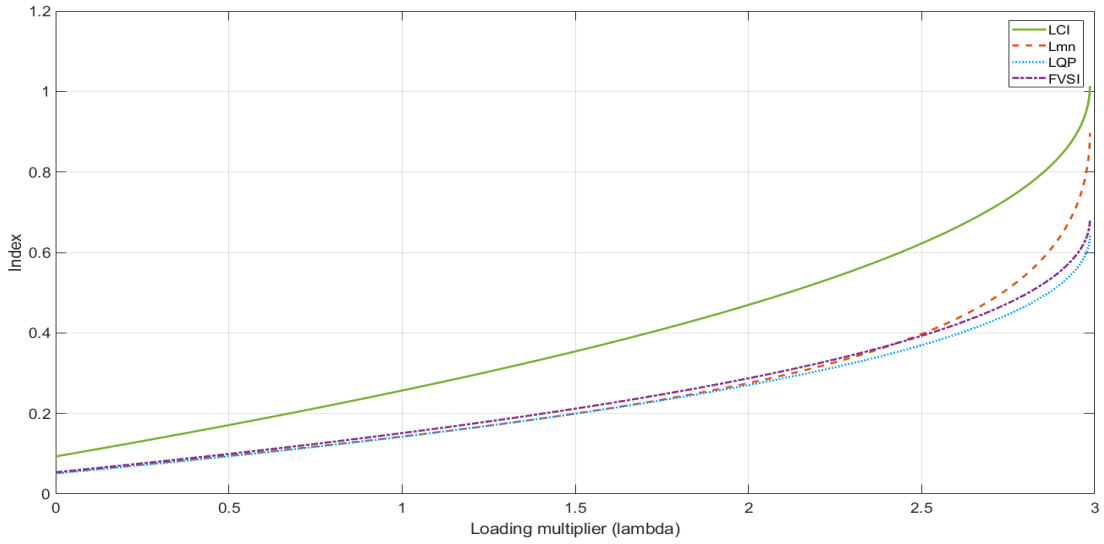

Figure 4.12 Comparison of line index performance vs system loading for line 10

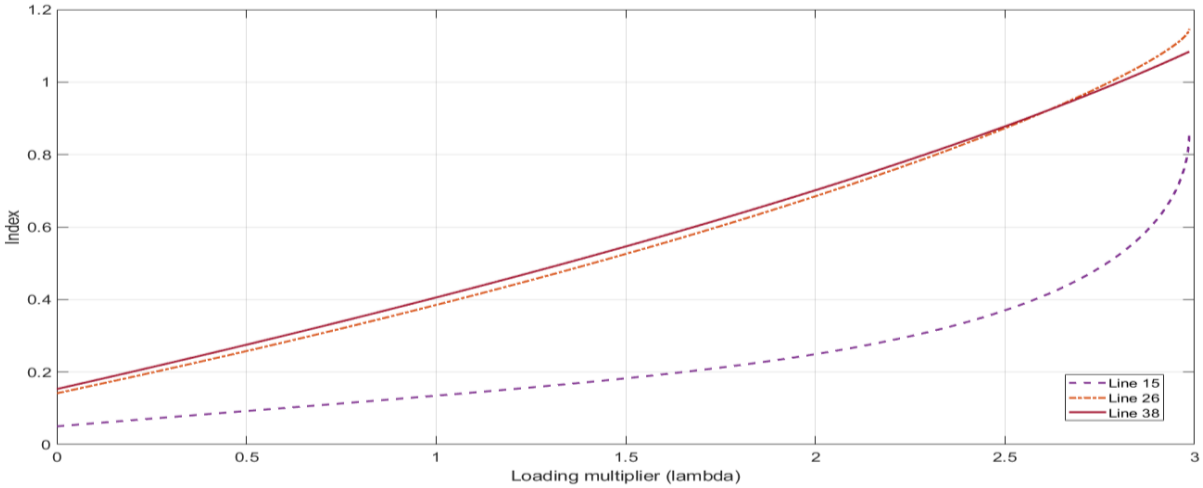

Figure 4.13 Comparison of LCI index and system loading for lines 15, 26,38

4.2.3 Comparison of index performance in the IEEE 118 bus test system against L_{mn}, LQP and FVSI indices

Similar to the previous study, voltage stability assessment via continuation power flow was performed to evaluate the performance of the proposed index relative to existing line indices for the IEEE 118 test network (figure 4.14). Results generally indicate the accuracy and improved performance of the LCI index when compared to the existing indices under a number of operating conditions. Table 4.2 shows the index values for LCI, LQP and L_{mn} or lines 164-186. The indices in this scenario are generally very comparable in magnitude across all the lines relative to the previous test case which demonstrates the scalability and accuracy of the proposed approach for larger network stability assessment. It can also be seen that the index values across the lines are relatively lower than in the previous test case indicating a generally more stable system as the indices do not reach the critical stability limit across the network. This illustrates that the LCI method can be a reliable indicator in determining the proximity to voltage collapse for large networks at a given loading condition and is able to identify the available stability margins at a given loading condition. This is illustrated in figures 4.15a and 4.15b with active and reactive margins calculated from (15) and (16) respectively

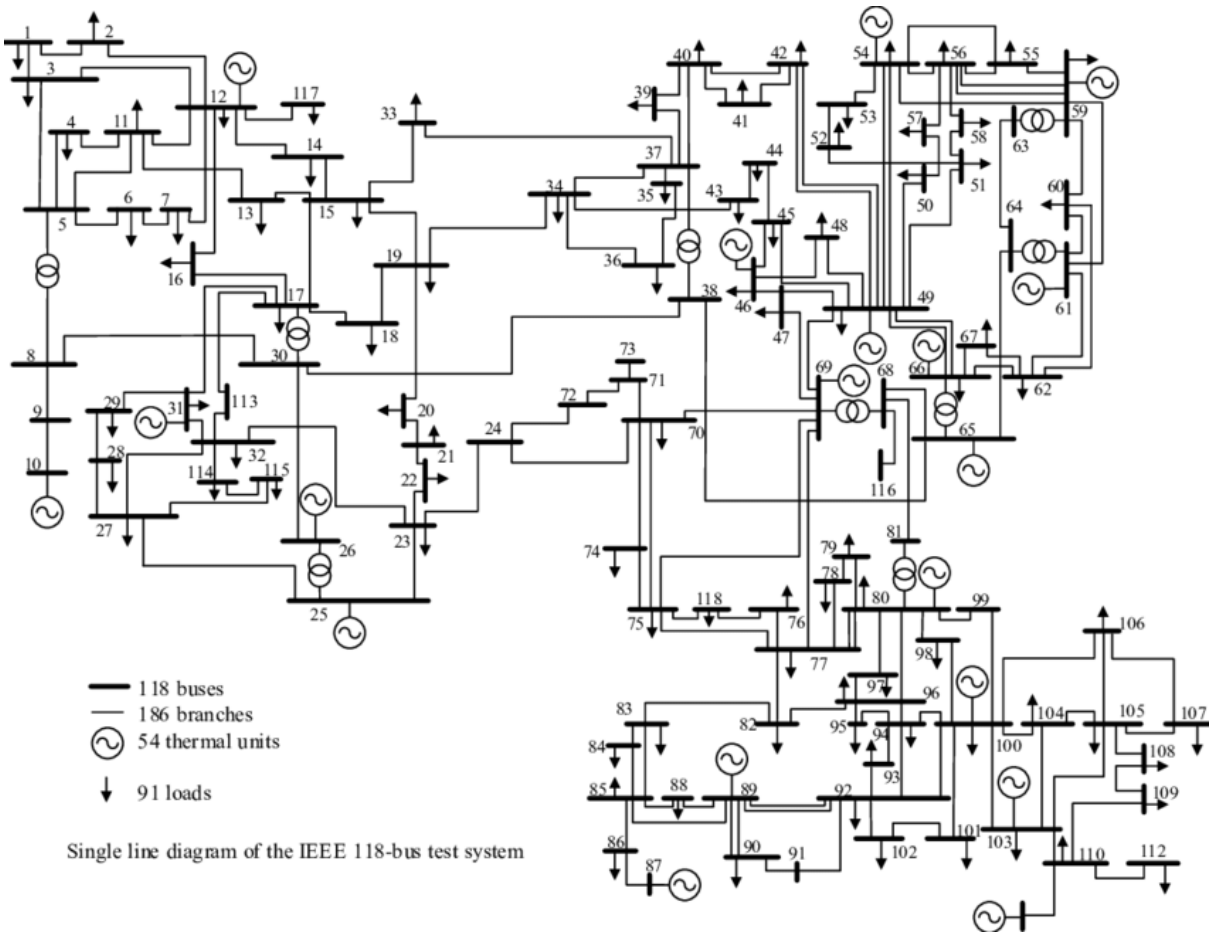

Figure 4.14 IEEE 118 bus test network

Table 4.2 Comparison of line stability indices for the IEEE 118 bus network for lines 164-186

Line	**LCI**	L_{mn}	**LQP**
164	0.64947	0.67941	0.63045
165	0.62164	0.65931	0.49560
166	0.73851	0.76977	0.52875
167	0.67637	0.51448	0.45393
168	0.97627	0.35067	0.13296
169	0.31118	0.23655	0.11995
170	0.41557	0.91575	0.30216
171	0.25415	0.02158	0.00985
172	0.53349	1.03857	0.33580
173	0.40045	0.04085	0.01201

174	0.67496	1.24852	0.68065
175	0.87439	4.49486	0.31794
176	0.33408	0.00000	0.00032
177	0.58887	1.45729	0.11226
178	0.09156	0.00000	0.00002
179	0.16558	0.00000	0.00360
180	0.05912	0.02529	0.02557
181	0.19465	0.07654	0.07114
182	0.05578	0.01147	0.01035
183	0.18507	0.00000	0.00000
184	0.13638	0.14788	0.14690
185	0.15824	0.11730	0.11279
186	0.18539	0.12567	0.11731

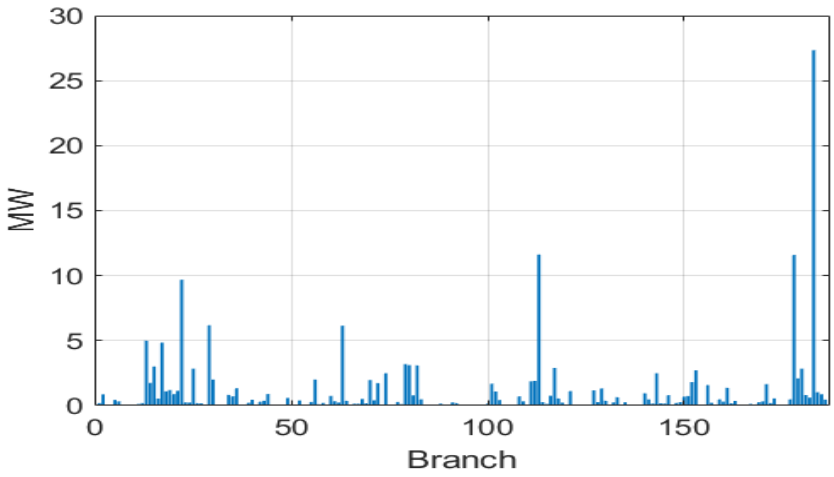

(a)

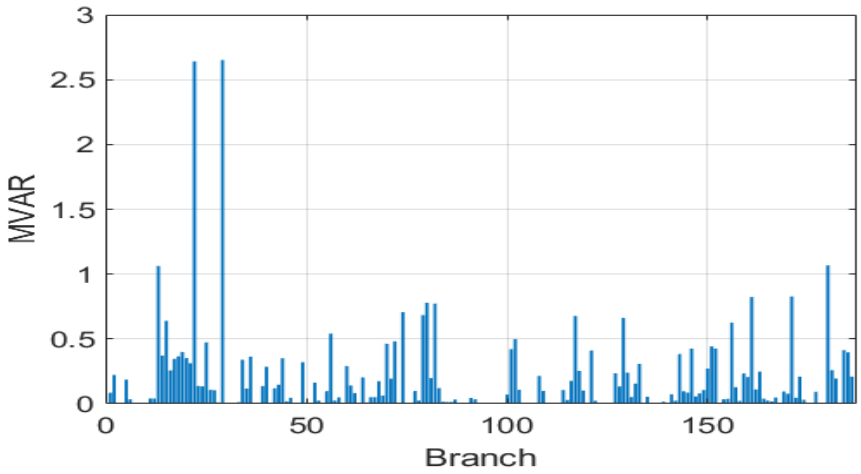

(b)

Figure 4.15 Available (a) MW and (b) MVAr margins at critical loadability condition

Figures 4.16a and 4.16b show that both the FVSI and LQP indices follow a similar trajectory to the LCI in terms of identifying the index values across the branches in the network. Both methods identify the critical lines (as indicated by index values of 1) but a general improvement in the performance of the LCI can be seen as the values of the indices are relatively high across all the lines during the simulated stressed condition when compared to the LQP and FVSI methods. These approaches are able to identify the lines whose indices are greater than 1 (critical) lines but the ability to determine the stability margins of the non-critical lines is generally less accurate (as indicated by the low index values). Similar to the IEEE 30 bus system test case, the LCI method produces similar index magnitudes to the L_{mn} approach and follow a similar characteristic across all the branches in the system. This is illustrated in figure 4.16c. This further demonstrates the proposed approach as a more reliable indicator when compared to the LQP and FVSI indices in assessing the stability condition and associated margins at a given loading condition.

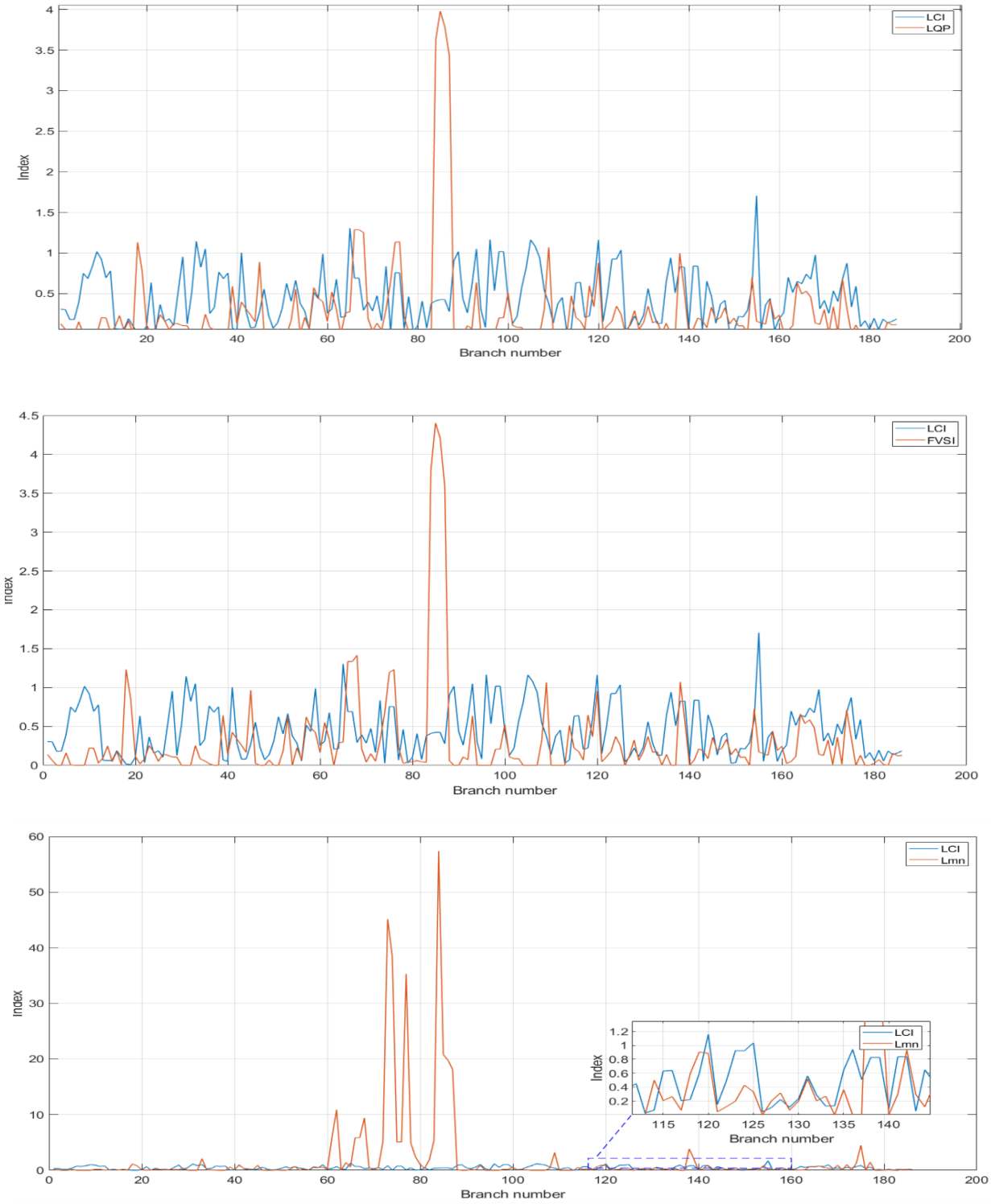

Figure 4.16 System line stability index performance for the IEEE 118 bus network against (a) FVSI (b) LQP index (c) Lmn index

Figure 4.17 illustrates the characteristic of line 164 for different line stability index values when the system is gradually increased to its stability limit.

Indices LCI, LQP and FVSI exhibit comparable characteristics as they start at a low index value at base load and proportionately increase to a maximum value at the critical loading condition. It should also be noted that despite the L_{mn} index exhibiting a different index characteristic, at the stability limit, it settles at a value of 0.679 and is comparable in magnitude to the LCI (0.649) and LQP (0.630) indices indicating good accuracy for a large network model. This illustrates the proposed approach is accurately able to determine index values for large networks for both critical and stable line conditions. The method also incorporates indices (LCI) in the OPF that account for shunt branch admittances which have not been previously utilized in index-based VSCOPF methods and is addressed in chapter 5.

Another advantage of this approach is its ability to assess stability conditions using steady-state parameters with minimal computation efforts. The LCI approach can therefore be used as a screening tool to identify the critical lines in the network and assist in taking corrective actions to improve stability performance and associated margins. As the index considers voltage and active power variation (through load and fault level calculation), in addition to the modelling of line shunt capacitance (from system admittance and bus impedance matrices), the approach can be regarded more accurate in capturing the stability condition and proximity to voltage collapse.

With the forecasted decline in network short circuit levels, risks of voltage instability are seen to be higher as a result of reduced power transfer capability and reactive resource availability. Accurate, reliable methods and tools in determining the stability condition of the network using stability indices can support maintaining the network below its steady-state stability limit through corrective and preventive action. The methodology of the proposed method is drawn from quasi steady-state analysis techniques and is based on the concept of impedance matching during voltage instability. The developed approach can potentially be used in other applications where the stability condition of the network can be improved through corrective action to enhance stability margins across the system. This methodology of utilising stability indicators has predominantly been used in power system optimisation problems

including DG placement and stability-constrained optimal power flow formulations [58, 59].

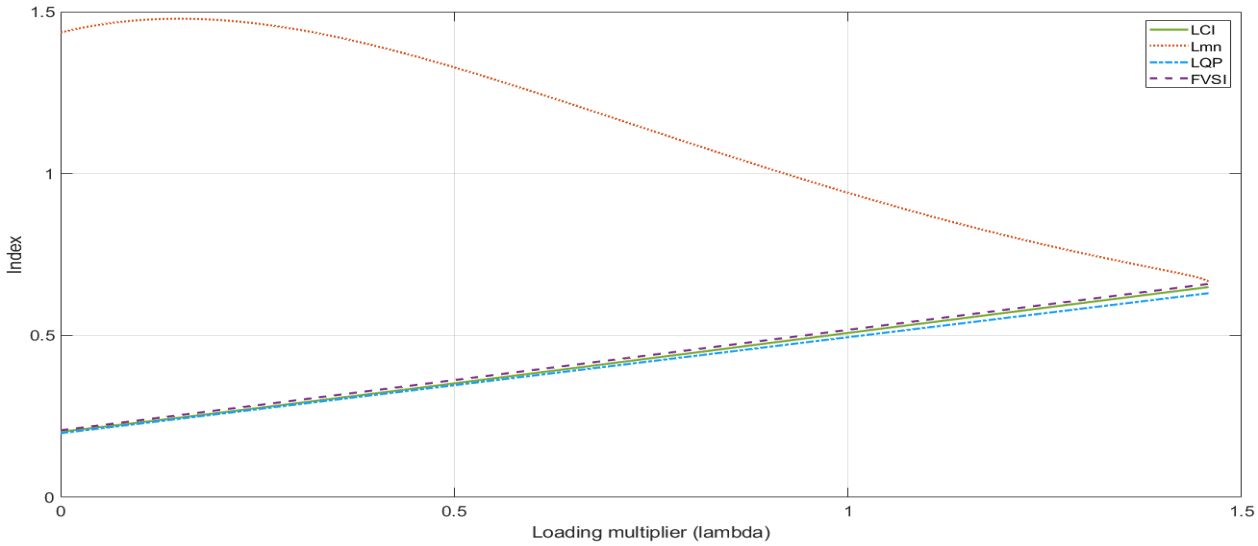

Figure 4.17 Line stability index characteristic vs system loading for line 164

4.2.4 Impact of transmission X/R ratio on line index performance

The purpose of this study is to evaluate the performance of the developed index with varying X/R ratio to simulate the effect of longer transmission distances and weaker network connections to the main power grid. The study also aims to evaluate the impact of X/R ratios on steady-state stability using the developed line index. For this case, line X/R ratios are varied between 2-10 and the resulting indices plotted against system loading and LCI magnitudes assessed at the critical condition for the branches in the network. From figure 4.18, it can be seen varied X/R ratios have negligible effects on the magnitudes of the indices, as all indicate a critical condition for line 25. However higher X/R ratios have a significant impact on the maximum loadability condition with larger X/R ratios resulting in lower maximum power transfers for the line under study. With higher transmission reactances, larger voltage drops are seen across the network causing a reduced active power transfer capability. Larger line reactances result in weaker network connections producing lower system short circuit levels which impose lower stability margins. This illustrates that in future network scenarios, lower short circuit levels from synchronous generation displacement may also result in similar reduced stability performance conditions as the system is weaker.

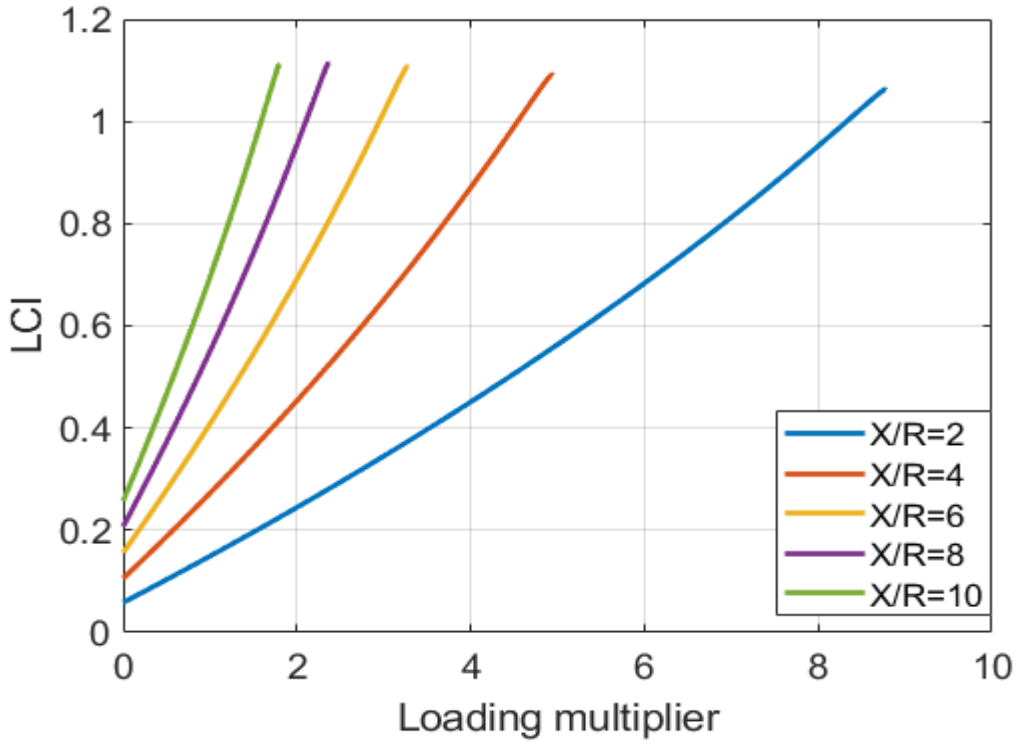

Figure 4.18 Impact of transmission X/R ratios on stability performance utilising LCI for line 25

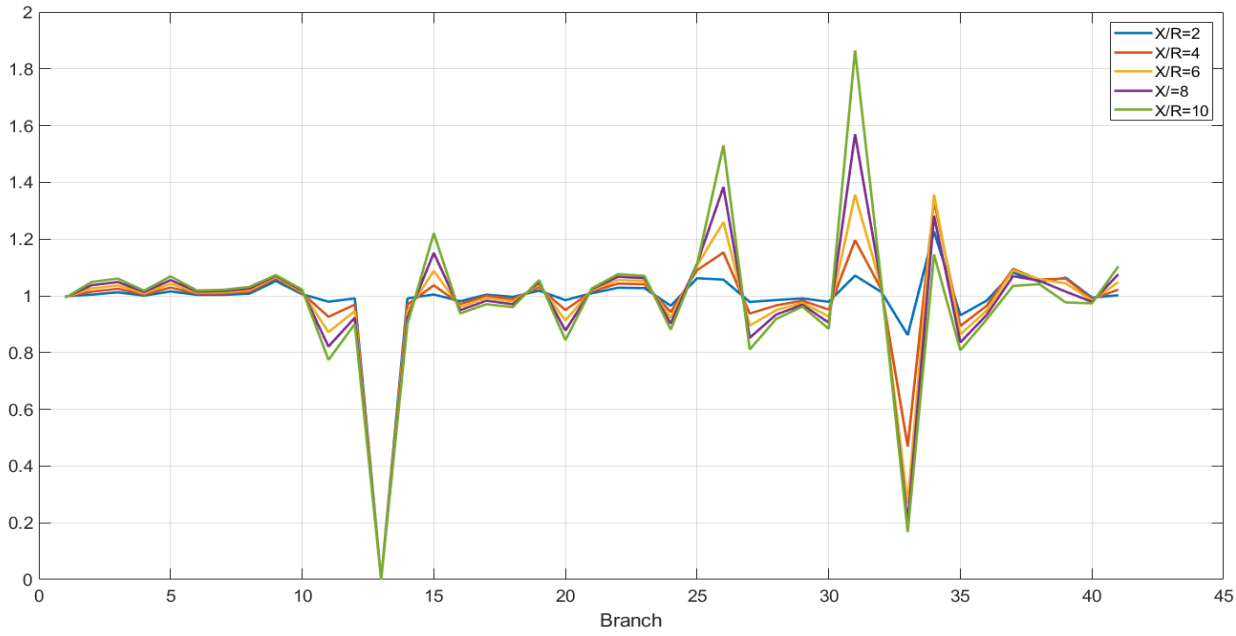

Figure 4.19 Impact of X/R ratios on system LCI indices

Figure 4.19 shows the impact of line X/R ratios on index magnitudes across the branches in the system under study. Similar to the previous assessment, the overall trend shows reduced system stability performance for larger X/R ratios. This relation can be regarded as proportional as higher line reactance and corresponding larger drops

and losses reduce the overall transfer capability of the system. However, the influence of X/R ratios is not uniform with some regions in the network experiencing reduced index magnitudes having higher margins and exhibiting improved stability performance than with low X/R ratios. From the figure, non-critical lines are seen to show improved stability performance with larger X/R ratios whilst critical lines result in larger index magnitudes for a given X/R value. However the overall trend shows significant reduction in the maximum transfer capability of the lines irrespective of its proximity to collapse as discussed in the previous study.

4.2.5 Impact of SST, constant voltage and constant power factor DG models and penetration levels on index performance

From the previously described SST load flow model, a study was conducted on the IEEE 14 bus network to evaluate the impact of SST reactive capability on the developed LCI . The study methodology, similar to the previously described SST study involved replacement of the conventional transformer between buses 5 and 6 with the SST. Reactive injections at the HV terminal (bus 5) are varied between 30-100 MVARs with index values compared with no SST installed. Figure 4.20 illustrates the LCI performance with and without SST compensation injected in the system. A proportional reduction in index values can be seen for line 12 with increasing injection as it is in close proximity to the SST location, however the line is seen to remain in a critical condition. The criticality of line 12 is shown to be lower with no SST connected with the system becoming more unstable with the SST connected at the same location. There is an overall reduction in the calculated expected fault current in line 12 as the previously connected compensator model at bus 6 was disabled resulting in a weaker system condition and hence higher index values are reached relative to the compensated network model with no SST connected. This illustrates that SSTs may not be effective in providing sufficient reactive compensation functions for stability enhancement and may be more suitable for voltage regulation and voltage profile improvement, however increased reactive compensation from SSTs may further facilitate increased DG capacity integration capability. Placement and sizing of compensation equipment including shunt capacitors, FACTs and condensers at

specified weak buses may therefore be more effective for instability prevention as stability phenomena is a localised network condition.

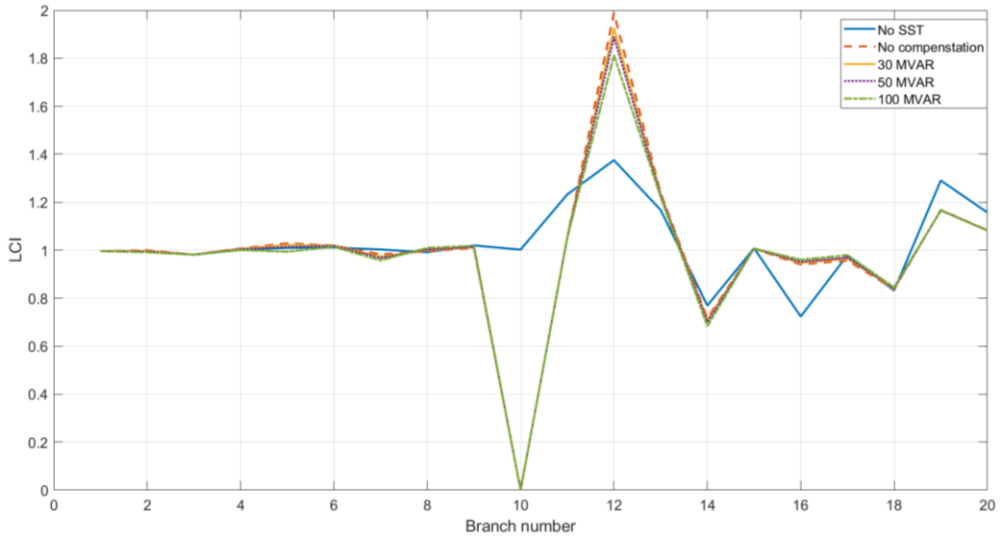

Figure 4.20 Impact of SST reactive injection on LCI performance

As previously mentioned, the purpose of the following study is to evaluate the performance of the developed indicator against various types of distributed generator models and operating modes. With the expected increase in DG penetration, operating at various control modes, the overall influence system stability and on the characteristic of line stability indices is investigated in this study. As discussed in the previous sections, the models employed rely on incorporating DG modelling methodologies adopted in steady-state analysis studies. In this regard, generic PV and PQ distributed generator models are utilised to simulate constant voltage and constant power factor control operating modes. As addressed in the previous chapters, depending on DG technology (inverter based, induction or synchronous), the control circuit functionality can either control P and V independently (PV model) or control P and Q independently for a constant power factor (PQ) model. Both steady-state models are incorporated in this study to evaluate the impact on the proposed line stability indicator. The PQ model is taken as a negative load whilst the PV generator utilizes a conventional voltage source model as described previously.

The studies investigated in this section aim to compare the performance of DG models with respect to the voltage stability index developed in this work. The overall influence of DG penetration levels on system stability performance and its effect on the index

characteristic at various operating conditions will also be studied. The IEEE 30 bus network will be utilised in this section to perform associated assessments. DG models are connected at bus 13 replacing the active and reactive power generation of the conventional unit connected at the bus and neighbouring nodes are studied to evaluate voltage stability performance via the developed index.

Figures 4.21 and 4.22 illustrate the impact of multiple DG models at various operating modes on the network voltage profile (at the critical condition) and system PV curve respectively. Incorporating PV models has the least improvement in system voltage profile relative to the PQ DG models. Operating a PQ generator at 0.95 power factor provides additional reactive support and results in higher voltages across the network. It can therefore be seen that PQ models can achieve stiffer bus voltages at a given loading condition. In terms of voltage stability improvement, the adoption of constant voltage generator models result in higher active power transfers when compared to no DGs connected in the network. Conversely the use of constant power factor models cause a significant reduction in the voltage stability margins and reach their respective critical state at higher voltage magnitudes. Having the PQ generator operating at 0.95 power factor increases the maximum loading capability of line 15 as additional reactive injection is supplied by the generator, however constant voltage control DG models offer improved stability performance overall as higher active power transfers can be sustained. It can therefore be deduced the PQ model-based DG would require additional reactive compensation to maintain stability margins within acceptable limits.

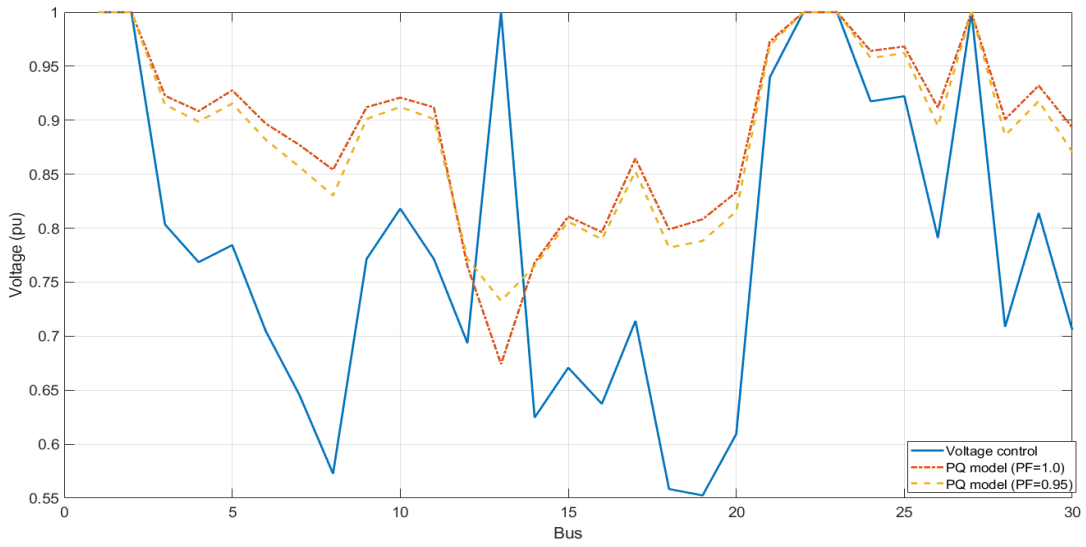

Figure 4.21 Voltage profiles under various DG models at the critical condition

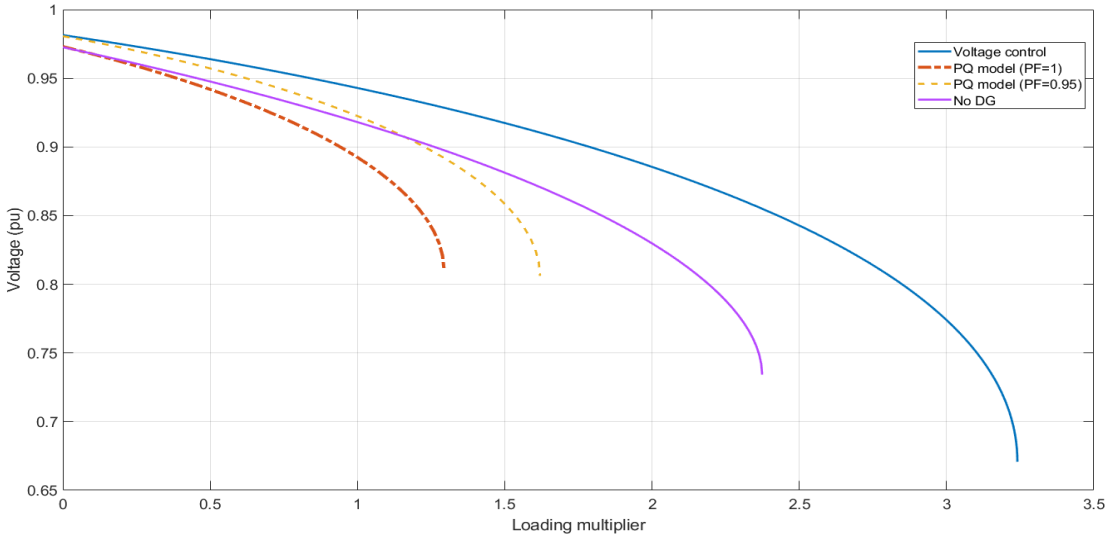

Figure 4.22 System PV curve for bus 15 for constant voltage and constant power factor DG models

Figures 4.23 and 4.24 illustrate the impact of the DG control modes (connected at bus 13) on the performance of the developed line index. As illustrated in the PV study, the application of PQ control (negative load model) result in lower active power transfers across line 15 with the unity power factor model showing inferior performance as no reactive power is injected by the generator. The use of constant voltage models demonstrates a significant improvement in the maximum loadability of the system however the impact of the DG models on the magnitude of the index at the critical condition is less severe. From figure 13, the impact of PV DG models results in relatively lower indices across the system illustrating improved stability performance

relative to constant PQ models. As with the previous studies, higher power transfers can be achieved when utilising PV models on neighbouring nodes and across the overall network. DGs operating at various power factors have negligible effect on the magnitude of the indices across the system at the critical condition. The application of reactive compensation from alternative sources (shunt capacitors, STATCOM, etc.) can therefore be more effective in improving system stability when operating DGs at constant power factor modes.

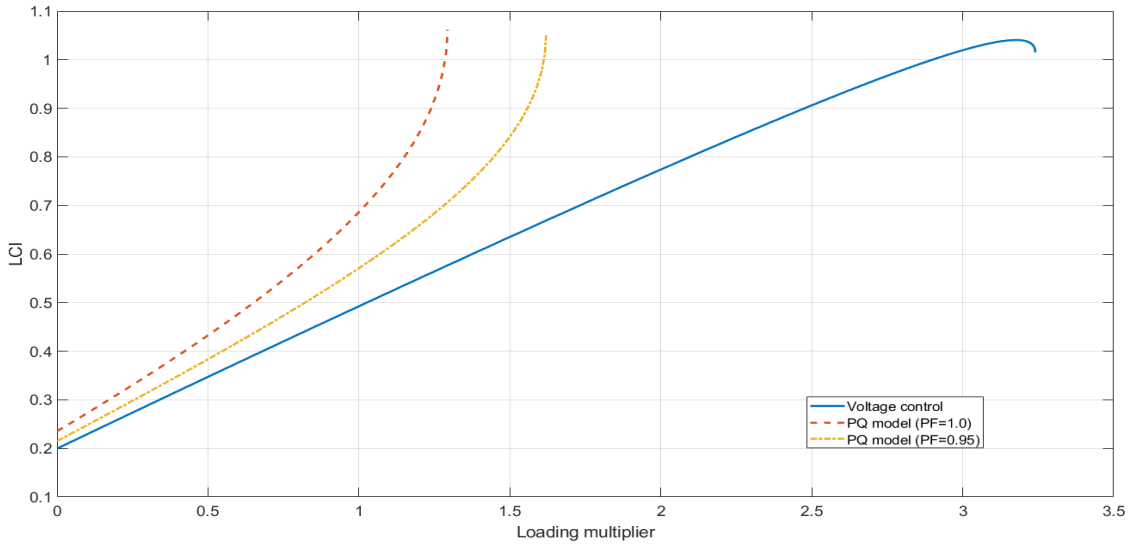

Figure 4.23 Impact of DG model operating mode on system stability utilising developed line index

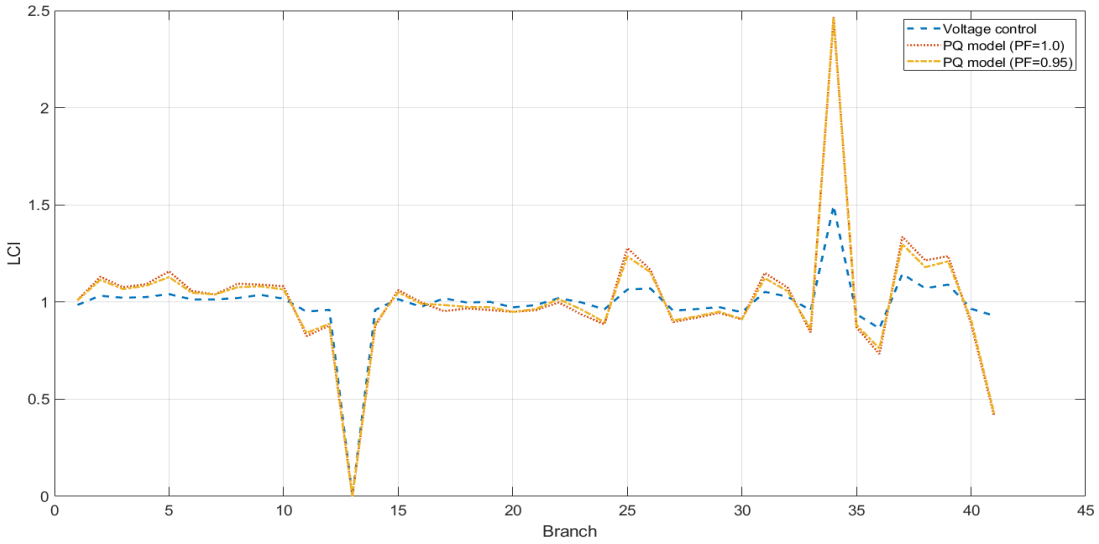

Figure 4.24 Impact of DG operating mode on system LCI indices

With increasing DG penetration levels, the overall trend shows a proportional reduction in system stability performance for line 15 when utilising PQ models (figure

4.25). As system loading is gradually increased, the maximum power transfer the line can withstand is significantly reduced. In other words, higher penetration of DG (at constant power factor modes) can result in weakened system conditions and thus the maximum loadability of a line is proportionately reduced. Conversely, the increase of PV based DG impacts the network stability characteristic differently than when using a PQ based DG.

From figure 4.26, having DG penetration of up to 20% initially improve the associated stability margins as the impact on maximum loadability is minimal with 5% penetration resulting in lower indices and higher active power transfers. With no DG connected, line 15 is seen to remain stable and not reach the critical condition. A 20% penetration level or higher results in a critical condition on with proportional reduction in the maximum transfer the line can sustain with the worst-case scenario at 50%. However, the overall performance of the system utilising constant voltage DG modes show improved stability margins and lower index magnitudes at the critical network state. From this study, the utilisation of PV models can result in higher DG penetration levels and reduced impact on system stability performance when compared to PQ operating modes. This also results in lesser reactive compensation requirements to maintain stability margins within acceptable limits.

With the expected decline of network short circuit levels due to the displacement of large synchronous generation with small scale distributed generation, the overall impact can be seen to significantly reduce the steady-state voltage stability capability of the network. It can therefore be deduced that regions in the network experiencing reduced stability performance (e.g. weak regions) would benefit from increasing penetration levels of specific generation technologies operating at constant voltage modes as lesser reactive compensation requirements are needed (when compared to PQ modes) from other sources connected in the network resulting in reduced operating costs.

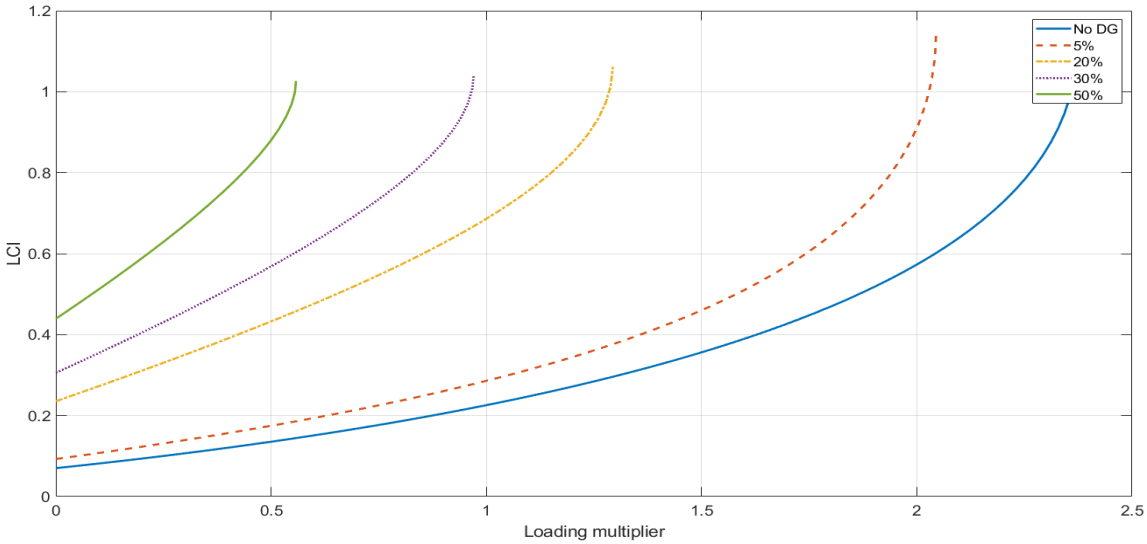

Figure 4.25 Increasing DG penetration levels for constant power factor mode (line 25)

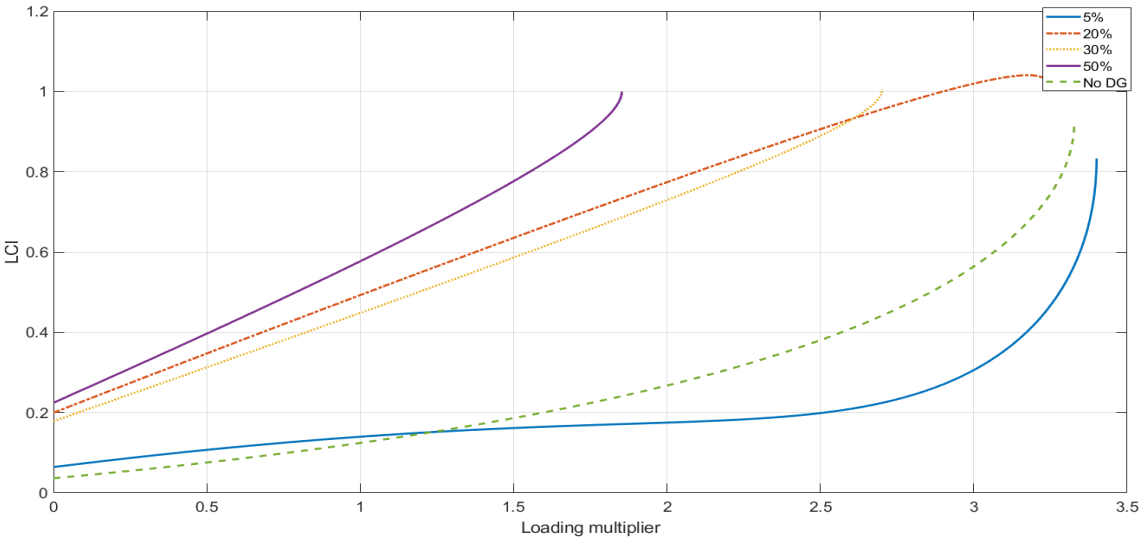

Figure 4.26 Increasing DG penetration levels for constant voltage mode (line 25)

4.2.6 Testing and validation studies of the proposed bus current index (BCI) method

To evaluate the performance of the proposed bus-based stability index, similar to the previous studies, active and reactive loading of all load buses was increased until system voltage collapses. The developed BCI is calculated at each loading point from (18) where the index performance is evaluated for the IEEE 14 bus and 30 bus test systems. Figure 4.27 illustrates the behaviour of the index as loading is increased to

the collapse point for buses 5,8 and 14. It can be seen both buses 8 and 14 start at a stable point at base case loading and gradually increase with bus 14 reaching instability with a final index value of 1.079 pu (at critical loading) and bus 8 remaining stable at 0.769 pu. Bus 5 is seen to approach the critical limit from base loading and reaches 1.002 at critical loading. It can therefore be deduced from the figure that both buses 5 and 14 are weak buses with bus 5 and 14 the strongest and weakest buses. Table 4.3 summarises the BCI values at the stability limit for the IEEE 14 bus system.

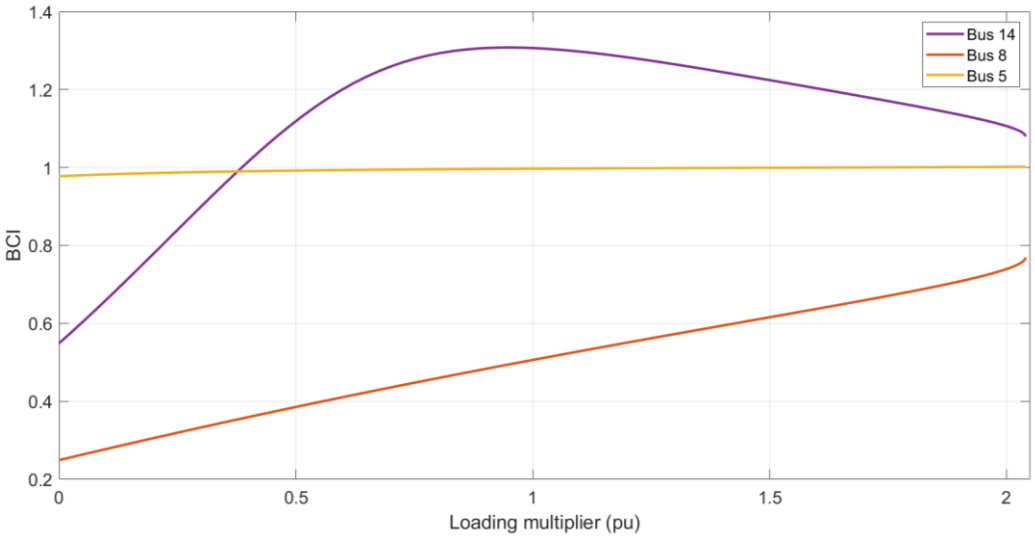

Figure 4.27 Bus current index performance for buses 5, 8, and 14 for the IEEE 14 bus test system

Table 4.3 BCI values at the critical condition for the IEEE 14 bus network

Bus	BCI
1	0
2	0.99606
3	0.98083
4	1.00541
5	1.0021
6	1.00235
7	0.99136
8	0.76912
9	1.01184
10	0.72376
11	1.01239
12	1.37523
13	1.18221
14	1.0794

Similarly, figure 4.28 shows the index characteristic for buses 12, 26 and 30 when the system is loaded to the collapse point. Both buses 26 and 30 are seen to be exceeding 1 pu BCI value indicating an unstable condition with bus 12 reaching 0.872 pu at the critical limit. Both buses 26 and 30 are regarded as the weak buses with bus 26 ranked as the weakest in this scenario with the highest BCI magnitude. At base case loading both buses 26 and 30 exhibit high BCI values which illustrate a weak bus characteristic at low loading conditions.

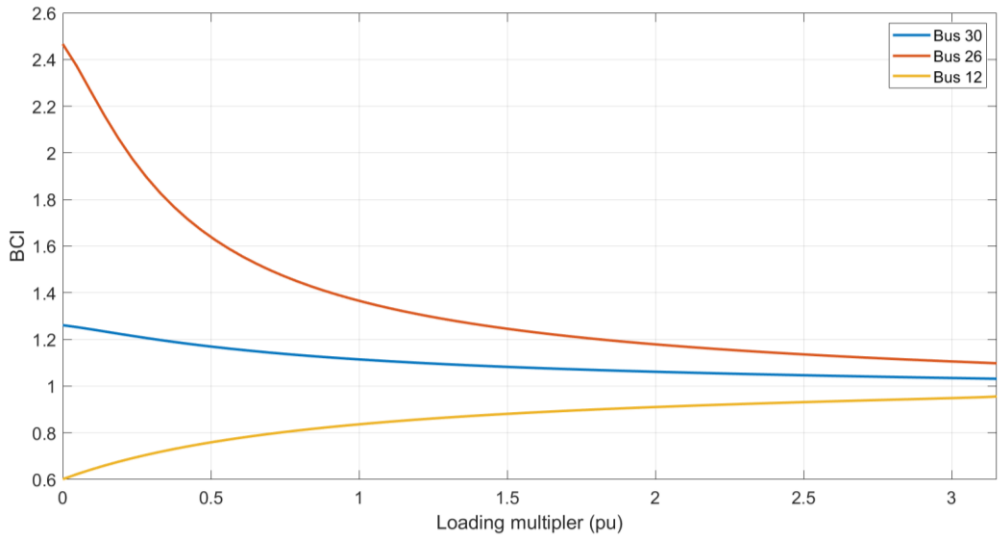

Figure 4.28 Bus current index performance for buses 12, 26 and 30 for the IEEE 30 bus test system

4.3 Chapter summary and conclusions

In this chapter a bus-based and line-based static voltage stability index based on impedance matching concepts was presented to evaluate the steady-state instability of a network during critical loadability. The developed line current index is based on the ratio of the load current flowing in a line to the expected fault current flowing in the same line for a fault at the receiving end bus. Similarly, the proposed bus current index is based on the ratio of the sum of load current injections into a bus to the sum of expected fault current flowing into the same bus. The indices vary between 0 at normal loading and 1 at the critical condition and can be utilised to identify the critical lines and weak buses in a network. The developed approach is based on a two-bus equivalent π transmission line model considering shunt susceptance parameters which

have been predominantly neglected in two-bus equivalent index methods. The developed indices are tested and validated on several test networks and case studies with performance compared to existing line-based indices. Enhanced performance of the developed index is demonstrated against multiple line index methods which fail to identify critical lines in some cases as maximum index values at the stability limit are not reached. The impact of DG power factor and constant voltage operating modes and SST power flow models on index performance were also reported in this chapter. The developed index obtained comparable index values relative to existing methods for both small and large networks during critical loadability, accounts for shunt susceptance parameters having been previously neglected in existing methods illustrating improved performance and can be expressed as both line and bus based stability indices, enhancing evaluation capability.

5. Development of a constraint-based and multi-objective VSCOPF using a novel static line stability index

This chapter proposes an index-based voltage stability-constrained OPF procedure to enhance steady-state voltage stability performance during critical loadability through re-dispatch of system control variables and components (e.g. synchronous generation, shunt capacitors, etc.). In the previous section, a novel line current stability index is proposed to evaluate the steady-state voltage stability of a power network under stressed system conditions. The proposed VSCOPF procedure incorporates the previously developed line current index (LCI) into an optimal power flow formulation to achieve secure system operation and improve stability margins through re-dispatch of system generation via preventive action. The developed approach implements the LCI both as an inequality constraint (constrained based) and a multi-objective (cost function) OPF formulation simultaneously minimizing generation costs and line indices across the system based on the proposed VSCOPF models. Introducing stability indices as inequality constraints for example applies upper and lower bounds on the indices as a function of the OPF variables in the model thus constructing a constrained-based VSCOPF procedure. An overview of recent methodologies that incorporate optimal power flow as a tool for managing emerging network bottlenecks in the context of increasing penetration of nonsynchronous generation is given. A critical review of existing literature in the application of VSCOPF techniques and methods is described in chapter 2 with gaps/shortcomings in existing indexed based VSCOPF methods outlined in terms of adopted concepts (e.g. impedance matching, power voltage quadratic equation solution) and index accuracy (neglected shunt branch parameters), and how the proposed VSCOPF solution procedure developed in this research addresses them.

The conventional OPF model is briefly reviewed and the proposed VSCOPF model is formulated utilising the developed LCI index. The proposed optimisation procedure is

tested on the IEEE 30-bus and 118-bus test networks with results compared to existing index-based VSCOPF formulations. A discussion of the findings and the main conclusions of the studies is also provided.

As previously described, to meet climate change targets, power systems are experiencing a significant increase in the instantaneous penetration of wind and solar generation across both transmission and distribution networks. To meet decarbonisation objectives, system operators are facing significant operational challenges relating to secure and economic management of the system. It has therefore become a requirement to adopt a holistic, coordinated approach for managing arising technical issues which drive consideration of the development of new tools in the control centre environment [97]. Recent challenges regarded as being critical for future network operation with high penetration of renewables include reduced system inertia and higher RoCoFs following disturbances, lower availability of dispatchable reactive power resources and availability of reactive power control, reduced transient stability margins and a reduction in short circuit levels which can exacerbate the depth and reach of the propagation of voltage dips throughout the system, potentially negatively impacting voltage stability, generator (and load) ride-through and possibly compromising network and generator protection performance.

These arising technical challenges have driven the need for the development of online tools [97] for safe and secure operation of power systems under high renewable penetration. Conventionally, the use of offline studies, tools and model-based methodologies have been the adopted approach by system operators for reliable network operation. These arising challenges are posing significant complexities and operational risks with the intermittency of generation and reliance on offline studies can no longer ensure secure, economic system operation. This may also lead to over-commitment of synchronous generation for the provision of inertia and system strength services increasing operational costs and limiting renewable penetration and alternative tools are desirable. The development and addition of decision support tools has therefore become a major requirement for managing network bottlenecks in real-time to facilitate high penetration of renewable resources.

A number of decision support tools have recently been developed by operators to address the aforementioned issues. This includes the real-time monitoring of operational metrics including non-synchronous penetration levels, system inertia and RoCoF (following disturbances) and wind dispatch tools, allowing real-time control of wind-generation levels through localised and global curtailment of generation outputs (to manage network constraints)[97]. Other useful tools include a security assessment tool which performs real-time security assessments (transient and voltage stability), to identify the safe levels of wind generation that can be accommodated. This tool makes use of RMS-based models to perform stability (and contingency) studies utilising real-time snapshots of the system (retrieved from a state estimator) at 5 minute intervals. Figure 5.1 shows the overall functionality provided by the wind security assessment tool (WSAT[98]). The network data/files are initially pre-processed (using python scripts) to construct a load flow solution of the given network snapshot/operating condition (base case scenario). This is then combined with other "files" including contingency lists, system integrity protection schemes, capability curves, etc. to undertake static (voltage stability) and dynamic (transient stability) assessments which are then displayed at the grid controller workstation. Based on the outputs of the security assessments, grid controllers would initiate preventive control actions of generators and line flows to restore the system to a secure state through the provision of new setpoints.

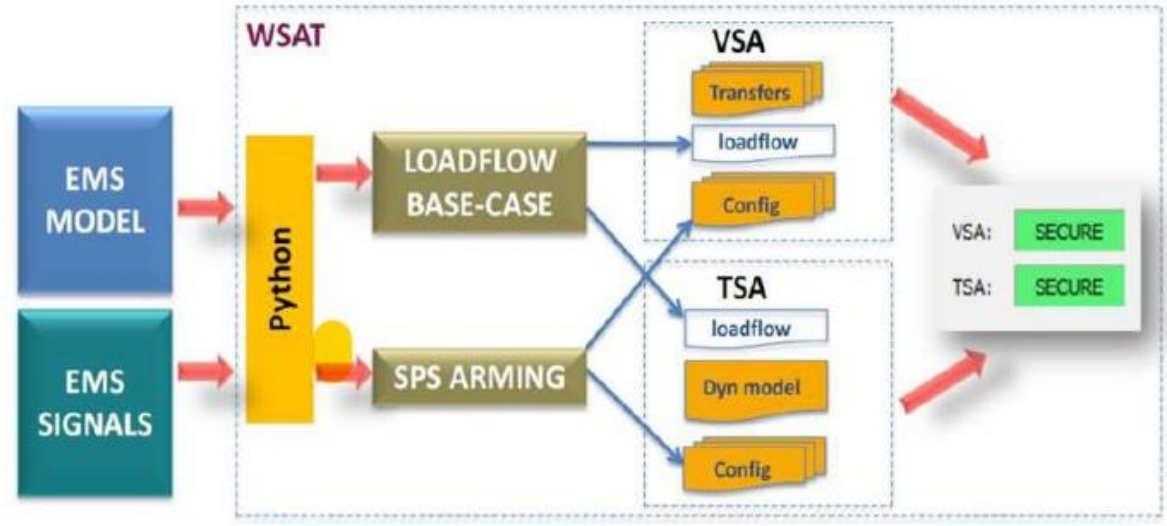

Figure 5.1 Workflow of an online security assessment tool [97]

As previously described in section 2.6.3, optimal power flow has been shown to be an effective and robust tool in power system planning and operation (65,66) and has been gaining increasing attention in its utilisation in deregulated networks where a number of DER resources are integrated in the system. The utilisation of OPF has been considered to assisting in solving a wide range of network issues and constraints at both transmission and distribution level including thermal, voltage constraints, DER and FACTs placement, system stability enhancement, etc [67,70].

An approach for online power flow management [99] of MV networks is achieved through an OPF procedure where DG output is curtailed to alleviate the network during thermal overloads. Increasing penetration of DG also risks fault levels on the network that the DG is connected to exceeding switchgear fault level make and break limits. An approach in [90] implements a fault level constrained OPF mechanism to allocate and readjust new and existing distributed generation capacity considering short circuit constraints to bring fault levels within switchgear specifications. Recent efforts aim to maximise the utilisation of DER resources and the expansion of existing power markets through the introduction of new network services[100]. Certain regions in the GB power system, for example, require that power transfers be capped from high DER penetration regions across major transmission corridors. Under predetermined contingencies/outages, low short circuit level conditions arise, limiting power exports across long lines (maximum transfers/ stability limits) to avoid system voltage collapse [101] which incur cost implications (for managing the constraint). An approach has been developed which utilises OPF methodologies to request distribution DER based reactive support during network [97, 101] congestions to support transmission operation. In this work, the OPF is utilised to provide DER and tap changer setpoints at a GSP for reactive power service provision to the SO facilitating transmission/distribution operator interaction (regarded as a key component/application to the DSO transition[102]). This further illustrates the effectiveness in utilising OPF based tools for dispatching network components and improve system operation to address system wide constraints in future scenarios under high nonsynchronous generator penetration.

With the expected uptake of inverter-based generation (IBG), issues related to reduced short circuit contribution under high penetrations are expected to arise across weak

regions. With the need to operate grids close to their operating limits [67] and increasingly weakened regions across the network, methods to improve system performance are gaining increasing attention[4]. The inclusion of voltage stability criteria in OPF models have conventionally been utilised to maintain networks within security limits by ensuring adequate stability margins through preventive control action and re-dispatching of system components. The incorporation of VSIs in an OPF formulation can be an effective approach to improve steady-state stability performance due to its simplicity (in modelling voltage stability criteria) and computational efficiency and is the methodology adopted in this work. In this chapter, the main motivation is therefore to develop a VSCOPF approach suitable for online applications where utilisation of index-based methods is chosen as static, RMS-based network models can be readily utilised to assess voltage stability and implement a VSCOPF solution for preventive action during stressed system conditions. From the previous chapter, a line-based LCI index is proposed based on a two-bus equivalent (π model) which incorporate impedance matching concepts and system variable-based methodologies considering shunt susceptance effects. The developed approach is utilised in this chapter to implement an index based VSCOPF solution procedure during stressed, critical loading conditions. The proposed VSCOPF model is evaluated against existing index-based methods and performance assessed utilising a number of test networks and case studies.

A summary of the advantages of incorporating the developed LCI index in a VSCOPF model and solution procedure include:

1. Modelling transmission shunt branch parameters through LCI considers a π transmission line model (two-bus) for index evaluation which improves accuracy and performance of stability index constraints and criteria imposed in the OPF as shunt branch parameters are modelled. These parameters have been previously neglected in existing line index based VSCOPF solution procedures.
2. Applying impedance-based stability constraints through LCI is a current based approach and is a function of both system loading and fault current levels [90] (load and Thevenin impedances). This shows that risks of instability can be

directly modelled in the OPF as a function of both maximum loadability and short circuit conditions and therefore incorporate stability and fault level constraints in the OPF formulation.

3. Previous impedance-based detection methods have predominantly been applied for bus based VSCOPF[103] formulations and have had limited application in line based VSCOPF solution procedures.
4. Accounting for line charging/susceptance effects via the LCI may reduce reactive power dispatch requirements from synchronous generation improving operational reactive reserves (for other voltage control services) and facilitating localised reactive support thereby reducing system losses.

5.1 Development of voltage stability-constrained OPF procedure utilising a novel static line current stability index method

5.1.1 Conventional OPF formulation

As previously mentioned, the main motivation in this research is to develop an approach to enhance/improve the steady-state stability performance of a network through the application of optimisation procedures. This is achieved via redispatch of system variables to enhance security margins during stressed system conditions via VSCOPF. Reliance on conventional security limits such as bus voltage magnitudes/angles and line thermal limits (equality and inequality constraints) may be insufficient in ensuring adequate security margins when the network is critically stressed or experiencing weak system conditions. In this regard, the incorporation of voltage stability criteria in the OPF formulation can address these shortcomings through the dispatch of appropriate controls to maintain the system within steady-state operating conditions to improve system power transfer capability. This section outlines the standard OPF model used to incorporate voltage stability in the OPF solution

The generalised AC optimal power flow problem aims to minimise an objective function (system losses/generation costs) which can be described using the following generalised equations

$$\min f(x) \tag{5.1}$$

Subject to equality constraints

$$g(x) = 0 \tag{5.2}$$

equality constraints

$$h(x) = 0 \tag{5.3}$$

Inequality constraints and variable bounds

$$x_{min} \leq x \leq x_{max} \tag{5.4}$$

The objective function, the OPF problem aims to minimise to obtain optimal generation costs and optimal control setpoints can be described using

$$min \sum_{i=0}^{n_g} f_p^i \, (P_g^i) \tag{5.5}$$

Where $f_p^i(P_g^i)$ is the generation fuel cost function to be minimised. This is subject to equality constraints which represent the active and reactive power balance equations

$$P_{G_i}\text{-}P_{D_i} = V_i \sum_{k=1}^{N} V_k(G_{ik}\cos(\theta_i - \theta_k)\text{+}B_{ik}\cos(\theta_i - \theta_k)) \tag{5.6}$$

$$Q_{G_i}\text{-}Q_{D_i} = V_i \sum_{k=1}^{N} V_k(G_{ik}\sin\theta_i - \theta_k)\text{+}B_{ik}\sin(\theta_i - \theta_k)) \tag{5.7}$$

P_{G_i} and $P_{D_i}$are the active power generation and demand at bus i. V_i, V_k are the voltage magnitudes at buses i and k, θ_i, θ_k are voltage angles for buses i and k. $G_{ik}$and B_{ik} are the conductance and susceptance respectively for lines i,k The inequality constraints include the maximum load flowing in the lines $S_{ij\,max}$, active and reactive generation limits. Imposed network operating limits also include bus voltage magnitudes and angles across the system.

$$\left|S_{ij}(\theta, V_m)\right|\text{-}S_{ij\,max} \leq 0 \tag{5.8}$$

$$\theta_{ref}^{i,min} \leq \theta_i \leq \theta_{ref}^{i,max} \qquad i \in \mathcal{L}_{ref} \tag{5.9}$$

$$V_m^{i,min} \leq V_m \leq V_m^{i,max} \qquad i = 1 \dots n_b \tag{5.10}$$

$$P_g^{i,min} \leq P_g \leq P_g^{i,max} \qquad i = 1 \dots n_g \tag{5.11}$$

$$Q_g^{i,min} \leq Q_g \leq Q_g^{i,max} \qquad i = 1 \dots n_g \tag{5.12}$$

$V_m^{i,min}$, $V_m^{i,max}$, $\theta_{ref}^{i,min}$, $\theta_{ref}^{i,max}$ represent the upper and lower limits of the bus voltage magnitudes and angles respectively and $P_g^{i,min}$, $P_g^{i,max}$, $Q_g^{i,min}$, $Q_g^{i,max}$ are the upper and lower bounds of generation active and reactive power respectively

5.2 Line current index-based VSCOPF models utilising constrained based and multi-objective formulations

In a general form, voltage stability constrained OPF is a nonlinear, nonconvex large scale optimization problem containing discrete and continuous variables [104]. The inclusion of voltage stability criteria in an OPF can be modelled using several approaches as discussed in the previous section. The application of static indices can be utilised to account for system voltage stability limits in an OPF by relating the indices to the optimisation vector x as a function of the OPF variables (equation (5.13). In this work, a novel line current index previously developed is incorporated into the OPF model so as to implement a VSCOPF solution. The index-based approach incorporates stability conditions as a function of load current flowing in the line to expected prevailing fault current level flowing in the same line. This criteria for identifying instability is based on the impedance matching condition during maximum power transfer (steady-state limit). When the index reaches unity, the line under study is said to have reached its critical state and re-dispatch of system variables should be initiated via the OPF for preventive control action, thus ensuring voltage security.

$$x = \begin{bmatrix} \theta \\ V_m \\ P_g \\ Q_g \end{bmatrix} \tag{5.13}$$

Modelling the line index in the optimisation problem can be applied using a number of approaches and methodologies. In this work, the LCI index is incorporated both as part of the objective function to be minimised in a multi-objective formulation and as inequality constraints in the OPF model. These are described in the next section.

5.2.1 Multiobjective based VSCOPF model

The previously described line index can be directly incorporated into the OPF objective function so as to minimise the total generation cost and total LCI indices across the lines of a given network. This can be described using

$$LCI_T = \sum_{i=1}^{N_L} LCI_i \tag{5.14}$$

Where LCI_T is the total line current index of the lines in the system and LCI_i is the line current index for line i in a given network. In this regard, the overall objective function to be minimised in the optimisation problem is therefore given by

$$min \sum_{i=0}^{n_g} f_p^i \left(P_g^i\right) + min \sum_{i=0}^{n_L} f_c^i \left(LCI_L^i\right) \tag{5.15}$$

Where the additional cost term $f_c^i\left(LCI_L^i\right)$ in the objective function can be represented as a function of the optimisation variables as

$$f_c^i\left(LCI_L^i\right) = \frac{\sum I_L z_{ij}}{\sum (V_i - V_j - V_f(FSF_{if} - FSF_{jf}))} \tag{5.16}$$

5.2.2 LCI-VSCOPF using index-based constraints

Alternatively, voltage stability criteria can directly be modelled in the OPF as inequality constraints so as to maintain stability margins within prespecified limits. As the developed LCI is a function of the OPF variables, it can be incorporated in the OPF as an algebraic model similar to voltage and thermal limits. The voltage stability state of the system can be directly quantified using the LCI at a given loading condition with the addition of upper and lower bounds to ensure steady-state stability during maximum loadability. The inequality constraints in the given problem can be described by

$$LCI_{min} \leq LCI_i \leq LCI_{max} \quad (5.17)$$

Where LCI_{max}, LCI_{min} are the upper and lower bounds of the LCI index.

5.3 Testing and validation of the developed VSCOPF models

5.3.1 IEEE 30 bus network

To illustrate the effectiveness of the proposed VSC-OPF models, a number of case studies are investigated on the IEEE 30 bus system previously described. Network load and generation is uniformly increased at each bus until the steady-state stability limit is reached. The proposed models are applied at the stressed condition in order to enhance the stability performance of the network through re-dispatch of system components. The proposed constrained-based and multi-objective model performances are compared against the application of a standard OPF solution in addition to existing index-based VSCOPF methods during the described stressed operating condition. A summary of the bus voltages, active and reactive power demand at the critical condition with no VSCOPF solution implemented is shown in table 5.1

Table 5.1 Bus voltages and active/reactive loading at the critical condition (PV knee point)

Bus	Voltage magnitude (pu)	Voltage angle (degrees)	Active power (MW)	Reactive power (MVAR)
1	1	0	0	0
2	1	-5.4420	124.280	72.7358
3	0.7838	-11.5257	13.7453	6.87267
4	0.7490	-14.297	-43.5269	-9.1635
5	0.7465	-16.9745	0	0
6	0.6503	-21.8927	0	0
7	0.5897	-26.9421	130.5808	62.4267
8	0.5027	-29.6805	171.8168	171.8168
9	0.7704	-33.5368	0	0
10	0.8432	-38.2137	33.21792	11.4544
11	0.7704	-33.5368	0	0
12	0.8258	-19.3808	64.1449	42.9542
13	1	1.6730	0	0
14	0.7651	-27.1648	35.5088	9.16356
15	0.7953	-28.5322	46.9632	14.3180

16	0.7649	-30.1312	20.045	10.3090
17	0.7787	-38.0138	51.5450	33.2179
18	0.6900	-39.4966	18.3271	5.15450
19	0.6681	-44.6158	54.4086	19.4725
20	0.7039	-43.3753	12.5999	4.00905
21	0.9460	-40.6137	100.2264	64.1449
22	1	-40.4836	0	0
23	1	-27.6652	18.3271	9.1635
24	0.9207	-34.600	49.8268	38.3724
25	0.9250	-26.8546	0	0
26	0.7979	-30.2130	20.045	13.1726
27	1	-20.631	0	0
28	0.6567	-23.8905	0	0
29	0.8226	-29.5420	13.7453	5.15450
30	0.7196	-37.9424	60.7086	10.8817

Figure 5.2 compares the voltage profiles of the network at the critical condition when the LCI index is incorporated in the VSCOPF model. The application of the index constraint VSCOPF result in negligible voltage profile improvement whilst the cost function model results in an overall increase in bus voltage magnitudes across the network. The profiles also follow a similar trajectory when compared to the standard OPF solution with no VSCOPF applied as it dictated by system characteristics (line impedances, generation location, voltage levels, etc).

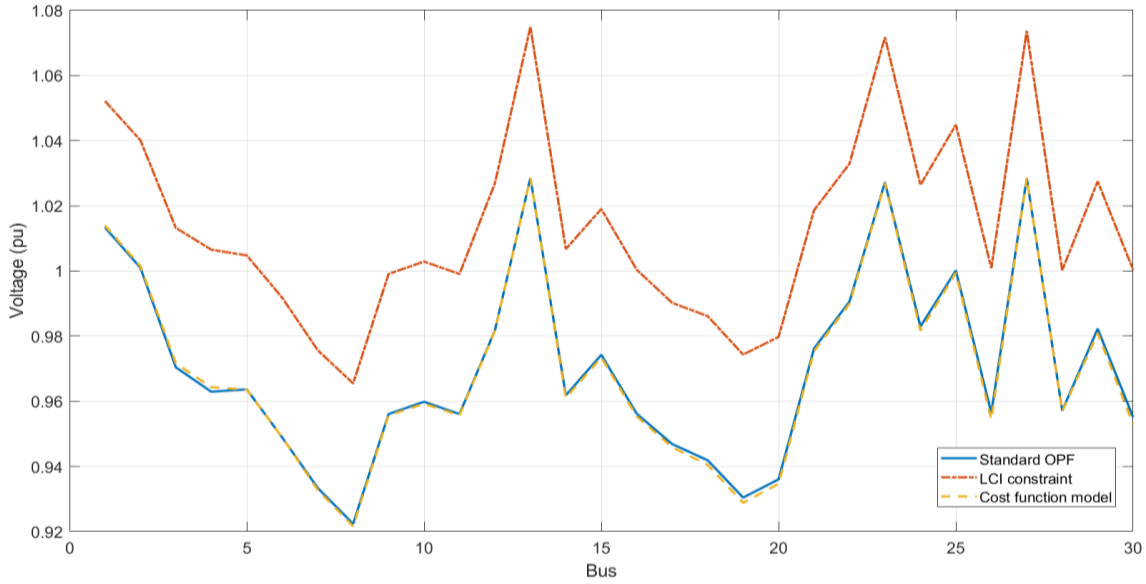

Figure 5.2 Voltage profile improvement of the system at the critical condition (IEEE 30-bus system)

The impact of the developed VSCOPF models on network stability margins are illustrated from the PV curves shown in figure 5.3 for bus 28. Including the proposed line index both as constraints and as a multiobjective formulation demonstrate an increase in the overall margins as higher maximum loadability (knee-point) is achieved and therefore voltage security is improved. This illustrates the effectiveness of both models in enhancing system security levels as a higher critical condition is reached and therefore the system is able to accommodate higher loading levels and remain stable. It can be seen that the cost function model has a larger impact in enhancing stability relative to the LCI constraint as the maximum loadability is raised to a value

of 3.59 pu compared to the 2.9 pu value for a standard OPF model yielding a 24.1% increase in the stability margins.

Figure 5.3 Stability margin enhancement through VSCOPF implementation (IEEE 30-bus system)

The VSCOPF solutions also shows increased active power generation output (figure 5.4) for both the constrained based and multi-objective approach, illustrating the additional re-dispatch required to improve system security. This also results in in an overall increase in system operating costs as imposing voltage security limits introduce

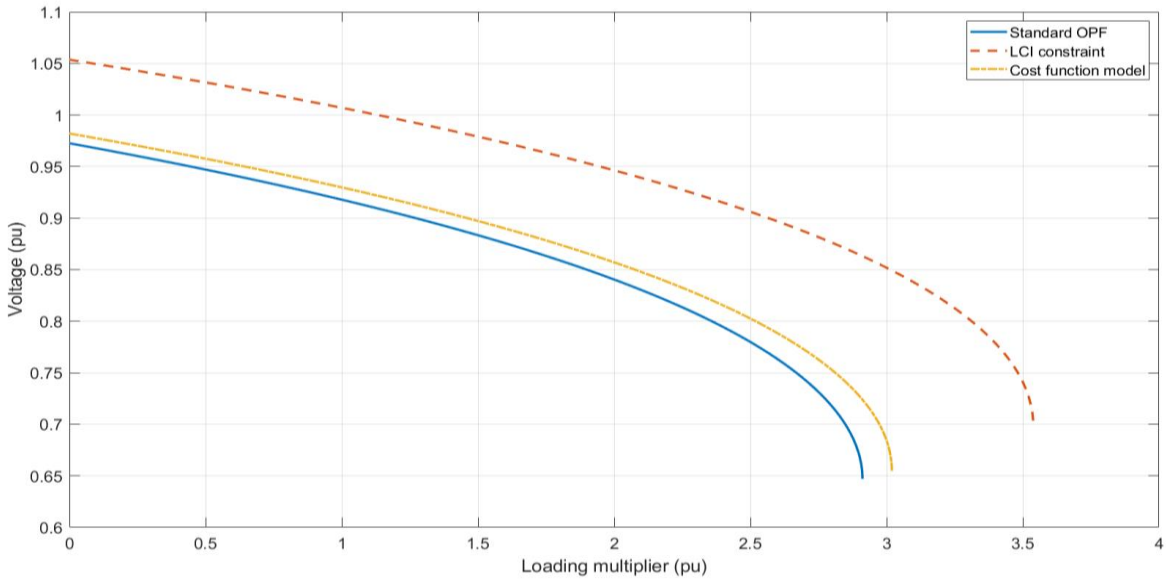

an additional cost for maintaining secure system operation. Higher active power output from the generators is therefore required to maintain system stability and improve voltage security. The cost function model shows a slightly higher generation output when compared to the linear constraint model. Reactive power generation follows a similar trend (figure 5.5) as output also increases proportionately for both VSCOPF formulations to move the system away from the stressed condition. The constraint-based approach illustrates a higher reactive power output when compared to the standard and multi-objective-based models.

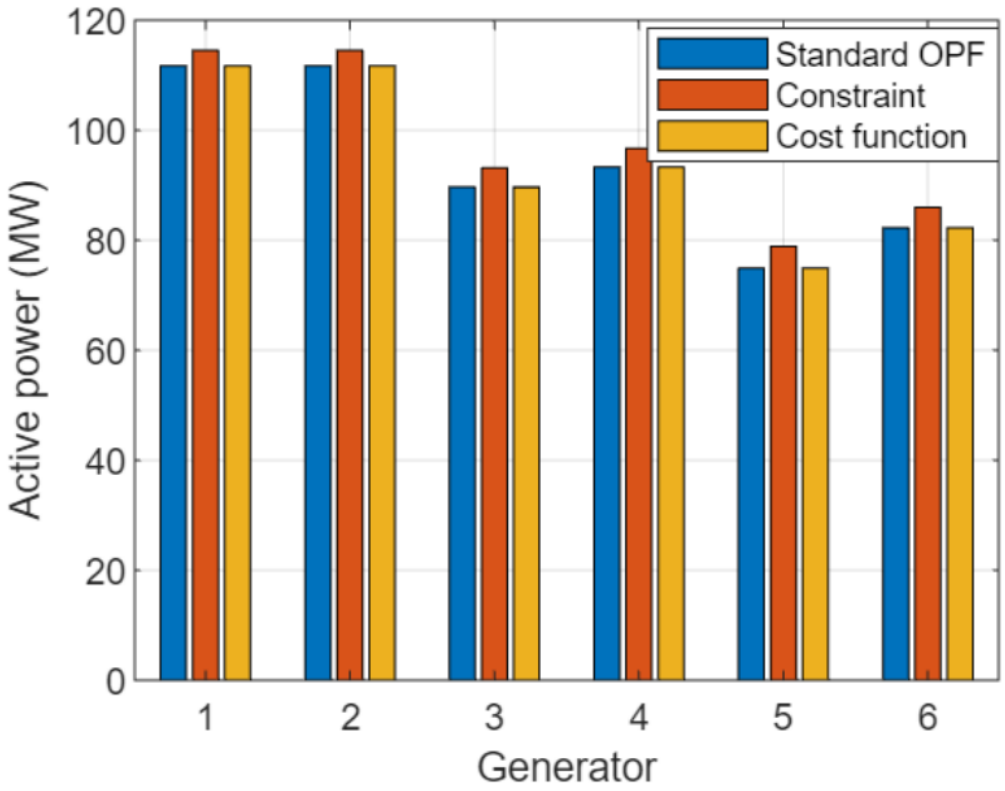

Figure 5.4 Comparison of active power generation re-dispatch at the stressed condition (IEEE 30-bus system)

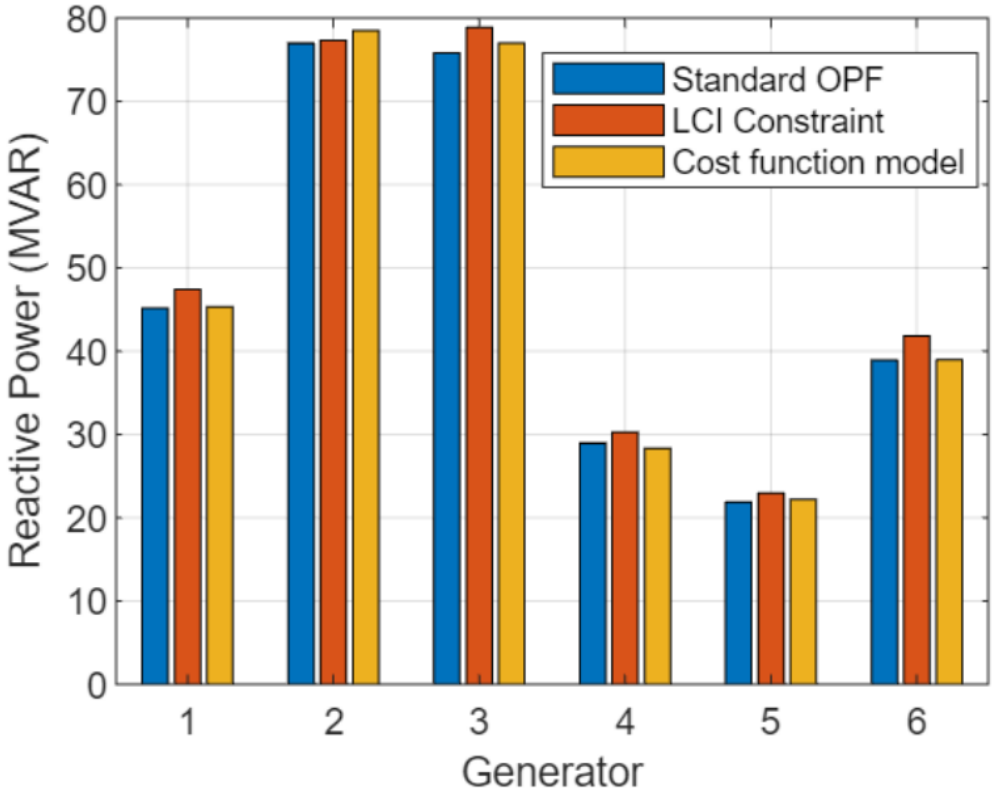

Figure 5.5 Comparison of reactive generation re-dispatch at the stressed condition (IEEE 30-bus system)

An overall increase the in the operating costs (objective function value) are seen when implementing both stability index constraints and objective function models as an additional cost is imposed for introducing voltage security in the OPF (table 5.2). This may be a function of the additional re-dispatching required to move the system away from the stressed condition. It can also be seen that implementation of the cost function approach imposes a higher cost when compared to the constraint-based approach. It can therefore be concluded that both proposed VSCOPF models can improve voltage security with the multi-objective approach exhibiting superior performance in stability margin and voltage profile improvement during stressed conditions. It should also be noted that implementing the LCI constraint offers reduced operating costs and lower system losses but exhibit reduced voltage security improvement.

Table 5.2 Fuel cost and system loss comparison of VSCOPF models (IEEE 30-bus system)

	Standard OPF	**Constraint**	**Constraint % Difference (Std OPF)**	**Cost function**	**Cost function % Difference (Std OPF)**
Fuel cost ($/MW)	2.636×10^3	2.6939×10^3	2.196 %	2.7831×10^3	5.58 %
Losses (MW)	40.4968	38.5863	-4.717 %	41.2222	1.79 %

Applying stability inequality constraints in the OPF offer flexibility in implementing the stability enhancement as weighting factors can be added to vary the overall stability threshold and cost of improving the stability margins. This is illustrated in figure 5.6. Lower weighting factors imposes higher voltage security limits which result in higher operating costs. Conversely, reducing levels of system security through higher weighting factor magnitudes reduce system operating costs but may increase risks of instability. The overall trend however is that imposing tighter voltage security thresholds results in improved stability performance but at higher operating costs. Inclusion of additional variables in the OPF to support voltage stability include reactive power resources (FACTs, condensers), DG contribution, demand response, etc., through the provision of control setpoints from the OPF solution may also impact voltage security costs depending on the cost of service.

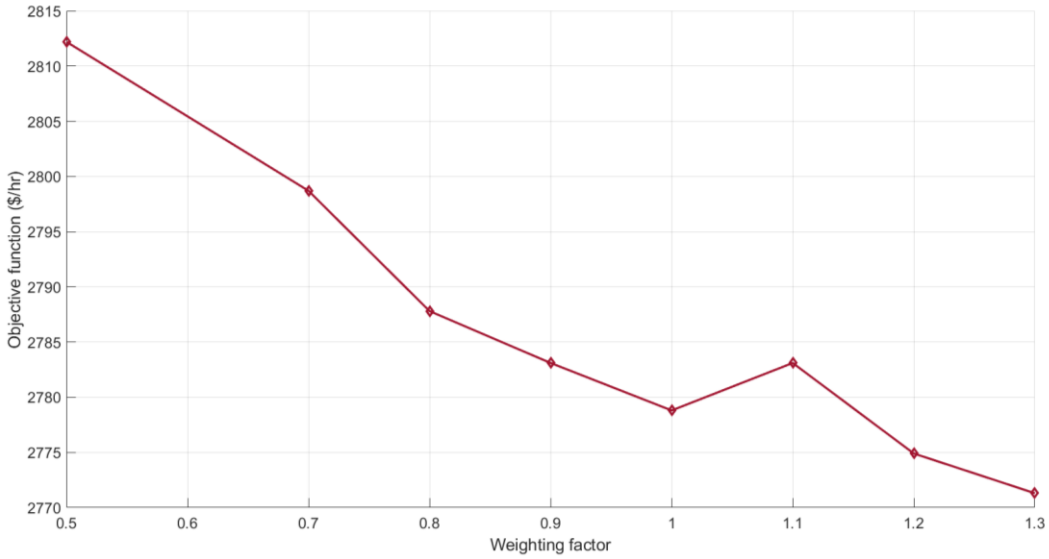

Figure 5.6 Effect of voltage security level variation on system operating costs using weighting factors

A comparison is made between the proposed and existing constraint based VSCOPF models utilising established line indices. Incorporating the L_{mn} index as a constraint in the OPF offers similar improvements in implementing the VSCOPF solution as in the case of adding an LCI constraint. Figure 5.7 illustrates the overall voltage profile improvement across the system when utilising both indices. Enhanced voltage performance of the network during critical conditions is seen when applying both index based VSCOPF formulations. Figure 5.8 show the PV curves of the network for bus 28 when utilising the L_{mn} and LCI indices in the VSCOPF. Both models illustrate improved stability performance as higher knee point values are reached relative to the standard OPF solution. The figure also shows a higher stability margin reached when utilising the LCI index for the constraint based VSCOPF formulation indicating improved stability performance of 3.44% relative to the L_{mn} formulation. For the IEEE 30-bus test network, with the VSCOPF applied, the system is relieved from the stressed condition with the application of the cost function model being more effective in increasing the stability margins across the lines.

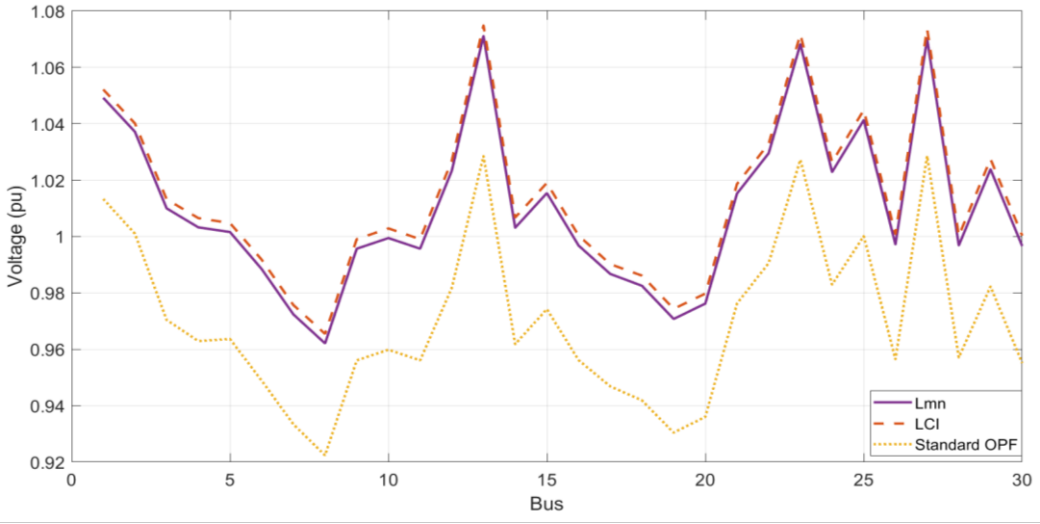

Figure 5.7 Comparison of existing and developed VSCOPF methods on voltage profile improvement at the critical condition

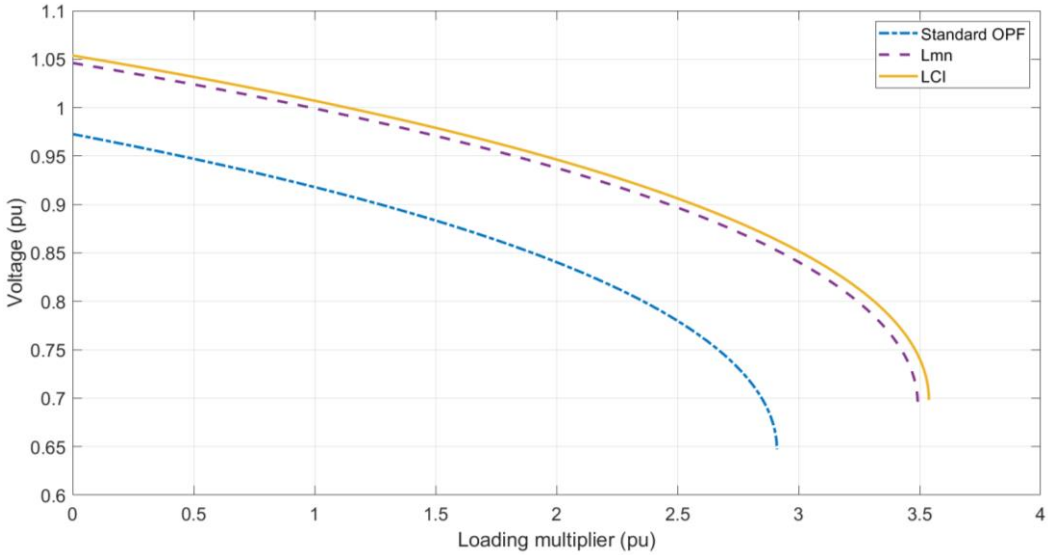

Figure 5.8 Comparison of existing and developed VSCOPF methods on stability margin improvement

To evaluate shunt admittance/susceptance and line charging effects on VSCOPF performance a case study was performed where line charging magnitude was varied across the lines in the network. Figures 5.9 and 5.10 show the influence of shunt susceptance of various magnitudes on network performance including voltage profiles and line reactive injection. There is a proportional increase voltage magnitudes and reactive flows in the system with increasing susceptance indicating enhanced stability support. This in addition

to the index calculation procedure considering shunt branches incorporated in the VSCOPF model. The impact of accounting for shunt admittance parameters on VSCOPF performance are shown in figures 5.11, 5.12 and 5.13. An overall reduction in the generation reactive power dispatch levels are seen across the units with increased line reactive injection. This further improves network performance as reduced reactive demand from generators enhance available reactive resource due to increased voltage support from line charging and branch admittances. A reduction in line losses is also inherent with increased line susceptance as localised reactive power provision reduces reactive power supply from remotely connected generation being transmitted which results in a reduction in the reactive loss. This further supports available loading margins and increased loadability as there is a reduced drop in system voltage in supplying demand at the critical condition and thus stability margins are further increased. Reduced line losses therefore indicate an improved stability performance of the lines in the presence of line charging. Susceptance parameters however have minimal impact on estimated line indices at the stressed condition and therefore do not significantly impact imposed constraints on the OPF solution procedure.

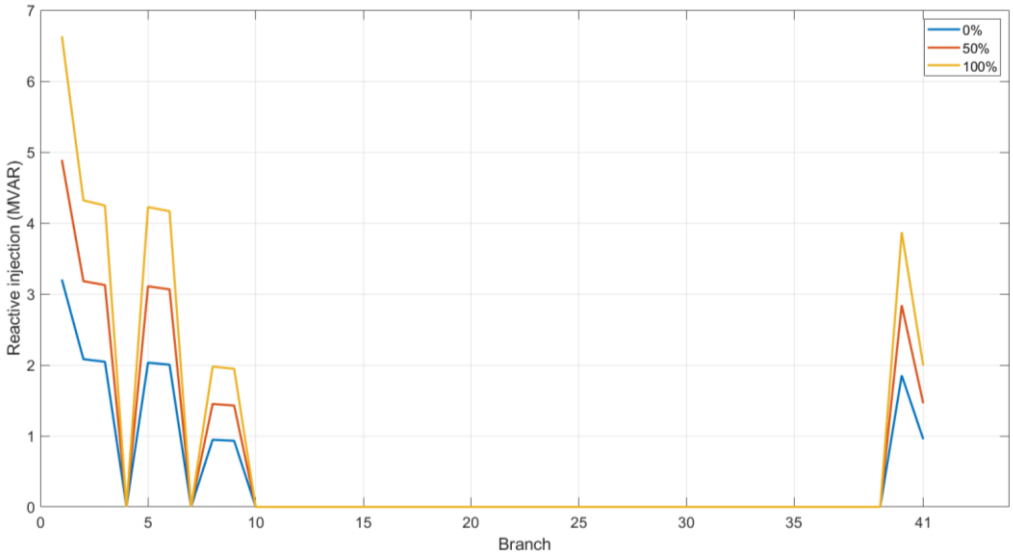

Figure 5.9 Impact of increased shunt susceptance on line reactive injection

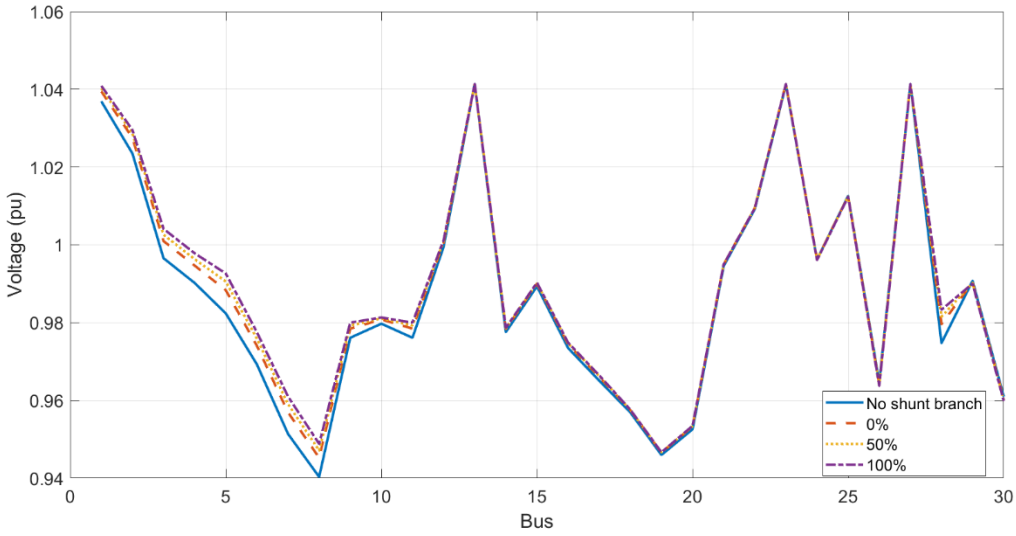

Figure 5.10 Impact of shunt susceptance magnitude on system voltage profile

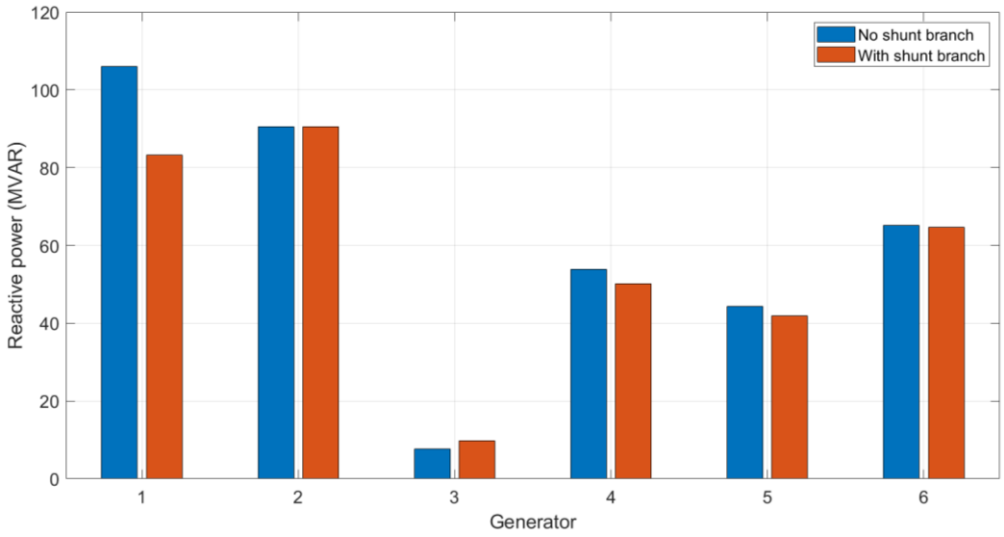

Figure 5.11 Impact of line shunt susceptance of reactive power generation dispatch

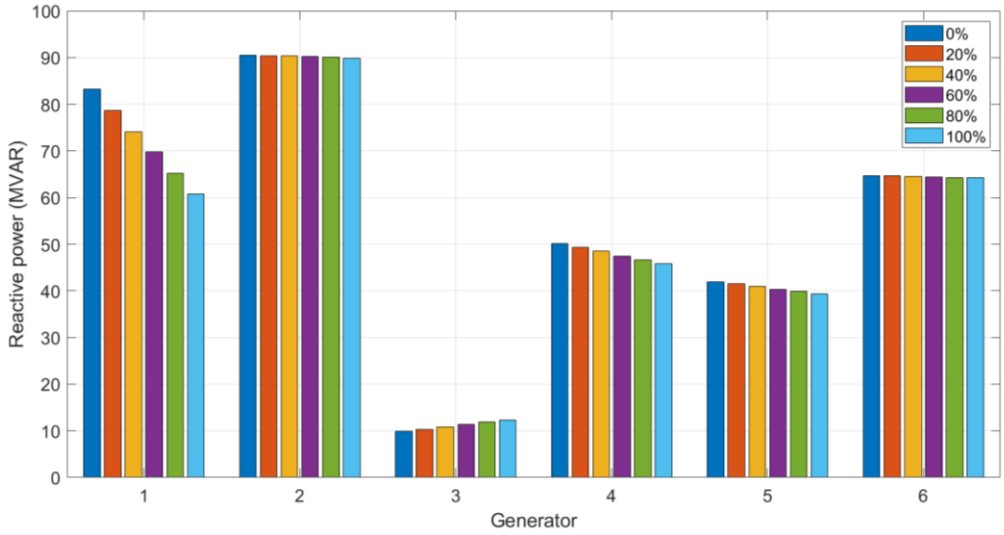

Figure 5.12 Impact of shunt susceptance magnitude on reactive power generation

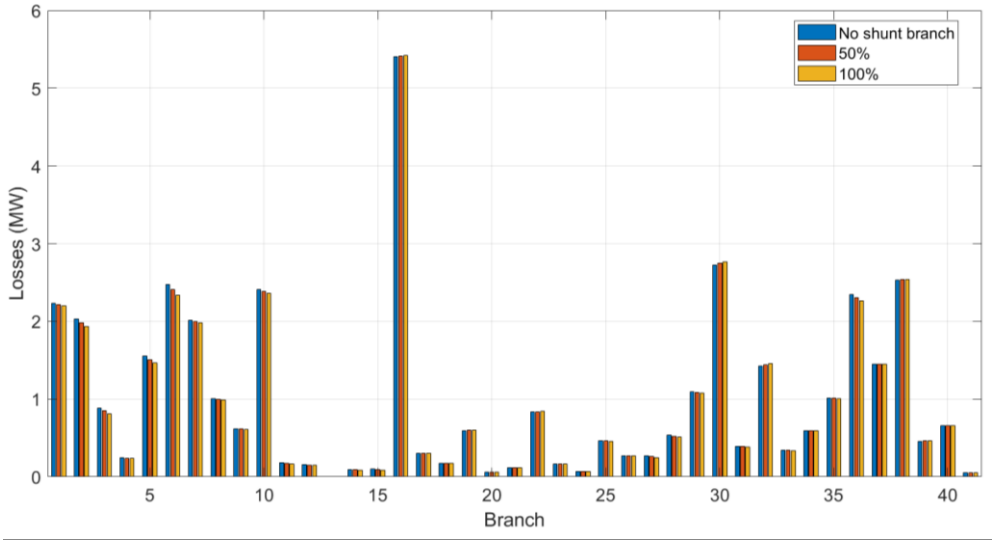

Figure 5.13 Impact of shunt susceptance magnitude on line losses

5.3.2 IEEE 118 test network

Similar the previous study, the proposed VSCOPF models are evaluated on a larger network, namely the IEEE 118-bus system. This model has been previously analysed to investigate its voltage stability performance using the developed LCI index. In this section the stability-constrained OPF is applied on the test network with results compared to the standard OPF solution at the critical condition. Figure 5.14 shows the overall voltage profiles of the system when the optimisation procedure is solved for the standard OPF and the VSCOPF models. As in the previous study, the voltage performance is improved when utilising both VSCOPF models indicating enhanced

stability performance during maximum loadability. The overall trend, similar to the IEEE 30-bus case, show higher profiles when utilising the multi-objective based VSCOPF. For the solution utilising the constraint-based model, a number of buses exceed the specified voltage magnitude limits (1.1 pu). This indicates reduced performance capability when compared to the cost function approach. Figures 5.15 and 5.16 compare the active and reactive generation dispatch respectively at the critical condition. At the given loading level, the active power generation is seen to reach the specified generation limits (in the OPF model) and may therefore unable to guarantee the system is re-dispatched to a secure operating condition. In this regard, when the system is loaded to the critical operating point, the active power generation reaches its maximum capability.

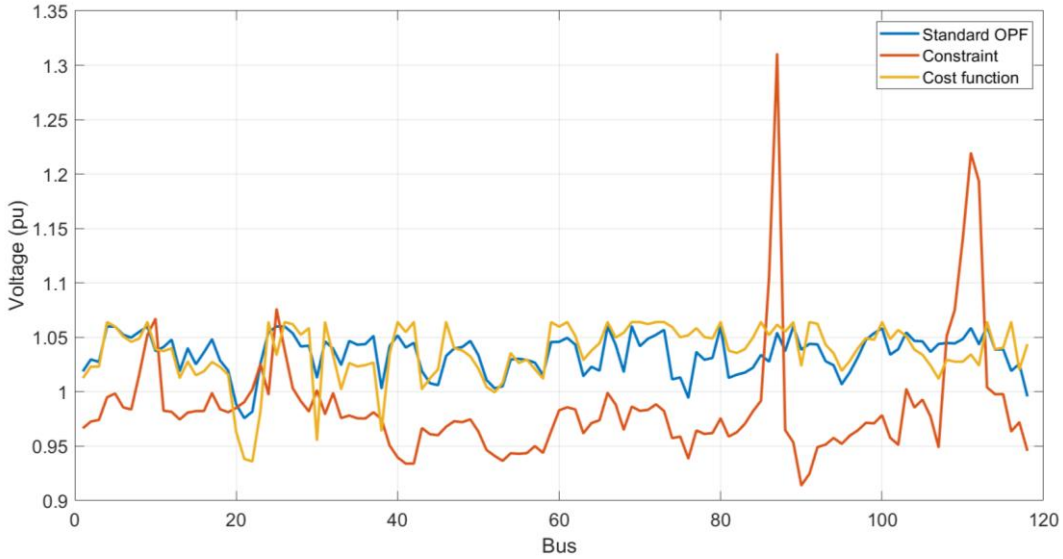

Figure 5.14 Voltage profile improvement of the system at the critical condition (IEEE 118-bus system) with generation limits imposed

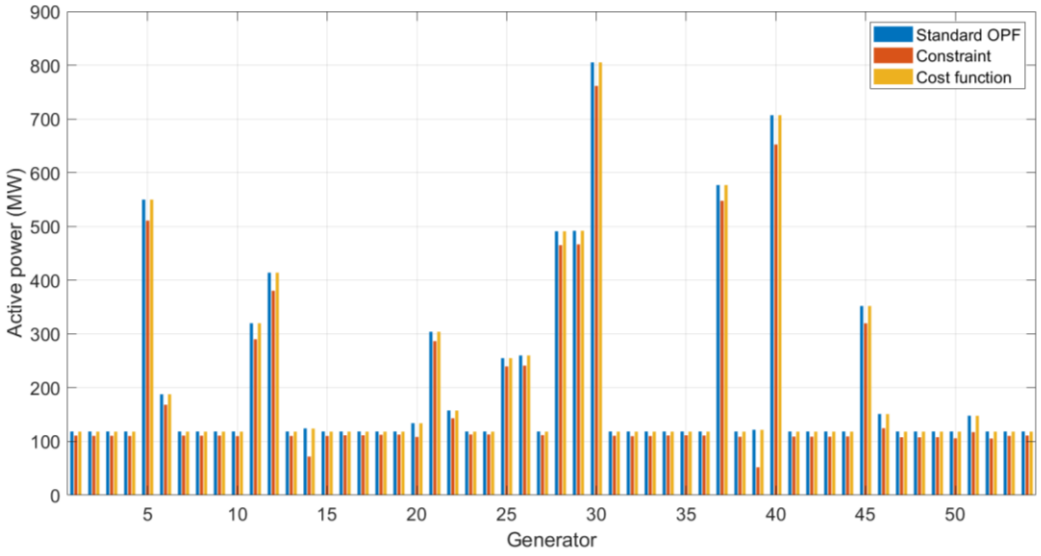

Figure 5.15 Comparison of active power generation re-dispatch at the stressed condition (IEEE 118-bus system) with generation limits imposed

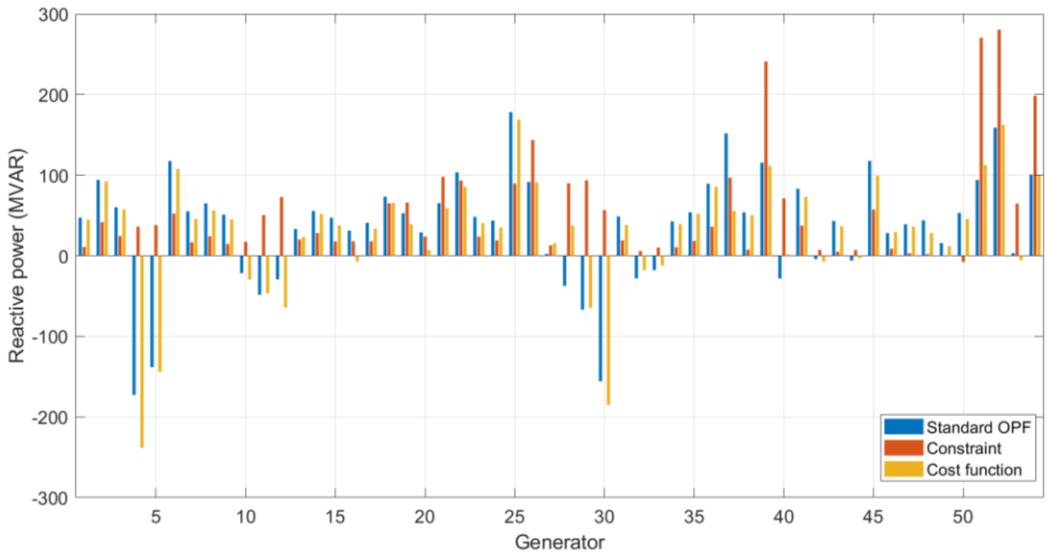

Figure 5.16 Comparison of reactive power generation re-dispatch at the stressed condition (IEEE 118-bus system) with generation limits imposed

To illustrate improvements in system performance when relaxing generation limits, figure 5.17 show the voltage profiles of the system with no generation limits imposed. In this scenario, both multi-objective and constraint-based models exhibit stable voltage performance with bus voltage magnitudes maintained within specified limits and at a higher level relative to the standard OPF solution. An overall increase in the active power generation for both the constraint and cost function models illustrate improved re-dispatching action when generation limits are removed (figure 5.18). The

reactive power dispatch of the cost function model is seen to significantly improve relative to the standard OPF and constraint models as additional MVAR injection in the system further enhance voltage stability performance (figure 5.19). In this scenario, λ_{max} is seen to increase from 1.5113 to 1.5563 pu for the cost function model relative to the standard OPF solution thereby increasing MW loadability. The multi-objective model, similar to the 30-bus case, also exhibit higher active (and reactive) power dispatch levels when compared to the constrained-based solution demonstrating increased effectiveness for maintaining a secure operating condition at critical loadability.

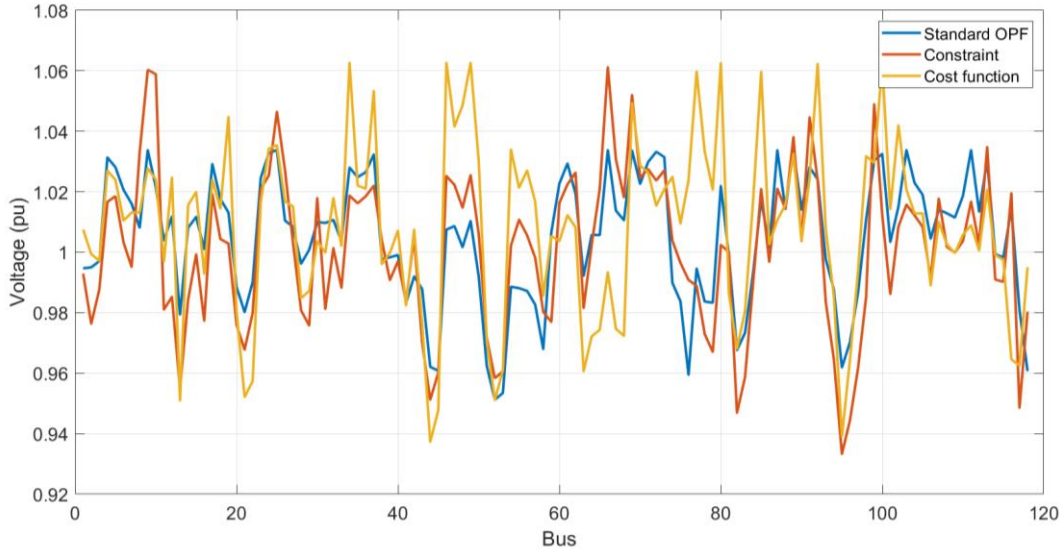

Figure 5.17 Voltage profile improvement of the system at the critical condition (IEEE 118-bus system) with active and reactive power limits relaxed

From the findings of this study, the multi-objective VSCOPF model can be regarded as superior to the linear constraint model in initiating preventive re-dispatching action to enhance system stability performance during stressed conditions as higher active/reactive generation dispatch levels are reached and improved voltage profiles are observed across the buses. It should also be noted that for large networks, the constrained-based model is less reliable in improving stability performance as insufficient re-dispatching action may occur which limit adequate margin improvement. Enhancing system generation capability (maximizing active and reactive generation limits in the system) by committing larger units may further improve system performance during critical loading conditions. This may be implemented through connecting large generators in the network or dispatching

additional generation during stressed conditions to maintain sufficient stability margins. Alternatively, preventive control action can be imposed through additional reactive resource devices (shunt capacitors, FACTs, condensers, etc.) which can be modelled in VSCOPF formulations to determine new control setpoints during stressed conditions and reduce the need to commit large synchronous generation for system strength provision. With the move towards increased transmission-distribution interaction and services, transmission operational limits (e.g. steady-state stability) can be further improved through DER-based reactive injection service provision which provide further localised support enhancing system performance and reducing losses.

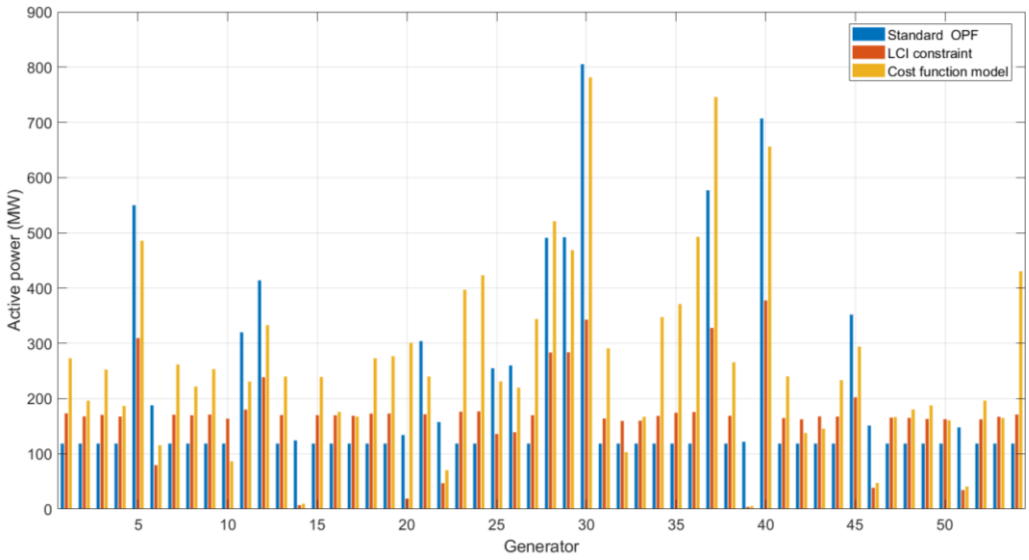

Figure 5.18 Comparison of active power generation re-dispatch at the stressed condition (IEEE 118-bus system) with generation limits relaxed

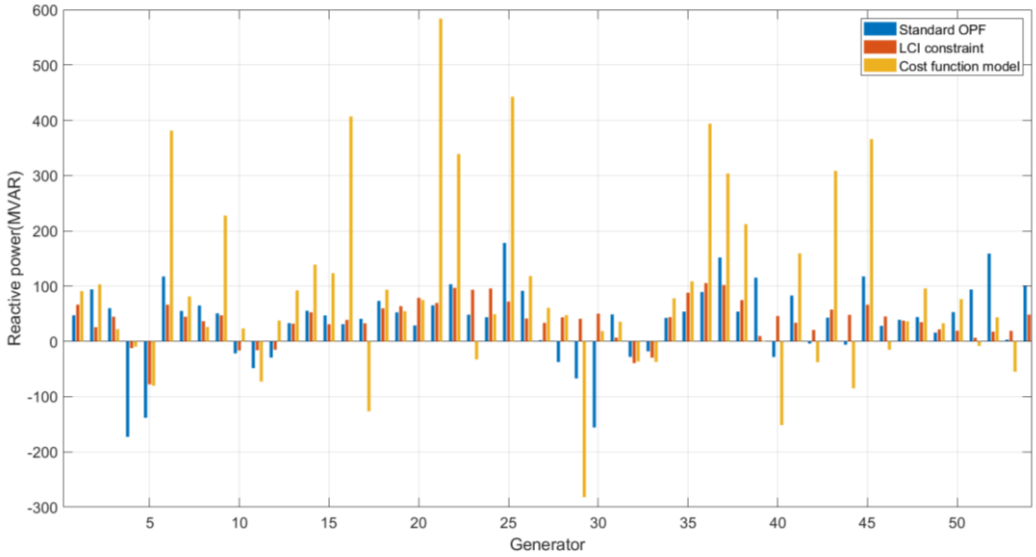

Figure 5.19 Comparison of reactive power generation re-dispatch at the stressed condition (IEEE 118-bus system) with generation limits relaxed

5.4 Chapter summary and conclusions

In this chapter, two voltage stability-constrained OPF solution procedures were proposed based on the previously developed line current index incorporated as a multi-objective and inequality constraint formulation in the OPF. Simulation based studies demonstrate the developed models enhance system voltage performance through increased voltage profiles, higher active and reactive generation dispatch levels and improved stability margins and critical loadability at the stressed condition. This demonstrates the proposed solution procedure improves system security levels and alleviates voltage instability issues. The developed VSCOPF models are validated on the IEEE 30 bus and IEEE 118 bus test systems with results compared against standard optimal power flow and existing line index-based VSCOPF methods. Simulation results also demonstrate improved stability margin enhancement relative to existing VSCOPF models and a reduction in system losses when a constrained based VSCOPF procedure is implemented. The multi-objective model was found superior in improving system voltage performance and enhancing loading margins at critical loadability. Studies also show that with limited generation capability in the network, risks of voltage instability increase as a limited level of security margin improvement is achieved. Committing larger generation units with higher active and reactive

capability limits can further increase system security margins but at higher operating costs.

6. Conclusions and future work

6.1 Summary

With the increasing uptake of inverter interfaced distribution energy resources, continuous changes in power system behaviour have resulted in emerging challenges needing to be closely managed. Changing system strength in transmission and distribution networks have led to growing issues in maintaining network security and operation whilst facilitating timely DER connections. MV distribution networks have seen increasing fault level constrained regions and bottlenecks due to the growing penetration of DER which reduce available short circuit capacity headroom without costly network reinforcement. This has raised the requirement for online and active management of fault level constrained regions through measurement-based monitoring of network fault levels. In this research, enhancement to existing passive short circuit estimation can provide efficient, cost-effective means in managing fault levels and validating network models in poorly instrumented areas in MV networks utilising recursive least square parameter estimation.

Declining system strength in transmission networks have also introduced several operational challenges including steady state stability that require additional preventive action to maintain networks within required security limits and reliability. In this thesis, steady-state voltage stability monitoring via static stability indices can provide effective means for online monitoring and identification of critical lines and weak buses of a given network. This research also focuses on the application of stability constrained OPF procedures to optimize generation dispatch and improve critical loadability and available stability margins through constrained based and multiobjective VSCOPF.

To this end, this thesis has presented a recursive least square-based passive fault current level estimation method based on a perturbation coefficient technique, an enhanced bus-based and line-based static stability index for steady state voltage stability monitoring and an enhanced VSCOPF procedure based on the incorporation

of an improved static line index as a multi-objective and constrained-based formulation. The performance of the proposed methods have been validated through simulation based studies utilising several realistic test networks with comparisons made against existing methods. The next section summarises the main conclusions and identifies additional areas for future work.

6.2 Conclusion

The contributions of the research reported in this thesis can be summarised in the following subsections discussed in detail

6.2.1 Passive short circuit current monitoring utilising recursive least square estimation in MV distribution networks

With the move towards measurement-based techniques for fault level management of distribution networks to support flexible connections and integration of DER, short circuit current monitoring has presented an effective means in monitoring and managing fault levels in constrained regions without immediate reinforcement of network infrastructure. A number of limitations have been outlined in the available literature including short comings in the statistical models adopted for effective short circuit parameter estimation. The application of ordinary least squares and frequency distribution histograms for short circuit monitoring may be inefficient for time sensitive applications as a large number of perturbation events are required to be collected and stored for analysis. Based on the identified challenges and shortcomings highlighted on existing methods, the following enhancements have been realised utilising the proposed approach

- Utilising recursive least square methodologies enhances existing ordinary least square passive estimation processes as the sum of square of measurement errors are continuously and recursively minimised as additional perturbation events are collected with parameter estimates updated.
- Improved modelling of a downstream load perturbation event irrespective of load type modelled as a net active power increment at a bus neglecting the active power loss from system voltage drops during a load increase with the approach derived from Jacobian and power flow methodologies.

- Separate resistance and reactance based RLS estimators allows effective means of deriving the overall short circuit impedance and current which reduces the absolute error of the short circuit current estimate. Errors were seen to be within $\pm 3\%$ for an unbalanced MV distribution network model for load events occurring at LV with voltage disturbances <1% of rated value.
- Negligible error magnitudes have been observed for events located in close proximity to monitoring location, with errors increasing significantly for events occurring at locations greater than 400 m (28%) at LV. Distances larger than 400 m result in higher active power losses which deteriorate the accuracy of the approach as active power loss at the assumed bus is neglected in the net active power increment model. This therefore illustrates a critical distance in which the accuracy of the approach may be compromised due to high voltage drops
- Perturbation magnitudes of 1250 MW causing a 0.49% voltage change yielded errors up to 8.9%. This illustrates large load event changes yield increased estimation errors as the method neglect active power loss which may become significant for large load perturbation (higher load currents) and can be regarded as a limitation in the accuracy of the developed approach
- Continuous reduction in the absolute error (and sum of square of errors) of the parameter estimates through recursive updating of impedance estimates (via gain vectors) for identified perturbation events addresses short comings of ordinary least square estimation methodologies and provides an enhanced passive estimation procedure

6.2.2 Improved static bus-based and line-based voltage stability indices with enhanced accuracy

Some of the major limitations of existing indices that have been highlighted in this thesis include

- Two-bus equivalent model-based stability indices have predominantly neglected shunt susceptance parameters which may compromise the accuracy of exiting approaches.

- Limitations in the concepts utilised to derive transmission line stability indices may further be expanded through the application of impedance matching concepts which have been utilised in bus based index applications

To overcome these shortcomings, a novel static line and bus-based stability index based on a full π transmission line two-bus equivalent model considering shunt branch admittances utilising impedance matching concepts is developed. The proposed line index is based on the load current flowing in a line to the expected prevailing fault current level flowing the same line for a receiving end bus fault. The physical significance of the index shows that when the voltage drop across the line becomes equal in magnitude to the receiving end bus voltage then the stability limit is reached. Alternatively, this index can be expressed in terms of a bus stability index taken as the ratio of the sum of load current injection into a bus to the total expected fault current infeed into the same bus. Flexibility in defining and expressing both indices may provide additional enhancements in the stability assessment as the voltage stability condition of both lines and buses can be evaluated using the proposed indices. In comparison to existing line indices, the proposed approach has shown to identify critical lines at maximum loadability by reaching/exceeding the theoretical limit of 1 with existing approaches reaching values below the theoretical limit and hence misclassify instability conditions of lines in some cases.

Limitations of the developed indices include high index values across the network during critical conditions which may misclassify stable lines as critical. This is seen for the IEEE 30 bus network case. The developed line based index is seen to perform well in larger node networks (IEEE 118 bus case) with index values in close proximity to existing line based methods. This generally indicates reduced performance capability for smaller networks relative to larger system models. Other limitations include improved performance of the line based index relative to the BCI method as the instability condition is derived from the expected prevailing fault current flowing in the line and therefore increased inaccuracies are introduced when incorporating the BCI approach.

6.2.3 Enhanced line based VSCOPF procedure based on an improved static line index approach

Based on previous evaluations of line based static indices and identified short comings, performance of VSCOPF models incorporating these indices may be less effective in enhancing system security and increasing stability margins during stressed system conditions. Previous indices have also neglected shunt susceptance parameters in calculated indices which impact index accuracy The development of constrained based and multi-objective VSCOPF solution procedures using the developed line index has shown to be effective in initiating preventive re-dispatch to maintain system security and increase system stability margins during critical conditions. Higher voltage profiles, improved critical loadability and higher active and reactive power generator injections were observed when implementing both solutions illustrating voltage security enhancement. The constrained based model has shown to cause a reduction in system losses with both formulations yielding higher operating costs for voltage security improvement. The multi-objective formulation was seen to be superior in enhancing stability performance relative to the constrained based model with an overall 24.1% increase in stability margins observed when compared to the standard OPF solution during critical loadability. In comparison to an existing established line based VSCOPF formulation, the developed approach was seen to yield an additional stability margin improvement of 3.44%

6.3 Future work

Based on the research reported in this thesis the following potential areas for future work are summarised in the following section which can advance and enhance performance of short circuit measurement methods, static voltage stability monitoring and optimisation.

6.3.1 Enhancing technology readiness levels of the proposed passive fault level monitoring method

The performance of the developed short circuit estimation method has been validated using simulation-based studies. The evaluation can be further advanced utilising laboratory-based experiments that can support addressing issues that may

hinder its deployment in MV distribution networks. Optioneering various measurement, data acquisition and communication technologies may identify the appropriate equipment for seamless substation integration. Assessment of power quality meters, phasor measurement units, distributed monitoring and protection relays may also assist in selection of appropriate specification in aspects relating to signal processing, processing and filtering requirements.

The developed scheme may also be tested in MW scale environments such as 11kV test beds to benchmark performance against actual fault events collected in digital fault recorders. The application of resistive and inductive load banks may also demonstrate real-time estimation capability in realistic network conditions through the provision of artificial disturbances. Investigation and selection of suitable event source location and identification methods (ESLI) for discriminating between upstream and downstream perturbation events prior to estimation may also further method applicability. Investigation of various load types (constant impedance, constant current and constant power models) on method performance may further highlight practical limitations of the proposed method. Incorporation of additional fault infeed sources including downstream load infeed, motor contribution and DG converter technologies (fully rated, doubly fed) may further improve method accuracy. Expanding the developed fault level estimator for single phase estimation functionality in addition to upstream ½ cycle (10 ms) fault level estimates for both radialized and interconnected sections of a test network [23] as discussed in section 2.2.3.

6.3.2 Developing a coordinated stability-constrained optimisation solution incorporating emerging reactive compensation models

To further improve economic and technical performance of the proposed VSCOPF models, development and incorporation of emerging reactive compensation devices in the OPF model may provide coordinated and cost-effective enhancements in voltage security. The emergence of new reactive power service providers in reactive power markets including hybrid STATCOM-condenser technologies, aggregate DER reactive injection sources (at GSPs), synchronous compensators may be directly incorporated as inequality constraints in the

VSCOPF solution procedure. With voltage stability being a localised and regional issue, utilisation of reactive power sources in close proximity to weak points may improve operational performance (loss reduction) and reduction in operating costs. Advancements in optimisation algorithms may be utilised to improve computational efficiency and performance of VSCOPF solutions. In this work, mixed integer linear programming solvers were incorporated in the solution procedure, evaluation of conventional and emerging optimisation solvers for VSCOPF implementation may further enhance method performance.

6.3.3 Application of measurement-based methodologies for static voltage stability assessment

Based on the developed line-based and bus-based stability indices and the advancements of various monitoring technologies including phasor measurement units, index assessment using hybrid methodologies incorporating network model parameters and actual network measurements may further enhance accuracy. The utilisation of network measurements for system wide monitoring using state estimation may be exploited for static stability monitoring using the developed index. The proposed perturbation-coefficient equivalent impedance method reported in this research may be utilised in dynamic voltage stability applications through the development of a PMU-based bus stability index based on impedance matching instability condition identification.

References

[1] "Net Zero Strategy: Build Back Greener" Available: Net Zero Strategy: Build Back Greener - GOV.UK (www.gov.uk)

[2] H. Gu, R. Yan and T. Saha, "Review of system strength and inertia requirements for the national electricity market of Australia," in *CSEE Journal of Power and Energy Systems*, vol. 5, no. 3, pp. 295-305, Sept. 2019, doi: 10.17775/CSEEJPES.2019.00230.

[3] NERC, "Integrating Inverter Based Resources into Low Short Circuit Strength Systems, Reliability Guideline," North American Reliability Corporation (NERC), 2017.

[4] H. Gu, R. Yan, T. K. Saha, and E. Muljadi, "System Strength and Inertia Constrained Optimal Generator Dispatch Under High Renewable Penetration," *IEEE Transactions on Sustainable Energy*, vol. 11, no. 4, pp. 2392-2406, 2020, doi: 10.1109/tste.2019.2957568.

[5] J. Outram, G.Murphy, R.Bryans, M.Bebbington, "Real Time Fault level Monitoring," *25th International Conference on Electricity Distribution*, 2019.

[6] R. Aljarrah, H. Marzooghi, J. Yu, and V. Terzija, "Monitoring of fault level in future grid scenarios with high penetration of power electronics-based renewable generation," *IET Generation, Transmission & Distribution*, vol. 15, no. 2, pp. 294-305, 2020, doi: 10.1049/gtd2.12021.

[7] S. Jupe A. Kazerooni, J.Berry, N.Murdoch, "Sensitivity Analysis of Fault Level Assesments in HV Networks," *CIRED Workshop*, 2014.

[8] T. N. Boutsika and S. A. Papathanassiou, "Short-circuit calculations in networks with distributed generation," *Electric Power Systems Research*, vol. 78, no. 7, pp. 1181-1191, 2008, doi: 10.1016/j.epsr.2007.10.003.

[9] *IEC 60909-0 : Short-circuit currents in three-phase a.c. systems - Part 0: Calculation of currents*, IEC, 2016.

[10] N. G. ESO, "System Operability Framework: Impact of Declining Short Circuit Levels" 2018, Available: https://www.nationalgrideso.com/document/135561/download

[11] C. Collins and B. Stojkovksa, "The Power Potential Project: Trialling the Procurement of Reactive Power Services from Distribution-Connected Assets," *2018 15th International Conference on the European Energy Market (EEM)*, 2018, pp. 1-4, doi: 10.1109/EEM.2018.8469905.

[12] J. Modarresi, E. Gholipour, and A. Khodabakhshian, "A comprehensive review of the voltage stability indices," *Renewable and Sustainable Energy Reviews*, vol. 63, pp. 1-12, 2016, doi: 10.1016/j.rser.2016.05.010.

[13] I. Musirin and T. K. A. Rahman, "On-line voltage stability based contingency ranking using fast voltage stability index (FVSI)," *IEEE/PES Transmission and Distribution Conference and Exhibition*, 2002, pp. 1118-1123 vol.2, doi: 10.1109/TDC.2002.1177634.

[14] C. Reis and F. P. M. Barbosa, "A comparison of voltage stability indices," *MELECON 2006 - 2006 IEEE Mediterranean Electrotechnical Conference*, 2006, pp. 1007-1010, doi: 10.1109/MELCON.2006.1653269.

[15] S. Ratra, R. Tiwari, and K. R. Niazi, "Voltage stability assessment in power systems using line voltage stability index," *Computers & Electrical*

Engineering, vol. 70, pp. 199-211, 2018, doi: 10.1016/j.compeleceng.2017.12.046.

[16] B. de Metz-Noblat, C. Poulain, "Calculation of short-circuit currents," in Cahier techniques, 2005. Available: https://www.studiecd.dk/cahiers_techniques/Calculation_of_short_circuit_currents.pdf

[17] "DIgSILENT PowerFactory User Manual," 2017. Available: https://www.digsilent.de/en/downloads.html

[18] N.Murdoch, J.Berry, A.Kazerooni, "Distributed generation connections undera fault-level active network management scheme," *24th International Conference & Exhibition on Electricity Distribution (CIRED)*, 2017.

[19] X. Wang, P. Wang, Y. Wang, and F. Shi, "Online Estimation of Short-Circuit Fault Level in Active Distribution Network," *Applied Sciences*, vol. 10, no. 11, 2020, doi: 10.3390/app10113812.

[20] K. O. H. Pedersen, A. H. Nielsen, and N. K. Poulsen, "Short-circuit impedance measurement," *IEE Proceedings - Generation, Transmission and Distribution*, vol. 150, no. 2, 2003, doi: 10.1049/ip-gtd:20030193.

[21] K. Srinivasan, C. Lafond and R. Jutras, "Short-circuit current estimation from measurements of voltage and current during disturbances," in *IEEE Transactions on Industry Applications*, vol. 33, no. 4, pp. 1061-1064, July-Aug. 1997, doi: 10.1109/28.605749.

[22] B. B. D. Gheorghe, "Fault Level Monitoring in Distribution Grids," *CIGRE SESSION*, 2020.

[23] TNEI"LCNF Fault Level Monitoring and Modelling of ENW Network" 2017. Available: https://www.enwl.co.uk/globalassets/innovation/respond/respond-key-documents/fault-level-network-monitoring-and-modelling.pdf

[24] S. S. Kieran Bailey, Paul Marshall, "Configuration of NMS and installation/ commissioning of Fault Level Assessment Tool software," 2016.

[25] S. Jupe, J.Berry, M.Meisinger, J.Outram, "Implementation of an Active Fault Level Monitoring System for Distrbuted Generation Integration" *D 22nd International Conference on Electricity Distribution*, 2013.

[26] B. D. Gheorghe, "Fault Level Monitoring in Distribution Grids" *CIGRE*, 2020.

[27] J. M. Xueguang Wu, Nick Jenkins and Goran Strbac, "An investigation of Network Splitting for Fault Level Reduction," 2003.

[28] C. E. T. Foote, G. W. Ault, J. R. McDonald and A. J. Beddoes, "The impact of network splitting on fault levels and other performance measures," *CIRED 2005 - 18th International Conference and Exhibition on Electricity Distribution*, 2005, pp. 1-5, doi: 10.1049/cp:20051375.

[29] T. L. C. Chandraratne, R. T. Naayagi and W. L. Woo, "Overview of Adaptive Protection System for Modern Power Systems,," *IEEE Innovative Smart Grid Technologies - Asia (ISGT Asia), 2018*, 2018, doi: 10.1109/ISGT-Asia.2018.8467827.

[30] WSP "Adaptive Protection Safety Justification" 2018. Available: https://www.enwl.co.uk/globalassets/innovation/respond/respond-key-documents/adaptive-protection-safety-case.pdf

[31] M. S. Rawat and S. Vadhera, "Voltage Stability Assessment Techniques for Modern Power Systems," in *Novel Advancements in Electrical Power*

Planning and Performance, (Advances in Environmental Engineering and Green Technologies, 2020, ch. chapter 6, pp. 128-176.

[32] E. Vittal, M. O'Malley, and A. Keane, "A Steady-State Voltage Stability Analysis of Power Systems With High Penetrations of Wind," *IEEE Transactions on Power Systems,* vol. 25, no. 1, pp. 433-442, 2010, doi: 10.1109/tpwrs.2009.2031491.

[33] J. Xu *et al.*, "Voltage instability detection based on the concept of short circuit capacity," *International Transactions on Electrical Energy Systems,* vol. 26, no. 2, pp. 444-460, 2016, doi: 10.1002/etep.2098.

[34] M. Cupelli, C. Doig Cardet and A. Monti, "Voltage stability indices comparison on the IEEE-39 bus system using RTDS," *2012 IEEE International Conference on Power System Technology (POWERCON)*, 2012, pp. 1-6, doi: 10.1109/PowerCon.2012.6401284.

[35] L. Ramirez Perdomo, A.Lozano, "Evaluation of indices for voltage stability monitoring using PMU measurements," *Ingenieria e Investigación,* pp. 44-49, 2014, doi: 10.15446/ing.investig.v34n3.43002. .

[36] I. Musirin and T. K. Abdul Rahman, "Novel fast voltage stability index (FVSI) for voltage stability analysis in power transmission system," *Student Conference on Research and Development*, 2002, pp. 265-268, doi: 10.1109/SCORED.2002.1033108.

[37] A. K. H. Sinha, "A Comparative Study of Voltage Stability Indices Used for Power System Operation," *International Journal of Electrical Power & Energy Systems,* pp. 589-596, 2000, doi: 10.1016/S0142-0615(00)00014-4. .

[38] P. Mandoulidis and C. Vournas, "A PMU-based real-time estimation of voltage stability and margin," *Electric Power Systems Research,* vol. 178, 2020, doi: 10.1016/j.epsr.2019.106008.

[39] M. P. Sambarta Dasgupta, Umesh Vaidya, and Ajjarapu V, "PMU-based model-free approach for short term voltage stability monitoring," *IEEE Power and Energy Society General Meeting - Conversion and Delivery of Electrical Energy in the 21st Century,* pp. pp. 1-8, 2012, doi: 10.1109/PESGM.2012.6345522.

[40] C. D. Vournas, C. Lambrou, and P. Mandoulidis, "Voltage Stability Monitoring From a Transmission Bus PMU," *IEEE Transactions on Power Systems,* vol. 32, no. 4, pp. 3266-3274, 2017, doi: 10.1109/tpwrs.2016.2629495.

[41] M. Kamel, A. A. Karrar, and A. H. Eltom, "Development and Application of a New Voltage Stability Index for On-Line Monitoring and Shedding," *IEEE Transactions on Power Systems,* vol. 33, no. 2, pp. 1231-1241, 2018, doi: 10.1109/tpwrs.2017.2722984.

[42] UKPN, "Transmission & Distribution Interface 2.0 (TDI 2.0) " 2017. Available:

https://www.ofgem.gov.uk/sites/default/files/docs/2016/11/final_submission_tdi_2.0.pdf

[43] C. Dobson, Thierry & Vournas, C & Demarco, C.L. & Venkatasubramanian, M & Overbye, T & Canizares, "Voltage Stability Assessment: Concepts, Practices and Tools," 2002.

[44] P. P. Kundur, Neal J. Balu, and Mark G. Lauby, *Power System Stability and Control*. 1994.
[45] Y. Lee and S. Han, "Real-Time Voltage Stability Assessment Method for the Korean Power System Based on Estimation of Thévenin Equivalent Impedance," *Applied Sciences*, vol. 9, no. 8, 2019, doi: 10.3390/app9081671.
[46] V. Ajjarapu and C. Christy, "The continuation power flow: a tool for steady state voltage stability analysis," *[Proceedings] Conference Papers 1991 Power Industry Computer Application Conference*, 1991, pp. 304-311, doi: 10.1109/PICA.1991.160593.
[47] R.D. Zimmerman, C.E. Murillo-S´anchez "Matpower 6.0b1 User's Manual," 2016. Available: https://matpower.org/docs/MATPOWER-manual-6.0b1.pdf
[48] Zhu, P.; Taylor, G.; Irving, M.: 'Performance analysis of a novel Q-limit guided continuation power flow method', IET Generation, Transmission & Distribution, 2009, 3, (12), p. 1042-1051, DOI: 10.1049/iet-gtd.2008.0504
IET Digital Library, https://digital-library.theiet.org/content/journals/10.1049/iet-gtd.2008.0504 [49] M. Moghavvemi and M. O. Faruque, "Effects of FACTS devices on static voltage stability," presented at the 2000 TENCON Proceedings. Intelligent Systems and Technologies for the New Millennium (Cat. No.00CH37119), 2000.
[50] C. A. Caiiizares, "On bifurcations, Voltage Collapse and Load Modelling," *IEEE Transactions on Power Systems*, vol. 10, 1995.
[51] C. A. Canizares, "Calculating optimal system parameters to maximize the distance to saddle-node bifurcations," *IEEE Transactions on Circuits and Systems I: Fundamental Theory and Applications*, vol. 45, pp. pp. 225-237, 1998, doi: 10.1109/81.662696.
[52] G. B. J. M.M. Aman, H. Mokhlis, A.H.A. Bakar, "Optimal placement and sizing of a DG based on a new power stability index and line losses," *International Journal of Electrical Power & Energy Systems*, vol. 43, no. 1, pp. 1296-1304, 2012, doi: https://doi.org/10.1016/j.ijepes.2012.05.053.
[53] Aman, M.M, Jasmon, G.B. Bakar, A.H.A. and Mokhlis "Optimum Capacitor Placement and Sizing for Distribution System Based on an Improved Voltage Stability Index," *International Review of Electrical Engineering*, 2012.
[54] S. Kim e. al, "Development of voltage stability constrained optimal power flow (VSCOPF)," *2001 Power Engineering Society Summer Meeting. Conference Proceedings (Cat. No.01CH37262)*, vol. 3, pp. 1664-1669 2001, doi: 10.1109/PESS.2001.970325.
[55] B. Cui and X. A. Sun, "A New Voltage Stability-Constrained Optimal Power-Flow Model: Sufficient Condition, SOCP Representation, and Relaxation," *IEEE Transactions on Power Systems*, vol. 33, no. 5, pp. 5092-5102, 2018, doi: 10.1109/tpwrs.2018.2801286.
[56] C. D. C. M. Cupelli, A. Monti, "Comparison of Line Voltage Stability Indices using Dynamic Real Time Simulation," *3rd IEEE PES Innovative Smart Grid Technologies Europe (ISGT Europe)*, 2012.
[57] C. S. a. M. G. Ganness, "Determination of Power System Voltage Stability Using Modal Analysis," *International Conference on Power Engineering,*

Energy and Electrical Drives, pp. pp. 381-387, 2007, doi: 10.1109/POWERENG.2007.4380124.

[58] V.Murty, A.Kumar "Optimal placement of DG in radial distribution systems based on new voltage stability index under load growth," *International Journal of Electrical Power & Energy Systems*, vol. 69, pp. 246-256, 2015, doi: https://doi.org/10.1016/j.ijepes.2014.12.080.

[59] T. Zabaiou, L. Dessaint and I. Kamwa, "A comparative study of VSC-OPF techniques for voltage security improvement and losses reduction," *2014 IEEE PES General Meeting | Conference & Exposition*, 2014, pp. 1-5, doi: 10.1109/PESGM.2014.6939000.

[60] R. P. Tamta, S.Painuli, M.Rawat, S.Vadhera,"Comparison of Line Voltage Stability Indices for Assessment of Voltage Instability in high Voltage Network," *1st International Conference on New Frontiers in Engineering, Science & Technology*, 2018.

[61] H. Z. X. Zhao, D. Shi, H. Zhao, C. Jing and C. Jones, "On-line PMU-based transmission line parameter identification," *CSEE Journal of Power and Energy Systems*, vol. 1, pp. 68-74,, 2015, doi: 10.17775/CSEEJPES.2015.00021.

[62] H. H. Goh, Q. S. Chua, S. W. Lee, B. C. Kok, K. C. Goh, and K. T. K. Teo, "Evaluation for Voltage Stability Indices in Power System Using Artificial Neural Network," *Procedia Engineering*, vol. 118, pp. 1127-1136, 2015, doi: 10.1016/j.proeng.2015.08.454.

[63] N. Upadhayay, M. Nadarajah and A. Ghosh, "System Strength Enhancement with Synchronous Condensers for Power Systems with High Penetration of Renewable Energy Generators," *2021 31st Australasian Universities Power Engineering Conference (AUPEC)*, 2021, pp. 1-5, doi: 10.1109/AUPEC52110.2021.9597835.

[64] SP Energy Networks, "Impact of SC / H-SC on existing balancing schemes and markets," 2021. Available: https://www.spenergynetworks.co.uk/userfiles/file/Phoenix_-_Impacts_Report_SDRC_2.5-v3.0.pdf

[65] I. M. Dudurych, "On-line assessment of secure level of wind on the Irish power system," *EEE PES General Meeting*, pp. pp. 1-7, 2010, doi: 10.1109/PES.2010.5588059.

[66] W. D. Rosehart, C. A. Canizares, and V. H. Quintana, "Multiobjective optimal power flows to evaluate voltage security costs in power networks," *IEEE Transactions on Power Systems*, vol. 18, no. 2, pp. 578-587, 2003, doi: 10.1109/tpwrs.2003.810895.

[67] F. Capitanescu *et al.*, "State-of-the-art, challenges, and future trends in security constrained optimal power flow," *Electric Power Systems Research*, vol. 81, no. 8, pp. 1731-1741, 2011, doi: 10.1016/j.epsr.2011.04.003.

[68] Z. D. S. Xia, M. Shahidehpour, K. W. Chan, S. Bu and G. Li, "Transient Stability-Constrained Optimal Power Flow Calculation With Extremely Unstable Conditions Using Energy Sensitivity Method," *IEEE Transactions on Power Systems*, vol. 36, no. 1, pp. 355-365, doi: 10.1109/TPWRS.2020.3003522.

[69] T. A. Reza Ardeshiri Lajimi, "A two stage model for rotor angle transient stability constrained optimal power flow," *International Journal of Electrical Power & Energy Systems,* vol. 76, pp. 82-89, 2016, doi: https://doi.org/10.1016/j.ijepes.2015.07.041.

[70] A. A. Mohamed and B. Venkatesh, "Voltage stability constrained line-wise optimal power flow," *IET Generation, Transmission & Distribution,* vol. 13, no. 8, pp. 1332-1338, 2019, doi: 10.1049/iet-gtd.2018.5452.

[71] H. Gu, R. Yan, and T. K. Saha, "Review of system strength and inertia requirements for the national electricity market of Australia," *CSEE Journal of Power and Energy Systems,* 2019, doi: 10.17775/cseejpes.2019.00230.

[72] J. Preetha Roselyn, D. Devaraj, and S. S. Dash, "Multi-Objective Genetic Algorithm for voltage stability enhancement using rescheduling and FACTS devices," *Ain Shams Engineering Journal,* vol. 5, no. 3, pp. 789-801, 2014/09/01/ 2014, doi: https://doi.org/10.1016/j.asej.2014.04.004.

[73] T. Niknam, M. R. Narimani, J. Aghaei, and R. Azizipanah-Abarghooee, "Improved particle swarm optimisation for multi-objective optimal power flow considering the cost, loss, emission and voltage stability index," *IET Generation, Transmission & Distribution,* vol. 6, no. 6, 2012, doi: 10.1049/iet-gtd.2011.0851.

[74] S. a. K. Moghadasi, Sukumar, "An architecture for voltage stability constrained optimal power flow using convex semi-definite programming," *2015 North American Power Symposium (NAPS),* pp. 1-6, 2015, doi: 10.1109/NAPS.2015.7335219.

[75] W. R. C. Canizares, A. Berizzi and C. Bovo, "Comparison of Voltage Security Constrained

Optimal Power Flow Techniques," *Power Engineering Society Summer Meeting. Conference Proceedings,* pp. 1680-1685, 2001, doi: 10.1109/PESS.2001.970328.

[76] T. Zabaiou, L. A. Dessaint, and I. Kamwa, "Preventive control approach for voltage stability improvement using voltage stability constrained optimal power flow based on static line voltage stability indices," *IET Generation, Transmission & Distribution,* vol. 8, no. 5, pp. 924-934, 2014, doi: 10.1049/iet-gtd.2013.0724.

[77] P. P. Biswas, Arora, P., Mallipeddi, R., " Optimal placement and sizing of FACTS devices for optimal power flow in a wind power integrated electrical network," *Neural Comput & Applic 33*, pp. 6753–6774, 2021, doi: 10.1007/s00521-020-05453-x.

[78] A. Lashkar Ara, A. Kazemi, S. Gahramani, and M. Behshad, "Optimal reactive power flow using multi-objective mathematical programming," *Scientia Iranica,* vol. 19, no. 6, pp. 1829-1836, 2012, doi: 10.1016/j.scient.2012.07.010.

[79] K. P. Bansilal D. Thukaram, "Optimal reactive power dispatch algorithm for voltage stability improvement," *International Journal of Electrical Power & Energy Systems,* vol. 18, no. 7, pp. 461-468, 1996, doi: https://doi.org/10.1016/0142-0615(96)00004-X.

[80] A. R. Nageswa Rao, P. Vijaya, and M. Kowsalya, "Voltage stability indices for stability assessment: a review," *International Journal of Ambient Energy,* vol. 42, no. 7, pp. 829-845, 2018, doi: 10.1080/01430750.2018.1525585.

[81] S. Kim, "Development of voltage stability constrained optimal power flow (VSCOPF)," *Power Engineering Society Summer Meeting. Conference Proceedings (Cat. No.01CH37262),* vol. 3, pp. 1664-1669 2001, doi: 10.1109/PESS.2001.970325.

[82] L. D. a. I. K. T. Zabaiou, "A Comparative Study of VSC-OPF Techniques for Voltage Security Improvement and Losses Reduction," *IEEE PES General Meeting | Conference & Exposition,* pp. 1-5, 2014, doi: 10.1109/PESGM.2014.6939000.

[83] M. Moghavvemi and O. Faruque, "Real-time contingency evaluation and ranking technique," *IEE Proceedings - Generation, Transmission and Distribution,* vol. 145, no. 5, 1998, doi: 10.1049/ip-gtd:19982179.

[84] F. Milano, C. A. Cañizares, and M. Invernizzi, "Voltage stability constrained OPF market models considering contingency criteria," *Electric Power Systems Research,* vol. 74, no. 1, pp. 27-36, 2005, doi: 10.1016/j.epsr.2004.07.012.

[85] R. Aljarrah, H. Marzooghi, V. Terzija, and J. Yu, "Modifying IEC 60909 Standard to Consider Fault Contribution from Renewable Energy Resources Utilizing Fully-Rated Converters," presented at the 2019 9th International Conference on Power and Energy Systems (ICPES), 2019.

[86] G. C. Cornfield, "Estimating system fault level from naturally occurring disturbances," *IEE Colloquium on Instrumentation in the Electrical Supply Industry,* pp. pp. 13/1-13/4., 1993.

[87] A. K. H. Sinha, D., " Comparative study of voltage stability indices in a power system," *International Journal of Electrical Power & Energy Systems,* pp. 589-596, doi: 10.1016/S0142-0615(00)00014-4. .

[88] A.Mohamed, S. Yusof, "A Static Voltage Collapse Indicator Using Line Stability Factors," *Journal of Industrial Technology,* 1998.

[89] I. Adebayo and Y. Sun, "New Performance Indices for Voltage Stability Analysis in a Power System," *Energies,* vol. 10, no. 12, 2017, doi: 10.3390/en10122042.

[90] P. N. Vovos and J. W. Bialek, "Direct Incorporation of Fault Level Constraints in Optimal Power Flow as a Tool for Network Capacity Analysis," *IEEE Transactions on Power Systems,* vol. 20, no. 4, pp. 2125-2134, 2005, doi: 10.1109/tpwrs.2005.856975.

[91] P. N. Vovos, G. P. Harrison, A. R. Wallace, and J. W. Bialek, "Optimal Power Flow as a Tool for Fault Level-Constrained Network Capacity Analysis," *IEEE Transactions on Power Systems,* vol. 20, no. 2, pp. 734-741, 2005, doi: 10.1109/tpwrs.2005.846070.

[92] S. Khushalani, J. M. Solanki, and N. N. Schulz, "Development of Three-Phase Unbalanced Power Flow Using PV and PQ Models for Distributed Generation and Study of the Impact of DG Models," *IEEE Transactions on Power Systems,* vol. 22, no. 3, pp. 1019-1025, 2007, doi: 10.1109/tpwrs.2007.901476.

[93] C. K. a. M. Liserre, "Operation and control of smart transformer for improving performance of medium voltage power distribution system," *2015 IEEE 6th International Symposium on Power Electronics for Distributed Generation Systems (PEDG),* pp. pp. 1-6, 2015, doi: 10.1109/PEDG.2015.7223092.

[94] D. S. a. M. L. Crow, "Online Volt-Var Control for Distribution Systems With Solid-State Transformers," *IEEE Transactions on Power Delivery,* vol. 31, pp. 343-350, 2016, doi: 10.1109/TPWRD.2015.2457442.

[95] J. E. H. a. J. W. Kolar, "Solid-State Transformers: On the Origins and Evolution of Key Concepts," *IEEE Industrial Electronics Magazine,* vol. 10, no. 3, pp. 19-28, doi: 10.1109/MIE.2016.2588878.

[96] G. M.-V. Guerra, Juan, "A Solid State Transformer model for power flow calculations," *International Journal of Electrical Power & Energy Systems,* pp. 40-51, 2017, doi: 10.1016/j.ijepes.2017.01.005.

[97] CIGRE, "CIGRE Science and Engineering," 2021. Available: https://www.cigre.org/GB/publications/cigre-cse

[98] I. M. Dudurych, "On-line assessment of Secure Level of Wind on the Irish Power System," *IEEE PES General Meeting,* pp. 1-7, 2010, doi: 10.1109/PES.2010.5588059.

[99] E. M. D. M. J. Dolan, I. Kockar, G. W. Ault and S. D. J. McArthur, "Distribution Power Flow Management Utilizing an Online Optimal Power Flow Technique," *IEEE Transactions on Power Systems,* vol. 27, no. 22, pp. 790-799, 2012, doi: doi: 10.1109/TPWRS.2011.2177673.

[100] I. Martínez Sanz, B. Stojkovska, A. Wilks, J. Horne, A. R. Ahmadi, and T. Ustinova, "Enhancing transmission and distribution system coordination and control in GB using power services from DERs," *The Journal of Engineering,* vol. 2019, no. 18, pp. 4911-4915, 2019, doi: 10.1049/joe.2018.9303.

[101] C. C. a. B. Stojkovksa, "The Power Potential Project: Trialling the Procurement of Reactive Power Services from Distribution-Connected Assets," *15th International Conference on the European Energy Market (EEM),* pp. 1-4, 2018, doi: 10.1109/EEM.2018.8469905.

[102] N. G. ESO, "Power potential (Tranmsission and Distribution interface 2.0) project closedown report," 2021. Available:

https://innovation.ukpowernetworks.co.uk/wpcontent/uploads/2021/08/Power Potential_CloseDownreport_FINAL.pdf

[103] X. C. D. Luo, H. He and T. Lu, "Fast approach for voltage stability constrained optimal power flow based on load impedance modulus margin," *2017 IEEE Industry Applications Society Annual Meeting,* pp. 1-12, 2017, doi: 10.1109/IAS.2017.8101702.

[104] F. Capitanescu, M. Glavic, D. Ernst, and L. Wehenkel, "Contingency Filtering Techniques for Preventive Security-Constrained Optimal Power Flow," *Power Systems, IEEE Transactions on,* vol. 22, pp. 1690-1697, 12/01 2007, doi: 10.1109/TPWRS.2007.907528.

[105] S. Ibrahim, “Experimental Measurements of Fault Level For Sceco west, Kingdom of Saudi Arabia,” Journal of King Abdulaziz University-Engineering Sciences, vol. 15, no. 1, pp. 83-102, 2004.

[106] Williamson, G.E.; Jenkins, N.; Cornfield, G.C. Use of naturally occurring system disturbances to estimate the fault current contribution of induction motors. IEE Proc. Gener. Transm. Distrib. 1996, 143, 243–248

[103] ANSI/IEEE Std. C37.010-1979, Application guide for AC high-voltage circuit breakers rated on a symmetrical basis.

[104] Engineering Recommendation G74, 1992

[105] S. Ibrahim, “Experimental Measurements of Fault Level For Sceco west, Kingdom of Saudi Arabia,” Journal of King Abdulaziz University-Engineering Sciences, vol. 15, no. 1, pp. 83-102, 2004.

[106] Williamson, G.E.; Jenkins, N.; Cornfield, G.C. Use of naturally occurring system disturbances to estimate the fault current contribution of induction motors. IEE Proc. Gener. Transm. Distrib. 1996, 143, 243–248

[107] Ha, H.; Subramanian, S. Predicting the prospective fault level on distribution grids and its impact on protective relaying. In Proceedings of the 2017 70th Annual Conference for Protective Relay Engineers (CPRE), College Station, TX, USA, 3–6 April 2017; pp. 1–4.

[108] Conner, S.; Cruden, A. An automatic transient detection system which can be incorporated into an algorithm to accurately determine the fault level in networks with DG. In Proceedings of the 47th International Universities Power Engineering Conference, Uxbridge, UK, 4–7 September 2012.

[109] Von Meier, A.; Stewart, E.; McEachern, A.; Andersen, M.; Mehrmanesh, L. Precision Micro-Synchrophasors for Distribution Systems: A Summary of Applications. IEEE Trans. Smart Grid 2017, 8, 2926–2936

[110] M. Farajollahi, A. Shahsavari, E. M. Stewart and H. Mohsenian-Rad, "Locating the Source of Events in Power Distribution Systems Using Micro-PMU Data," in *IEEE Transactions on Power Systems*, vol. 33, no. 6, pp. 6343-6354, Nov. 2018, doi: 10.1109/TPWRS.2018.2832126.

[111] A. C. Parsons, W. M. Grady, E. J. Powers and J. C. Soward, "A direction finder for power quality disturbances based upon disturbance power and energy," *8th International Conference on Harmonics and Quality of Power. Proceedings (Cat. No.98EX227)*, 1998, pp. 693-699 vol.2, doi: 10.1109/ICHQP.1998.760129.

[112] U. Hashmi, R. Choudhary and J. G. Priolkar, "Online thevenin equivalent parameter estimation using nonlinear and linear recursive least square algorithm," *2015 IEEE International Conference on Electrical, Computer and Communication Technologies (ICECCT)*, 2015, pp. 1-6, doi: 10.1109/ICECCT.2015.7225946.

[113] X. Chen, Y. Sun and R. Yin, "An Improvement Algorithm for Online Identification of Thevenin Equivalent Parameters," *2021 3rd Asia Energy and Electrical Engineering Symposium (AEEES)*, 2021, pp. 46-49, doi: 10.1109/AEEES51875.2021.9403072.

[114] P. -. Lof, G. Andersson and D. J. Hill, "Voltage stability indices for stressed power systems," in *IEEE Transactions on Power Systems*, vol. 8, no. 1, pp. 326-335, Feb. 1993, doi: 10.1109/59.221224.

[115] Yuanyuan Lou, Zhongxi Ou, Zhu Tong, Wenjing Tang, Zhencong Li, Kun Yang, "Static Volatge Stability Evaluation on the Urban Power System by Continuation Power Flow", *2022 5th International*

[116] I. Smon, G. Verbic and F. Gubina, "Local voltage-stability index using tellegen's Theorem," in *IEEE Transactions on Power Systems*, vol. 21, no. 3, pp. 1267-1275, Aug. 2006, doi: 10.1109/TPWRS.2006.876702.

[117] Y. Gong and N. Schulz, "Synchrophasor-Based Real-Time Voltage Stability Index," *2006 IEEE PES Power Systems Conference and Exposition*, 2006, pp. 1029-1036, doi: 10.1109/PSCE.2006.296452

[118] N. Thasnas and A. Siritaratiwat, "Implementation of Static Line Voltage Stability Indices for Improved Static Voltage Stability Margin," *Journal of Electrical and Computer Engineering*, vol. 2019, p. 2609235, 2019/05/02 2019, doi: 10.1155/2019/2609235.

[119] Moger, T. and Dhadbanjan, T. (2015), A novel index for identification of weak nodes for reactive compensation to improve voltage stability. IET Gener. Transm. Distrib., 9: 1826-1834.

[120] A. R. Phadke, M. Fozdar, and K. R. Niazi, "A new technique for computation of closest saddle-node bifurcation point of power system using real coded genetic algorithm," *International Journal of Electrical Power & Energy Systems*, vol. 33, no. 5, pp. 1203-1210, 2011/06/01/ 2011, doi: https://doi.org/10.1016/j.ijepes.2011.01.034.

[121] Y. Wen, C. Guo, D. S. Kirschen and S. Dong, "Enhanced Security-Constrained OPF With Distributed Battery Energy Storage," in *IEEE Transactions on Power Systems*, vol. 30, no. 1, pp. 98-108, Jan. 2015, doi: 10.1109/TPWRS.2014.2321181.

[122] Raheel Zafar, Jayashri Ravishankar, John E. Fletcher, Hemanshu R. Pota, "Multi-Timescale Voltage Stability-Constrained Volt/VAR Optimisation With Battery Storage System in Distribution Grids", *IEEE Transactions on Sustainable Energy*, vol.11, no.2, pp.868-878, 2020.

[123] S. Goh, T. Saha, and Z. Y. Dong, "Solving Multi-Objective Voltage Stability-constrained Power Transfer Capability Problem using Evolutionary Computation," *International Journal of Emerging Electric Power Systems*, vol. 12, 01/06 2011, doi: 10.2202/1553-779X.2544.

[124] Eladl, A.A., Basha, M.I. & ElDesouky, A.A. Multi-objective-based reactive power planning and voltage stability enhancement using FACTS and capacitor banks. *Electr Eng* (2022). https://doi.org/10.1007/s00202-022-01542-3

[125] Aljarrah, R, Marzooghi, H, Yu, J, Terzija, V. Monitoring of fault level in future grid scenarios with high penetration of power electronics-based renewable generation. *IET Gener Transm Distrib*. 2021; 15: 294– 305.

[126] I. Jarraya, J. Hmad, H. Trabelsi, A. Houari and M. Machmoum, "An Online Grid Impedance Estimation Using Recursive Least Square For Islanding Detection," *2019 16th International Multi-Conference on Systems, Signals & Devices (SSD)*, 2019, pp. 193-200, doi: 10.1109/SSD.2019.8893148.

[127] M. K. De Meerendre, E. Prieto-Araujo, K. H. Ahmed, O. Gomis-Bellmunt, L. Xu and A. Egea-Àlvarez, "Review of Local Network Impedance Estimation

Techniques," in *IEEE Access*, vol. 8, pp. 213647-213661, 2020, doi: 10.1109/ACCESS.2020.3040099.

[128] E. Ghahremani and I. Kamwa, "Optimal placement of multiple-type FACTS devices to maximize power system loadability using a generic graphical user interface," in *IEEE Transactions on Power Systems*, vol. 28, no. 2, pp. 764-778, May 2013, doi: 10.1109/TPWRS.2012.2210253.

[129] H. Xiong, H. Cheng, and H. Li, "Optimal reactive power flow incorporating static voltage stability based on multi-objective adaptive immune algorithm," *Energy Conversion and Management*, vol. 49, no. 5, pp. 1175-1181, 2008/05/01/ 2008, doi: https://doi.org/10.1016/j.enconman.2007.09.005.

[130] F. Capitanescu, M. Glavic, D. Ernst, and L. Wehenkel, "Contingency Filtering Techniques for Preventive Security-Constrained Optimal Power Flow," *Power Systems, IEEE Transactions on*, vol. 22, pp. 1690-1697, 12/01 2007, doi: 10.1109/TPWRS.2007.907528.

[131] D. Gan, R. J. Thomas and R. D. Zimmerman, "Stability-constrained optimal power flow," in *IEEE Transactions on Power Systems*, vol. 15, no. 2, pp. 535-540, May 2000, doi: 10.1109/59.867137.

[132] Z. Zou, J. Zhao, E. Pan, D. Xu and L. Dong, "Trajectory Sensitivity Based Voltage Stability Constrained Reactive Optimal Power Flow in Sending-End Power System with High Penetration Renewable Energy," *2020 12th IEEE PES Asia-Pacific Power and Energy Engineering Conference (APPEEC)*, Nanjing, China, 2020, pp. 1-5, doi: 10.1109/APPEEC48164.2020.9220481.

[133] A. Meddeb, H. Jmii, S. Chebbi "Security Analysis and the Contribution of UPFC for Improving Voltage Stability", Advances in Science, Technology and Engineering Systems Journal, vol. 3, no. 1, pp. 404-411 (2018).

[134] Tianjing Wang, Yong Tang, "Data-model driven rescheduling considering both rotor angle stability and transient voltage stability constraints", *IET Renewable Power Generation*, 2022.

[135] Wei Zhang, Zhaolin Liu, Yulin Zhao, "An Online Method to Identify the Voltage Stability of Power Systems during Transients", *2017 IEEE International Conference on Energy Internet (ICEI)*, pp.119-124, 2017.

[136] Mazhar Ali, Elena Gryazina, Oleg Khamisov, Timur Sayfutdinov, "Online assessment of voltage stability using Newton-Corrector algorithm", *IET Generation, Transmission & Distribution*, vol.14, no.19, pp.4207-4216, 2020.

[137] Stefan Polster, Herwig Renner, "Voltage stability monitoring methods for distribution grids using the Thevenin impedance", *CIRED - Open Access Proceedings Journal*, vol.2017, no.1, pp.1535-1539, 2017.

[138] W. H. Kersting, "Radial distribution test feeders," *2001 IEEE Power Engineering Society Winter Meeting. Conference Proceedings (Cat.*

No.01CH37194), Columbus, OH, USA, 2001, pp. 908-912 vol.2, doi: 10.1109/PESW.2001.916993.